

Data-Driven Modeling and Control of Batch
and Batch-Like Processes

DATA-DRIVEN MODELING AND CONTROL OF BATCH AND
BATCH-LIKE PROCESSES

BY

ABHINAV GARG, M.S. (R), B.Tech.

A THESIS

SUBMITTED TO THE SCHOOL OF GRADUATE STUDIES

IN PARTIAL FULFILMENT OF THE REQUIREMENTS

FOR THE DEGREE

DOCTOR OF PHILOSOPHY

McMaster University © Copyright by Abhinav Garg, August 2018

Doctor of Philosophy (2018)
(Chemical Engineering)

McMaster University
Hamilton, Ontario, Canada

TITLE: Data-Driven Modeling and Control of Batch and Batch-Like Processes

AUTHOR: Abhinav Garg
M.S. (R), B.Tech.

SUPERVISOR: Prof. Prashant Mhaskar

NUMBER OF PAGES: xx, 143

Dedicated to all my Teachers for their love and trust in my abilities.

Gurur Brahma Gurur Vishnu

Gurur Devo Maheshwaraha

Gurur Saakshaat Para Brahma

Tasmai Sree Guruve Namaha

"Guru (Teacher) is verily the representative of Brahma, Vishnu and Shiva. He creates, sustains knowledge and destroys the weeds of ignorance. I salute such a Guru."

Preface

This ‘sandwich’ thesis is composed of different research articles either published or submitted to a journal for publication. The details on the article are provided at the beginning of each chapter. In case of published articles, the content is a reproduced verbatim in the corresponding chapters.

A majority of this work is a result of industrial and academic collaboration resulting in multi-authored papers/manuscripts. The contribution of each author in the different chapters is as follows.

In Chapter 4, the entire work is done by the me under supervision of Prof. Prashant Mhaskar. Brandon Corbett helped in the formulation of the subspace identification problem for this work. Further, Gangshi Hu and Jesus Flores-Cerrillo were the collaborators from Praxair Inc. who provided the insights on the operation of their hydrogen plant and specified their requirements for this project.

In Chapter 5, I have made the primary contribution of designing the data-driven modeling and control strategy for the rotational molding process along with developing the Matlab based interface for the experimental setup. Felipe Pedro Gomes contributed by conducting the experiments and performing the quality tests for the samples. The project was done under the guidance of Prof. Prashant Mhaskar and Prof. Michael Thompson.

The rest of the chapters (2 and 3) were entirely my independent work done under the supervision of Prof. Prashant Mhaskar.

Abstract

This thesis focuses on data-driven modeling and control of batch and batch-like processes. These processes are highly nonlinear and time-varying which, unlike continuous operations, are characterized by the finite duration of operation and absence of equilibrium conditions. This makes the modeling and control approaches available for continuous processes not readily applicable and requires appropriate adaptations of the available approaches to handle a) batch data structure for modeling and b) a control objective different than that of maintaining a steady-state operation as often encountered in a continuous process.

With these considerations, this work adapted the batch subspace identification for modeling and control of a variety of batch and batch-like processes. A particular focus of this work was on the application of the proposed ideas on real engineering systems along with simulated case studies. The applications considered in this work are batch crystallization, a hydrogen plant startup dynamics in a collaboration with Praxair Inc. and a rotational molding process in collaboration with the polymer research group at McMaster University. For the seeded batch crystallization process, subspace identification techniques are adapted to identify a linear time invariant model for the, otherwise, infinite dimensional process. The identified model is then deployed in a linear model

predictive control (MPC) strategy to achieve crystal size distribution (CSD) with desired characteristics subject to both manipulated input and product quality constraints. The proposed MPC is shown to achieve superior performance and the ability to respect tighter product quality constraints as well as robustness to uncertainty in comparison to an open loop policy as well as a traditional trajectory tracking policy using classical control. In another contribution, merits of handling data variety in a subspace identification framework was demonstrated on the crystallization process. The proposed approach facilitates the specification of a desired shape of the particle size distribution required at the termination of the batch process. Further, novel model validity constraints are proposed for the subspace identification based control framework.

In the collaborative work on hydrogen plant startup, it is recognized as a batch-like process due to its similarity to batch processes. Firstly, in this work a high fidelity model of the Hydrogen unit was developed with relevant startup and shutdown mechanisms. This setup is used to mimic the trends in the key process variables during the startup/shutdown operation. The simulated data is used to identify a state-space model of the process and validated on new simulated startup. Further, the approach was demonstrated on real plant data from one of the Praxair's plants. The predictive capabilities of the model provide ample handle for the plant operator for averting failures and abrupt shutdown of the entire plant. This is expected to have immense economic advantages.

Finally, the subspace identification based modeling and control approach was applied to a lab-scale rotational modeling (RM) process. It is a polymer processing technique that is characterized by the placement of a polymer resin inside a mold,

subsequent closure of the mold, followed by the simultaneous application of uni-axial (as is the case in the present work) or bi-axial rotation and heat. The resin is deposited on the mold wall where it forms a dense unified layer following which, the mold is cooled while still rotating the mold. Once demolding temperatures are achieved, the finished part is removed from the mold. Its potential as a manufacturing process for polymeric components is limited by a number of concerns including difficulties in process control, in particular, determining efficiently the process operation to yield the desired product consistently, and produce new products. This work has contributed by developing optimal control strategies for the process to achieve user-specified product quality and reject variability across batches. The results obtained demonstrate the merits of the proposed approach.

Acknowledgements

At first, I would like to express my sincere gratitude to my advisor Dr. Prashant Mhaskar for his excellent and enthusiastic guidance during the entire course of my Ph.D. at McMaster University. He influenced me greatly not only at the technical level, but also at a personal level. He was a true friend, philosopher and guide. His in-depth knowledge of the subject and exceptional analytical skills helped me to bring my work to this level. I was extremely fortunate in pursuing my graduate research under his guidance. I have attempted my best to learn as much as possible from him and am sure his teachings will always help me throughout my career.

I am grateful to my supervisory committee members, Dr. Vladimir Mahalec, Dr. Shahin Sirouspour for their support and valuable guidance. I would also like to thank Dr. Michael Thompson for his guidance in our collaborative work on rotational molding control; and Jesus Flores-Cerrillo and Gangshi Hu from Praxair Inc. for providing industrial data and insights on their hydrogen plant. Further, I would like to express my gratitude to Lynn Falkiner, Michelle Whalen, Linda Ellis and Kristina Trollip for all the administrative help during my studies.

I would also like to take this opportunity to thank my Master's advisor Dr. Arun K. Tangirala for his continued guidance and motivation. Without his motivation, I might not have pursued doctoral studies. Further, I would be

failing in my duties if I don't acknowledge the selfless contributions of my school teachers in making me capable to reach this level. Without their belief in me, I would have never been able to achieve this.

It has been a wonderful experience working in McMaster Advanced Control Consortium (MACC). The group consists of people with a broad range of research interest and always has been a great place to discuss new ideas, particularly, discussions on subspace identification with Brandon Corbett. Further, I would like to thank my friends Jaffer Ghouse, Pulkit Mathur, Smriti Shyamal, Rahul Sadavarte, Shailesh Patel, Ganesh Niranjana, Avijit Mallick for making my stay enjoyable. Outside McMaster, I would like to acknowledge Avinash Sahu for being a great friend. I will always cherish the time that I have spent with them.

Finally, I would like to thank my family for their moral support and encouragement. In particular, I would like to thank my mother for being my strength in the times of difficulty.

Contents

Preface	iv
Abstract	vi
Acknowledgements	ix
List of abbreviations and symbols	xxi
Declaration	xxv
1 Introduction	1
1.1 Batch Process Control	1
1.1.1 Thesis Outline	4
2 Subspace Identification Based Modeling and Control of Batch Particulate Processes	6
2.1 Introduction	7
2.2 Preliminaries	10
2.2.1 Motivating Example: A Seeded Batch Crystallizer	11
2.2.2 Subspace Identification	15

2.3	Proposed Modeling and Control Approach	17
2.3.1	Model Identification	17
2.3.2	Model Validation	20
2.3.3	Model Predictive Controller Design	22
2.4	Applications to the Motivating Example	24
2.4.1	Model Identification	24
2.4.2	Predictive Control Of Batch Particulate Processes	30
2.5	Robustness Evaluation in Presence of Time Varying Parameters	38
2.5.1	Model Identification	39
2.5.2	Closed-loop Results	39
2.6	Conclusions	41
3	Utilizing Big Data for Batch Process Modeling and Control	42
3.1	Introduction	43
3.2	Preliminaries	47
3.2.1	Seeded Batch Crystallizer: Modeling and Dynamics	47
3.3	Handling data variety in modeling and control of batch processes	50
3.3.1	Model identification	51
3.3.2	Predictive control of volume of fines in batch particulate processes	59
3.3.3	Predictive control of shape of the particle size distribution	65
3.4	Conclusions	67
4	Subspace-Based Model Identification of a Hydrogen Plant Startup Dynamics	69

4.1	Introduction	70
4.2	Preliminaries	73
4.2.1	Process Description	73
4.2.2	Subspace Identification	76
4.3	Detailed First Principles Model Development	78
4.4	Identification of State-Space Model	80
4.4.1	Illustrative Simulations for Batch Subspace Identification Methodology	85
4.4.2	Model Identification & Validation for Simulated Data	90
4.4.3	Model Identification & Validation for Plant Data	92
4.5	Conclusion	95
5	Model Predictive Control of Uni-Axial Rotational Molding Process	96
5.1	Introduction	97
5.2	Preliminaries	100
5.2.1	Rotational Molding Process	100
5.2.2	Subspace Identification for Batch Processes	106
5.3	Data Driven Modeling and Control of a Rotational Molding Process .	110
5.3.1	Model Identification	110
5.3.2	Predictive Control Of Rotational Molding Process	114
5.3.3	Closed-Loop Experimental Results	119
5.4	Conclusions	127
6	Conclusions and Future Work	128
6.1	Conclusions	128

6.2	Future Work	130
-----	-----------------------	-----

List of Tables

2.2	Parameter values for the seeded batch cooling crystallizer of Eqs.2.1–2.3. [63]	13
2.3	Training database summary	26
2.4	MASE for validation batch using proposed approach (Figure 2.3) and conventional subspace identification (Figure 2.4).	27
2.5	Comparison of control strategies for 50 batches	37
2.6	Comparison of control strategies for 50 batches in presence of time varying parameters	40
3.7	Parameter values for the seeded batch cooling crystallizer of Eqs.3.32–3.34. [63, 24]	49
3.8	PI controller parameters	52
3.9	Comparison of control strategies for 25 batches	63
3.10	Control results for 25 batches	67
4.11	MASE for validation results in Figure 4.19	90
4.12	MASE for validation results in Figure 4.21 for predictions starting from 50th sampling instant onwards	93
5.13	Variables for the rotational molding process	106

5.14	Quality measurements for training batches, arranged in the increasing order of the MPC objective function values for case 1. Further the row corresponding to the minimum value of the MPC objective function for case 2 is highlighted.	112
5.15	Case 1: Quality measurements for MPC batches	120
5.16	Case 2: Quality measurements for MPC batches	122

List of Figures

2.1	Linear cooling control: (a) Jacket temperature profile, (b) reactor temperature profile, (c) reactor concentration profile and (d) the evolution of crystal size distribution.	14
2.2	Nominal seed distribution	25
2.3	Validation results for identification: (a) Reactor temperature, (b) Reactor concentration, (c) Saturation concentration, (d) Metastable concentration, (e) μ_1 , (f) μ_2 , (g) μ_3 , (h) μ_3^n , and (i) μ_3^s	28
2.4	Validation results for identification using conventional subspace identification: (a) Reactor temperature, (b) Reactor concentration, (c) Saturation concentration, (d) Metastable concentration, (e) μ_1 , (f) μ_2 , (g) μ_3 , (h) μ_3^n , and (i) μ_3^s	29
2.5	Distribution of μ_3^n for process under (a) Linear cooling, (b) PI and (c) MPC.	37
2.6	Results corresponding to best MPC batch scenario: (a) Input profiles, (b) Reactor temperature, (c) Reactor concentration and (d) Final CSD.	38

2.7	Results corresponding to best MPC batch scenario in presence of time varying parameters: (a) Input profiles, (b) Reactor temperature, (c) Reactor concentration and (d) Final CSD.	40
3.8	Validation results for identification: (a) Reactor temperature, (b) Reactor concentration, (c) Saturation concentration, (d) Metastable concentration, (e) n_1 , (f) n_{100} , (g) n_{200} , (h) n_{300} , (i) n_{400} , (j) n_{500} , (k) n_{600} , (l) n_{700} , (m) n_{800} , (n) n_{900} and (o) n_{1000}	57
3.9	Quality model prediction of the CSD at batch termination based on predicted terminal state estimates from 15 minutes onward.	58
3.10	Distribution of μ_3^n for process under Linear cooling, PI and MPC.	64
3.11	Results corresponding to MPC batch with lowest achieved μ_3^n : (a) Input profiles, (b) Reactor temperature, (c) Reactor concentration and (d) Final CSD.	64
3.12	Terminal PSD for the best and worst case scenario	68
4.13	A schematic of the hydrogen production process	75
4.14	Simulated startup: Manipulated variables profile	79
4.15	Simulated startup: Output variables profile	79
4.16	A Luenberger observer (red) is used to estimate the initial condition of the identified state space model till 20th, 60th and 80th sampling instant and then the identified model predictions are shown by blue dashed lines, green dotted lines and brown circles respectively. Black lines denote the plant output. The simulation illustrates the the prediction error goes down as the updated state estimate is used.	87
4.17	Residual plot from 20th, 60th and 80th sampling instants onward	87

4.18	Manipulated variables for the validation batch	89
4.19	Validation results	90
4.20	Input profiles for the validation startup batch from plant	92
4.21	Output profiles prediction for plant data, with open loop prediction starting from 50 (dotted lines) and 180 (solid blue line) sampling instance. The red dashed line shows outputs from the Luenberger observer.	92
5.22	Experimental setup for rotational molding	101
5.23	Finished product	103
5.24	Molded product with two ultrasonic transducers affixed to the top of one of the cubic surfaces using high vacuum grease for non-destructive (ultrasonic) testing	105
5.25	Mold internal temperatures for training batches	114
5.26	Case 1: Comparison of MPC objective function values between training and MPC batches	120
5.27	Mold internal temperatures for MPC batches	121
5.28	Case 2: Comparison of MPC objective function values between training and MPC batches	123
5.29	Case 2: Mold internal temperatures for MPC batches	124
5.30	MPC control signals (after switching from PI controller) for one candidate batch from the two cases for (a) heater 1, (b) heater 2 and (b) compressed air supply.	124
5.31	Case 1: Scatter plot for the quality values obtained in the training (red circles) and MPC batches (blue circles).	125

5.32 Case 2: Scatter plot for the quality values obtained in the training
(red circles) and MPC batches (blue circles). 126

List of abbreviations and symbols

Abbreviations

CSD	Crystal size distribution
CVA	Canonical variate analysis
EM	Expectation maximization
LTI	Linear time invariant
LTV	Linear time varying
MASE	Mean absolute scaled error
MHE	Moving horizon estimator
MLE	Maximum likelihood estimation
MOESP	Multivariable output error state space algorithm
MPC	Model predictive control
MWD	Molecular weight distribution
N4SID	Numerical algorithms for subspace state space system identification
NG	Natural gas
OPS	Operating procedure synthesis
P&ID	Piping and instrumentation diagram
PBE	Population balance equations

PCA	Principle component analysis
PE	Polyethylene
PEM	Prediction error minimization
PI	Proportional integral
PID	Proportional integral derivative
PLS	Partial least squares
PRBS	Pseudo random binary signal
PSA	Pressure swing adsorber
PSD	Particle size distribution
RET	Reformer exit temperature
RM	Rotational molding
SMR	Steam methane reforming
SOP	Standard operating procedure
SSE	Sum squared error
SVD	Singular value decomposition

Mathematical Nomenclature

$n(r, t)$	Crystal size distribution
C	Concentration / Cross time constant
T	Reactor Temperature
ρ	Density of crystals
k_v	Volumetric shape factor
U	Overall heat-transfer coefficient
A	Total heat-transfer surface area
M	Mass of solvent
T_j	Jacket temperature
ΔH	Heat of reaction
C_p	Heat capacity
μ_2	Second moment of PSD
$B(t)$	Nucleation rate
$G(t)$	Growth rate
E_b	Nucleation activation energy
E_g	Growth activation energy
b	Exponent relating nucleation rate to supersaturation
g	Exponent relating growth rate to supersaturation
C_s	Saturation concentration
C_m	Metastable concentration
μ_3	Third moment of PSD
t_f	Final time (in a batch)
A	State space model matrix
B	State space model matrix

C	State space model matrix
D	State space model matrix
\mathbf{x}_k	State of the process at time k
\mathbf{y}_k	Process outputs at time k
\mathbf{u}_k	Process inputs at time k
L	Luenberger observer gain
K_c	Controller gain
T_i	Reset time
l	Sampling instant
Q	Quality variable
η_0	Zero-shear viscosity parameter
η_∞	Infinity-shear viscosity parameter
m	Cross rate constant
$\dot{\gamma}$	shear rate constant

Declaration

I, Abhinav Garg, hereby declare that this thesis is entirely the product of my independent work under the guidance of my supervisor, Prof. Prashant Mhaskar with exceptions to the collaborative work as discussed in the Preface.

Chapter 1

Introduction

1.1 Batch Process Control

Batch processes are an indispensable constituent of chemical process industries and are universally used for manufacturing of high-quality products. The preeminent reason for their popularity can be attributed to their flexibility to control different grades of products by changing the initial conditions and input trajectories. However, a batch process is characterized by absence of equilibrium conditions and a highly nonlinear and time-varying dynamics, which make the classical approaches (for continuous processes) not directly applicable.

Typically, a batch process consists of the following main steps.

1. Reactor is charged with ingredients following some pre-defined recipe.
2. A transforming process is carried out over a finite duration of time.
3. Finally, the process is terminated upon meeting some predefined criterion.

Apart from conventional batch processes, start-ups and shutdowns in continuous plants also mimic batch behavior and are termed as batch-like processes in this work. A fundamental objective in a typical batch process is to achieve the final product quality specifications. The measurements related to the terminal quality are usually not available during the batch operation and can only be accessed at the end of batch operation. Thus, it is not feasible to directly measure/control the quality of the product during the operation and can be achieved indirectly via trajectory tracking approach.

Traditionally, simple open loop policy have been used to control batch processes where the idea is to implement the same time-indexed input-trajectory from a previous successful batch [7]. The underlying assumption in this approach is that implementing the same, previously successful, input trajectory will lead to similar product quality. Although these approaches are simple to implement and do not require any knowledge of the process model or online measurements, they are incapable of rejecting disturbances and batch to batch variations due to absence of feedback. A significant body of literature (see [44] for overview) is also dedicated to develop control strategies to mitigate batch to batch variations such as iterative learning control (ILC). The basic idea in these approaches is that it utilizes the information from previous batches to update control policies in the subsequent batches.

A common closed-loop control approach that then emerged is trajectory-tracking, where a pre-defined measured variable is tracked using a PI/PID controller. It is assumed in this approach that if the pre-defined trajectory, usually from past successful batches, is tightly followed, the desired product quality will

be achieved. However, even with perfect tracking, the desired product may not be obtained as the process dynamics may change significantly due to variability in the feedstock properties, process disturbances etc. Another limitation of this approach is that it does not allow altering the batch duration as they are inherently time-indexed.

Therefore, advanced control strategies such as model predictive control utilize a model of the process to overcome limitations mentioned before by predicting the batch process behavior to make decisions. Thus, building an accurate model of the process (first principles or data-driven) is an integral component of advanced control design [63, 6, 4, 3, 9, 8]. However, a high fidelity model of large-scale batch processes have limited applicability in practice due to modeling and computational challenges. Further, with an exponential increase in the availability of historical process data, data-driven approaches provide a more natural alternative.

Among data-driven approaches for modeling of batch processes, latent variable based methods have been widely used over past few decades in various applications [16, 40, 39, 17, 28, 29]. However, the limiting factor in these approaches have been the use of alignment variable to align batches with different batch lengths, which is a natural characteristic of batch processes. Recently, subspace identification algorithm was adapted for batch processes that does not require alignment of batch lengths due to its dependence on 'state' of the process rather than 'time' [11]. The paper compared their approach with the more established latent variable method for a simulated lumped parameter process. The results obtained looked promising enough to pursue and develop

it further to meet the requirements of industry 4.0. In summary, there exists a lack of results for model development using subspace identification techniques that demonstrate their ability to handle infinite dimensional processes, optimize startup operation and duration, and their implementation for closed-loop control on real (experimental or industrial) systems.

1.1.1 Thesis Outline

Considering the challenges in batch and batch-like processes as described above, this thesis demonstrate the novel subspace identification based modeling and control approach for these processes. The applications considered include several industrially relevant processes namely, seeded batch crystallization, hydrogen plant startup and rotational molding process. The rest of the thesis is organized as follows.

In Chapter 2, the problem of subspace based model identification and predictive control of particulate process subject to uncertainty and time varying parameters is considered. A linear model predictive controller (MPC) formulation is shown to achieve a particle size distribution with desired characteristics subject to both manipulated input and product quality constraints in comparison to traditional control practices.

In Chapter 3, a novel batch subspace identification model based predictive controller with explicit model validity constraint, capable of handling data variety, for batch particulate processes is proposed. The batch subspace identification method was adapted to handle data variety using a combination of a dynamic and static final CSD model, which is subsequently deployed within MPC. The

effectiveness of the proposed approach in terms of improved product quality are demonstrated through two different formulations.

In Chapter 4, the problem of determining a data-driven model for the startup of a hydrogen production unit is considered. To validate our approach, first a high fidelity model of the hydrogen plant capable of simulating startup and shutdown phase is developed in UniSim. Additionally, a simulated case study is presented to demonstrate the suitability of linear models in approximating nonlinear dynamics. The proposed approach is then demonstrated on both simulated and real plant data.

In Chapter 5, a novel data-driven model predictive controller for uni-axial rotational molding process is proposed. Batch subspace identification algorithm is used to identify a linear time-invariant state-space model of the process. The identified model is then deployed within MPC to achieve a desired quality of the mold. The results show the merits of the proposed approach in terms of improved quality, variability rejection across difference batches and the ability to achieve the specified grade of product.

Finally in Chapter 6, concluding remarks are made along with directions for future work.

Chapter 2

Subspace Identification Based Modeling and Control of Batch Particulate Processes

The results of this chapter have been published as:

JOURNAL PUBLICATIONS:

- A. Garg and P. Mhaskar. Subspace Identification-Based Modeling and Control of Batch Particulate Processes. *Industrial & Engineering Chemistry Research*, 56(26):7491–7502, jul 2017

REFEREED CONFERENCE PROCEEDINGS:

- A. Garg and P. Mhaskar. Subspace identification and predictive control of batch particulate processes. In *2017 American Control Conference (ACC)*, pages 505–510. IEEE, may 2017

2.1 Introduction

Particulates production has undergone phenomenal growth in the past few decades. They are used for manufacturing of numerous high-value industrial products such as crystals, polymers etc. The products are often manufactured using batch processes to provide the flexibility of achieving different products by changing recipes. The physio-chemical and mechanical properties of the end product are known to be linked to the particle size distribution (PSD). For instance, in case of emulsion polymerization, PSD strongly impacts the polymers' rheology (viscosity), adhesion, drying characteristics etc.[35] In addition to PSD, certain product qualities are also impacted by variables such as solids content [35] or molecular weight distribution (MWD).[2]

Traditional approach for control of batch processes (particulates or otherwise) have been to use open loop, recipe based policy. In this approach, a predefined input trajectory is applied to each batch.[7] The approach assumes that the desired product characteristics (often quantified via more than one measures) can be obtained by repeating historically successful input profiles. Although these approaches are easy to implement and do not require a model for the process, they are incapable of rejecting disturbances that affect the process. This has motivated the use of feedback control strategies.

A classical closed loop control approach in batch process is trajectory tracking. In this approach, one of the important (and measured) process variables is first selected. The trajectory of the said variable (obtained from past successful batches) is then tracked using proportional integral or other controllers, with the assumption that tracking the desired trajectory of one of the measured variables

will also lead to acceptable trajectories of the other important variables. When implementing trajectory tracking approaches (with PI or otherwise) even with perfect tracking, the relationship between the tracked variable and other important variables may change significantly with changes in the process conditions, thus possibly leading to off-spec product.

These challenges are addressed by control strategies that can readily handle the multivariable nature of the problem. One such approach, model predictive control (MPC), has increasingly been studied for the control of batch processes [63, 6, 4, 3, 9, 8]. The reasons for popularity of these control schemes is two fold: first, the feedback controller can counter the model uncertainty that are associated with model simplifications and measurement errors, the other being their ability to handle the ever present input/output constraints. In implementing these formulations, where possible, good first principles models are utilized due to the ability to predict process behavior beyond the data set used to estimate the model parameters [60, 47]. The model development and parameter estimation problem for first principles models is non-trivial. Given the even increasing sensing capabilities, large amounts of data is often available that can potentially be utilized for building a data driven model. In this manuscript, we will focus on a modeling and control approach that exploits the increased data availability without requiring the development of a first principles models, and therefore will not compare our results to scenarios where a first principles model is available.

The increasing availability of data has motivated the use of simpler, often linear, models derived from past batches database. A variety of approaches for development of data-driven models have been proposed. One of the most

celebrated and widely used approach is partial least squares (PLS), which models the process in a projected latent space. [16, 40, 39, 17, 28, 29] These models are essentially time-varying linear models, linearized around mean past trajectories, and therefore require the batches to be of same length, or to recognize an appropriate alignment variable. An alternate latent variable method was also presented [18, 74] which was based on using PCA with missing data formulation. This approach does not require the batches to be of uniform lengths for computation of the PCA model, but uses missing data imputation to compute the control trajectory (thus intrinsically tries to implement the same 'kind' of control action as seen in past batches, thus partly attempting to replicate the control law in use in the training batches). A multi-model approach to handle unequal batch lengths was recently proposed. [3] These developments were followed by contributions in the area of integration of these data-driven models with model predictive control formulations. [4, 3, 10] More recently a subspace identification based batch control approach was proposed [11], where a LTI state-space model of the batch process is identified.

The existing data-driven control formulations have, however, dealt generally with lumped parameter systems and the applications of data-driven approaches for PBE systems have been limited. Some variation of PLS approach have been proposed for distributed parameter processes. In one approach, [14] a PLS model is used in conjunction with the predictions obtained from PBEs for batch to batch optimization. In another result [52], a similar strategy is presented where only a PLS model is used for predicting the final PSD. As with other latent variable approaches, a limitation with the use of PLS models for batch processes is the

need to align the batch lengths. In summary, there exists a lack of results for data driven subspace modeling of batch particulate process that can readily handle non-uniform batch durations at the modeling and control stage.

Motivated by these considerations, this manuscript presents a subspace identification based modeling and control approach for batch particulate processes. The rest of the paper is organized as follows: Section 2.2 presents a seeded batch crystallizer as a motivating example, followed by an overview of subspace identification methods. Section 2.3.1 presents the subspace identification approach for batch particulate processes that does not require the training batches to be of uniform length. Section 2.3.2 presents the validation approach, and clarifies the necessity of an appropriate state estimator. The proposed model predictive control formulation is then presented in Section 2.3.3. In Section 2.4, an application of the proposed approach to the seeded batch crystallization example is presented with robustness evaluation in presence of time varying parameters discussed in Section 2.5. Finally, concluding remarks are made in Section 2.6.

2.2 Preliminaries

For a particulate process, the state of the system includes the particle size distribution (PSD), and the writing of appropriate balances results in so called population balance equations (PBEs) based first principles models for such processes. These PBEs describe the time evolution of properties of particulate entities such as particles, droplets etc, when interacting with each other and/or with their environment (usually continuous phase), and result in a set of equation comprising partial and ordinary non-linear integro-differential equations.

For the purpose of control, a number of studies have taken the approach of developing a first principles model based on these principles, estimating parameters (typically of a reduced order model), and using it for closed-loop control [60, 47]. For instances where the development of such a model is possible, it is expected that a good first principles based model will have better predictive ability, and thus better control performance. The focus in the present manuscript is on scenarios where the model is required to be identified from past data, without first developing the governing balances.

2.2.1 Motivating Example: A Seeded Batch Crystallizer

In this section, we briefly describe the simulation test bed. To this end, consider the seeded batch cooling crystallizer [60, 63], used in the manufacturing of potassium sulfate crystals. A first principle model describing the evolution of the crystal size distribution, $n(r, t)$, under the joint effects of nucleation and crystal growth yields two ordinary differential equations describing the evolution of the solute concentration, C , and reactor temperature, T and a partial differential equation of the following form:

$$\begin{aligned} \frac{\partial n(r, t)}{\partial t} + G(t) \frac{\partial n(r, t)}{\partial r} &= 0, \quad n(0, t) = \frac{B(t)}{G(t)} \\ \frac{dC}{dt} &= -3\rho k_v G(t) \mu_2(t) \\ \frac{dT}{dt} &= -\frac{UA}{MC_p} (T - T_j) - \frac{\Delta H}{C_p} 3\rho k_v G(t) \mu_2(t) \end{aligned} \quad (2.1)$$

where ρ is the density of crystals, k_v is the volumetric shape factor, U is the

overall heat-transfer coefficient, A is the total heat-transfer surface area, M is the mass of solvent in the crystallizer, T_j is the jacket temperature, ΔH is the heat of reaction, C_p is the heat capacity of the solution, and μ_2 is the second moment of the PSD given by

$$\mu_2 = \int_0^{\infty} r^2 n(r, t) dr \quad (2.2)$$

The nucleation rate, $B(t)$, and the growth rate, $G(t)$, are given by

$$\begin{aligned} B(t) &= k_b e^{-E_b/RT} \left(\frac{C - C_s(T)}{C_s(T)} \right)^b \mu_3, \\ G(t) &= k_g e^{-E_g/RT} \left(\frac{C - C_s(T)}{C_s(T)} \right)^g \end{aligned} \quad (2.3)$$

where E_b is the nucleation activation energy, E_g is the growth activation energy, b and g are exponents relating nucleation rate and growth rate to supersaturation, C_s is the saturation concentration of the solute (Equation 2.5), and μ_3 is the third moment of the PSD given by

$$\mu_3 = \int_0^{\infty} r^3 n(r, t) dr \quad (2.4)$$

Equation 2.5 defines the saturation and metastable concentrations corresponding to the solution temperature T . The solution concentration is required to be between these two concentrations, i.e., $C_s \leq C \leq C_m$ must hold during the whole batch run.

$$\begin{aligned}
 C_s(T) &= 6.29 \times 10^{-2} + 2.46 \times 10^{-3}T - 7.14 \times 10^{-6}T^2 \\
 C_m(T) &= 7.76 \times 10^{-2} + 2.46 \times 10^{-3}T - 8.10 \times 10^{-6}T^2
 \end{aligned}
 \tag{2.5}$$

Values of the process parameters are given in Table 2.2. To generate data from this virtual test bed, a second-order accurate finite difference method with 1000 discretization points is used. Figure 2.1 shows the evolution of the reactor temperature, T , the solution concentration, C , and the PSD under a linear cooling strategy, where the jacket temperature, T_j is cooled down linearly from 50°C to 30°C (see Figure 2.1(a)).

Table 2.2: Parameter values for the seeded batch cooling crystallizer of Eqs.2.1–2.3. [63]

Parameter	Value	Unit	Parameter	Value	Unit
b	1.45		g	1.5	
k_b	285.0	$1/(s \mu m^3)$	k_g	1.44×10^8	$\mu m/s$
E_b/R	7517.0	K	E_g/R	4859.0	K
ΔH	44.5	kJ/kg	C_p	3.8	$kJ/K \cdot kg$
M	27.0	kg	ρ	2.66×10^{-12}	$g/\mu m^3$
k_v	1.5		t_f	30	min
$T(0)$	50	$^\circ C$	$C(0)$.1742	g/g
UA	0.8	$kJ \cdot s \cdot K$			

Fines, or small crystals often formed by nucleation, pose difficulties in downstream processing equipment and affect product quality and process economics. This issue becomes more pronounced in case of a seeded batch crystallizer as the final products primarily grow from the seeds rather than from crystals formed by nucleation. Another downside of excessive fines is that it may require longer batch run time to achieve the desired crystal size distribution.

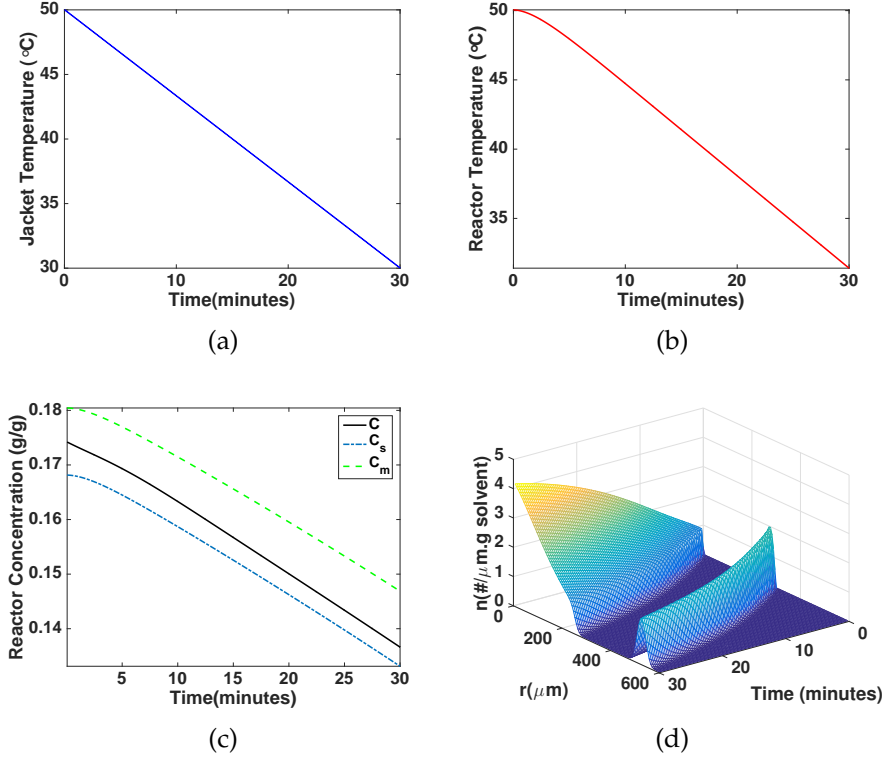


Figure 2.1: Linear cooling control: (a) Jacket temperature profile, (b) reactor temperature profile, (c) reactor concentration profile and (d) the evolution of crystal size distribution.

For the present application, crystals smaller than $300\mu m$ (denoted by r_g) are recognized as fines. From a crystal size distribution, one can therefore compute two moments corresponding to fines, and desired crystals, respectively. To be precise, the i th moments can be defined as,

$$\begin{aligned}\mu_i^n &= \int_0^{r_g} r^i n(r, t) dr \\ \mu_i^s &= \int_{r_g}^{\infty} r^i n(r, t) dr, \quad i = 0, 1, 2, 3.\end{aligned}\tag{2.6}$$

where the superscript, n , stands for nucleation, and s stands for seed. It

should be noted here that although in the present study the two modes happen to be distinct (non-overlapping) for the training batches, the proposed approach holds for processes with possibly overlapping modes. In essence, $\mu_3^n[t_f]$ and $\mu_3^s[t_f]$ quantify the total volume of fines (undesired) and the volume of crystals grown from seeds (desired) at the termination of the batch (denoted by time t_f) respectively. The control objective, therefore, is to minimize the volume of fines in the final product along with achieving a desired crystal growth while respecting constraints on the manipulated input, and concentration. Next, an overview of subspace identification based data-driven modeling method is presented.

2.2.2 Subspace Identification

Classical system identification methods are a class of iterative optimization based state space model identification algorithms that minimize the prediction errors (PEM) using methods such as maximum likelihood estimation (MLE) and expectation maximization (EM) algorithm. These methods have been widely studied[46, 27, 58, 31, 72, 70] and possess well-established theoretical properties including asymptotically achieving Cramér-Rao lower bound. However, the practical implementation of these approaches may not always be straightforward due to the underlying non-convex optimization formulation. Moreover, these approaches have been developed and studied for continuous processes and are not directly applicable to data collected from multiple batches.

In contrast to classical system identification methods, a relatively newer class of methods known as subspace identification are non-iterative in nature and rely on efficient matrix factorization techniques such as (singular value decomposition)

SVD and QR factorization for their implementation. These techniques have gained popularity in the last two decades in both theory and practice. Among these methods the most prominent ones are canonical variate analysis (CVA) [43], numerical algorithms for subspace state space system identification (N4SID) [51] and multivariable output error state space algorithm (MOESP) [66]. All these methods can be interpreted as a singular value decomposition of a matrix weighted differently in each method [65]. Apart from these, several other algorithms equivalent to the standard subspace identification have been proposed based on the application requirements [45, 67] (see also [64] for an excellent overview).

The deterministic identification problem (for a continuous process) can be explained as follows: If s measurements of the input $u_k \in \mathbb{R}^m$ and the output $y_k \in \mathbb{R}^l$ are given which are generated by the unknown deterministic system of order n :

$$\mathbf{x}_{k+1}^d = \mathbf{A}\mathbf{x}_k^d + \mathbf{B}\mathbf{u}_k, \quad (2.7)$$

$$\mathbf{y}_k = \mathbf{C}\mathbf{x}_k^d + \mathbf{D}\mathbf{u}_k, \quad (2.8)$$

the task is to determine the order n of this unknown system and the system matrices $\mathbf{A} \in \mathbb{R}^{n \times n}$, $\mathbf{B} \in \mathbb{R}^{n \times m}$, $\mathbf{C} \in \mathbb{R}^{l \times n}$, $\mathbf{D} \in \mathbb{R}^{l \times m}$ (up to within a similarity transformation). There are a number of algorithms available in the literature for estimation of these unknowns. The existing results however are designed primarily for continuous operation, and typically applied to lumped parameter systems.

2.3 Proposed Modeling and Control Approach

The first step in the proposed approach is to identify a linear state-space model of the batch particulate process using past batch database and identification batches. This is achieved by adapting the subspace identification algorithm for batch processes (also adapted for an application in the context of lumped parameter systems [11]). A key step in subspace identification algorithm is the arrangement of data in Hankel matrices. In case of continuous processes, the training datasets are collected from identification experiments done around a desired steady-state condition and can readily be incorporated in the Hankel matrices for subspace identification of the model. However, in case of batch processes, a meaningful steady-state is not available around which a model can be identified. Instead, a model for transient dynamics of the process is required over entire range of the process for different initial conditions. More importantly, typically data from multiple batches is available and this nature of the data requires specific adaptation of the database, and subspace identification method for continuous process cannot be directly implemented for batch processes.

2.3.1 Model Identification

Consider the output measurements of a batch process denoted as $y^{(b)}[k]$, where k is the sampling instant since the batch initiation and b denotes the batch index. The output Hankel submatrix for a batch b is the same as a 'standard' Hankel matrix,

given by:

$$\mathbf{Y}_{1|i}^{(b)} = \begin{bmatrix} \mathbf{y}^{(b)}[1] & \mathbf{y}^{(b)}[2] & \cdots & \mathbf{y}^{(b)}[j^{(b)}] \\ \vdots & \vdots & & \vdots \\ \mathbf{y}^{(b)}[i] & \mathbf{y}^{(b)}[i+1] & \cdots & \mathbf{y}^{(b)}[i+j^{(b)}-1] \end{bmatrix} \quad \forall b = 1, \dots, nb \quad (2.9)$$

where nb is the number of batches used for identification. The use of the above Hankel matrix by itself would not enable the use of data available from multiple batches. At the same time, a naive concatenation of the data across various batches would also lead to erroneous conclusion. More specifically, such a naive concatenation would suggest that the end point of one batch is the beginning of another, which clearly is not the case. The key, therefore, is to build an appropriate Hankel-like matrix for batch processes in a way that enables use of data across batches, without (incorrectly) assuming that the end point of one batch is the beginning of another. This is achieved by horizontally concatenating the individual matrices, from each batch, to form a single pseudo-Hankel matrix for both input and output data. Thus the pseudo-Hankel matrix takes the form:

$$\mathbf{Y}_{1|i} = \begin{bmatrix} \mathbf{Y}_{1|i}^{(1)} & \mathbf{Y}_{1|i}^{(2)} & \cdots & \mathbf{Y}_{1|i}^{(nb)} \end{bmatrix} \quad (2.10)$$

Similarly, pseudo-Hankel matrices for input data are formed. This approach for handling multiple batches nicely satisfies the requirements for subspace identification. A distinctive feature of this approach is that it does not impose any constraint on the length of different batches being equal.

Construction of appropriate pseudo-Hankel matrices for input and output

enable determination of state trajectories using any of the wide variety of subspace identification algorithms available in the literature (such as the deterministic algorithm [48] used in this work). A consequence of concatenation of the Hankel matrices is that the identified state trajectories will be comprised of concatenated state estimates for each training batch. Mathematically this can be represented as:

$$\hat{\mathbf{X}}_{i+1}^{(b)} = \begin{bmatrix} \hat{\mathbf{x}}^{(b)}[i+1] & \cdots & \hat{\mathbf{x}}^{(b)}[i+j^{(b)}] \end{bmatrix} \quad \forall b = 1, \dots, nb \quad (2.11)$$

$$\hat{\mathbf{X}}_{i+1} = \begin{bmatrix} \hat{\mathbf{X}}_{i+1}^{(1)} & \hat{\mathbf{X}}_{i+1}^{(2)} & \cdots & \hat{\mathbf{X}}_{i+1}^{(nb)} \end{bmatrix} \quad (2.12)$$

where nb is the total number of batches used for identification. Once this state trajectory matrix is obtained, the system matrices can be estimated easily using methods like ordinary least squares as shown below:

$$\mathbf{Y}_{reg}^{(b)} = \begin{bmatrix} \hat{\mathbf{x}}^{(b)}[i+2] & \cdots & \hat{\mathbf{x}}^{(b)}[i+j^{(b)}] \\ \mathbf{y}^{(b)}[i+1] & \cdots & \mathbf{y}^{(b)}[i+j^{(b)}-1] \end{bmatrix} \quad (2.13)$$

$$\mathbf{X}_{reg}^{(b)} = \begin{bmatrix} \hat{\mathbf{x}}^{(b)}[i+1] & \cdots & \hat{\mathbf{x}}^{(b)}[i+j^{(b)}-1] \\ \mathbf{u}^{(b)}[i+1] & \cdots & \mathbf{u}^{(b)}[i+j^{(b)}-1] \end{bmatrix} \quad (2.14)$$

$$\begin{bmatrix} \mathbf{Y}_{reg}^{(1)} & \cdots & \mathbf{Y}_{reg}^{(nb)} \end{bmatrix} = \begin{bmatrix} \mathbf{A} & \mathbf{B} \\ \mathbf{C} & \mathbf{D} \end{bmatrix} \begin{bmatrix} \mathbf{X}_{reg}^{(1)} & \cdots & \mathbf{X}_{reg}^{(nb)} \end{bmatrix} \quad (2.15)$$

Thus, \mathbf{A} , \mathbf{B} , \mathbf{C} and \mathbf{D} are the desired state-space model matrices.

Remark 2.1. It is important to recognize that the subspace identification problem using data from multiple batches is qualitatively different from the existing subspace identification applications. The formation of the pseudo-Hankel

matrices is critical in explicitly dealing with the batch nature of the problem, and in ensuring that consistent state estimates are obtained for data from multiple batches. In particular, let us consider the scenario where the traditional subspace identification approaches are used and for each batch, a corresponding state trajectory is independently obtained, and then a least squares problem is solved to determine the system matrices. The inherent problem with such an approach would be that when state estimates are obtained for a particular batch, they are on a certain basis, and this basis may be different for each batch. Thus, when state trajectories from different batches are used to determine a common system dynamics, it will inevitably lead to a mismatch. In contrast, in the proposed method, formation of the pseudo-Hankel matrix and determination of the state trajectories for each batch *by solving a single problem* leads to the state trajectories being identified on the same basis. Thus when the system dynamics are finally determined, they are consistent across data obtained from the multiple batches.

2.3.2 Model Validation

A model which captures the dynamics of the process reasonably well can be incorporated in a predictive control framework to achieve desired product specifications. This constitutes the second step of the approach. Good model predictions (using state-space models) are dictated primarily by two components: initial state estimate and the system matrices. A good estimate of the system matrices from the training data are obtained utilizing the subspace identification algorithm, which also involves determining the initial state of the system for each batch (based on the entire batch behavior). When implementing such an

approach online (i.e., for a new batch), the batch data is unavailable when a new batch starts, and thus the application of this approach *can not be done* without using an appropriate state estimation technique. Just as importantly, model validation should not be done using the estimator throughout the batch duration. To judge the ability of the identified model to predict the dynamic behavior, the state estimator should be taken out of the loop after the outputs have converged. Beyond that point, the identified model should be utilized to predict the variable trajectory for the rest of the batch, and compared with the observed values. Herein lies the utility of the identified model in determining the appropriate control trajectory for the remaining batch duration, starting from some time into the batch.

To quantify the prediction errors in the validation, once the model predictions are obtained, mean absolute scaled error (MASE)[34] is computed for all the variables. MASE can be computed using the following expression.

$$\text{MASE} = \frac{\sum_{t=1}^{t_p} |e_t|}{\frac{t_p}{t_p-1} \sum_{t=2}^{t_p} |Y_t - Y_{t-1}|} \quad (2.16)$$

where, e_t is the prediction error and Y_t is the measured value of a variable at any sampling instant t . t_p denotes the prediction horizon over which MASE is being evaluated.

In the present work, a Luenberger observer is used to illustrate the results. However, the method is not restricted to this choice of estimator/observer. Any other estimator, such as Kalman filter, or moving horizon estimator (MHE) can be readily used. Thus, to validate the model, for the initial part of the batch, a standard Luenberger observer of the following form is used to determine good

estimates of the states (based on convergence of the measured output):

$$\hat{\mathbf{x}}[k + 1] = \mathbf{A}\hat{\mathbf{x}}[k] + \mathbf{B}\mathbf{u}[k] + \mathbf{L}(\mathbf{y}[k] - \hat{\mathbf{y}}[k]) \quad (2.17)$$

where \mathbf{L} is the observer gain and is design to ensure that $(\mathbf{A} - \mathbf{L}\mathbf{C})$ is stable. The poles of the observer are placed appropriately in the unit circle. The initial state estimate could be chosen as zero, or initialized at the average of states in the training data set. After the observer has converged, the identified model can be deployed for predicting the rest of the batch profile (for a candidate input profile) both for the purpose of validation, and ultimately for feedback control.

2.3.3 Model Predictive Controller Design

For the case of batch processes, while the structure of the controller is similar to the standard MPC design, the control objective being different from that of operating around the steady state must be adequately accounted for in the controller implementation. Thus the MPC formulation takes the following form:

$$\begin{aligned} \min_{\mathbf{u}} \quad & f(y) \\ \text{s.t.} \quad & u_{min} \leq u \leq u_{max}, \\ & \alpha[k] \leq f_2(y[k]) \leq \beta[k], \\ & f_3(y[t_f]) \geq \gamma \\ & \mathbf{x}[k + 1] = \mathbf{A}\mathbf{x}[k] + \mathbf{B}\mathbf{u}[k] \\ & \mathbf{y}[k] = \mathbf{C}\mathbf{x}[k] + \mathbf{D}\mathbf{u}[k] \end{aligned} \quad (2.18)$$

where $f(y)$ represents the objective function which, depending on the application, could be 'stage cost' or simply depend on the terminal output $y[t_f]$, u_{min} and u_{max} denote the bounds for the manipulated input. The constraint on $f_2(y[k])$ denotes the output path constraints, while the constraint on $f_3(y[t_f])$ denotes the terminal quality constraint. The optimization problem is solved based on the predictions obtained from the identified (LTI) state-space model, utilizing the current state estimate provided by the state estimator. If the constraints and objective can also be described by linear functions, utilization of the subspace model enables converting the optimization problem to a linear/quadratic program that can be readily implemented online.

Remark 2.2. The ability to represent (or reasonably approximate) the dynamics described by PBEs through a linear time-invariant (LTI) state-space model stems from two factors; the first being the ability to approximate PBE models through finite moments models, and the other is the ability to approximate nonlinear dynamics with (possibly higher order) linear time systems for a finite duration. The approximation by an LTI system is enabled by the fact that the linear representation is not obtained by discretization of a nonlinear system around some nominal operating conditions. Instead, a sufficiently high order representation is estimated to explain the dynamics of the process over a finite duration.

2.4 Applications to the Motivating Example

In this section, first the identification of a state space model for the batch crystallization process using the subspace identification method is presented. This is followed by application of the predictive control formulation along with the comparison of the results against conventional approaches.

2.4.1 Model Identification

For the purpose of model identification, historical data from 40 different batches, along with 9 identification experiments was assumed to be available (see Table 2.3 for details). In these batches, a PI controller tracked the temperature trajectory that yielded the best results under linear cooling (out of 50 batches, also used later for the purpose of comparison with PI and MPC). A saturator is used in series with the PI controller to restrict the input moves between 50°C and 30°C and the gradient within 2°C/min. The parameters of the PI controller were: controller gain, $K_c = 0.1$ and reset time, $T_i = 1$. The nominal seed is taken to be a parabolic distribution (Figure 2.2), from 250 to 300 μm , and the maximum density of initial seed distribution, which is $2/\mu m \cdot g$ solvent, occurs at 275 μm , i.e.,

$$n(r, 0) = \begin{cases} 0 & r < 250\mu m \\ 0.0032(300 - r)(r - 250) & 250\mu m \leq r \leq 300\mu m \\ 0 & r > 300\mu m \end{cases} \quad (2.19)$$

To reflect variability across batches, for each batch the initial conditions for reactor temperature, reactor concentration and seed distribution vary (randomly) with a

zero mean Gaussian distribution around their nominal initial values as shown in Table 2.2.

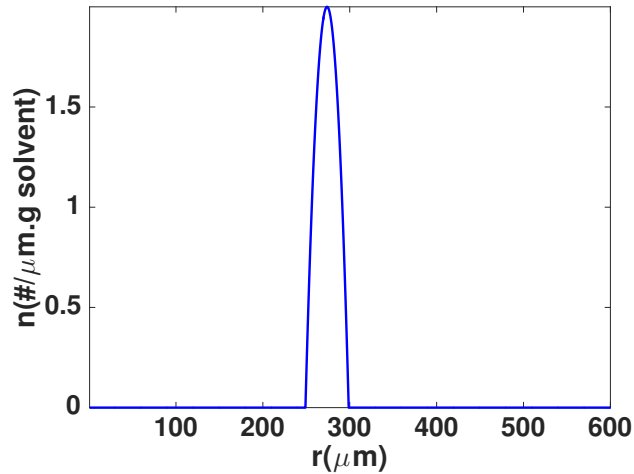


Figure 2.2: Nominal seed distribution

For the 49 simulated batches of 30 minutes duration each, measurements were collected (and feedback implemented) every ($\Delta_s =$) 3 seconds. As summarized in Table 2.3, the database consisted of PI controlled batches where in the last 9 batches, the tracking trajectory (reactor temperature) was also superimposed with a pseudo random binary signal (PRBS). The principle moments calculations are assumed to be available online through online measurements of PSD. Note that in practice, PSD measurements can be obtained using measurement techniques such as laser light scattering method. Further, the concentration and reactor temperature are also assumed to be measured in real time. The measurements of the reactor temperature, reactor concentration and crystal size distribution are corrupted by measurement noise drawn from a random Gaussian distribution with zero mean and a standard deviation of 0.001 (appropriately

scaled back to each variable by multiplying with the true value of that variable). A moving average filter, of window size 5, was implemented to filter out the measurement noise from the measurements before using them for the training and implementation of the controllers (the same filtering was utilized when implementing the classical controllers as well).

Table 2.3: Training database summary

Input policy	Number of Batches
PI trajectory tracking	40
PI trajectory tracking superimposed with PRBS	9
Total batches	49

The output vector for the crystallizer thus consists of 9 measurements, namely, reactor temperature, reactor concentration, saturation concentration, metastable concentration, μ_1 , μ_2 , μ_3 , μ_3^n and μ_3^s . The input and output data from the training batch database were used to identify a linear state-space model of the process. A parsimonious order of the system was selected based on its prediction accuracy for validation dataset. Thus, a 46th order state space model of the following form was identified:

$$\begin{aligned} \mathbf{x}[k+1] &= \mathbf{A}\mathbf{x}[k] + \mathbf{B}\mathbf{u}[k] \\ \mathbf{y}[k] &= \mathbf{C}\mathbf{x}[k] + \mathbf{D}\mathbf{u}[k] \end{aligned} \quad (2.20)$$

where $\mathbf{y} = [T \ C \ C_s \ C_m \ \mu_1 \ \mu_2 \ \mu_3 \ \mu_3^n \ \mu_3^s]'$ and $\mathbf{u} = T_j$.

Remark 2.3. In the present work, the model order is selected based on cross-validation results. In general, selecting a higher number of states reduces the error in the training data set but may result in increase of prediction errors (for

the validation data set) as the higher order of the model effectively attempts to capture the effect of the noise present in the data. Therefore, the order was chosen such that further increase in the model order did not result in any significant reduction in predictions errors in the validation data set.

To validate the identified model, 6 validation batches, different from the training batches, were assumed to be available. The validation batches were generated using PI trajectory tracking superimposed with PRBS. For validation tests on a new batch, once the observer has converged to a state estimate such that the predicted outputs match the observed outputs (this happens by 12.5 minutes for the application), the state estimate is used to predict the process output for the remainder of the batch using the remainder of the input sequence. This predicted output is compared to the measured output trajectory to gauge the quality of the estimated model. Results for one of the validation is presented in Figure 2.3 with the MASE values presented in Table 2.4. The validation results demonstrate the viability of using the developed model for feedback control within an MPC framework.

Table 2.4: MASE for validation batch using proposed approach (Figure 2.3) and conventional subspace identification (Figure 2.4).

	T	C	C_s	C_m	μ_1	μ_2	μ_3	μ_3^n	μ_3^s
Figure 2.3	0.7175	4.5885	4.5585	5.8187	2.4133	1.9012	1.7803	2.7412	2.3150
Figure 2.4	8.8×10^5	7.9×10^5	1.0×10^6	1.0×10^6	8.2×10^4	12.2	3.6	13.3	4.1

To further emphasize the merits of the proposed modeling approach, the model predictions were also obtained using the conventional subspace identification algorithm. To represent a conventional subspace identification approach, a single batch data was used for training while another batch is used for validation.

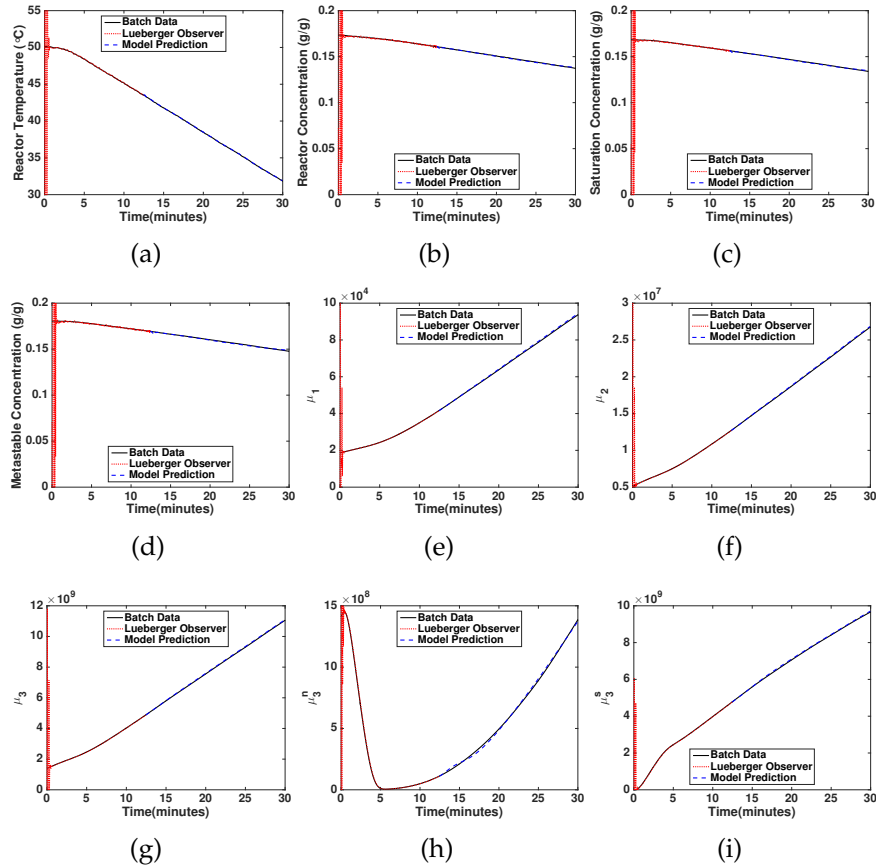


Figure 2.3: Validation results for identification: (a) Reactor temperature, (b) Reactor concentration, (c) Saturation concentration, (d) Metastable concentration, (e) μ_1 , (f) μ_2 , (g) μ_3 , (h) μ_3^n , and (i) μ_3^s .

For this the system identification toolbox in MATLAB was used to identify a deterministic state-space model using CVA algorithm. A model order of 25 was chosen (higher model order did not lead to improvements). The validation results are shown in Figure 2.4, with the MASE values presented in Table 2.4. As can be observed, the predictions obtained are overall worse. A possible reason for this is that data from a single batch may not exhibit the range of process dynamics that the process typically goes through, and thus may not be able to predict the dynamics of a new batch. This reiterates the necessity of including multiple

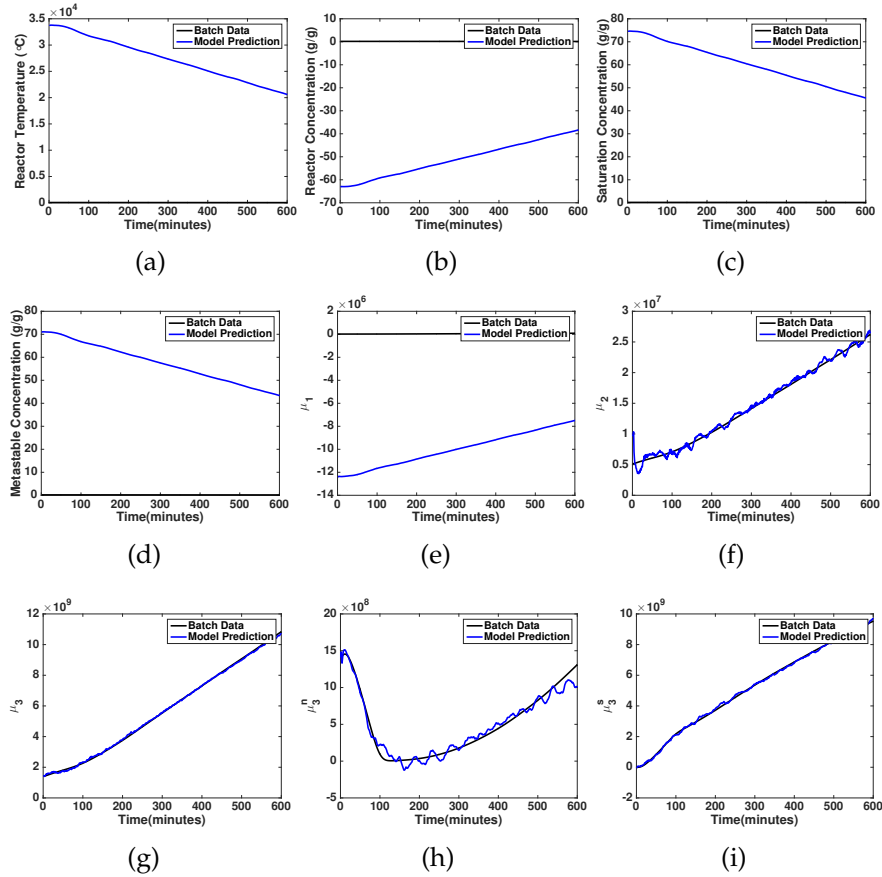


Figure 2.4: Validation results for identification using conventional subspace identification: (a) Reactor temperature, (b) Reactor concentration, (c) Saturation concentration, (d) Metastable concentration, (e) μ_1 , (f) μ_2 , (g) μ_3 , (h) μ_3^n , and (i) μ_3^s .

batches for identification of process dynamics. A naive implementation of the conventional subspace identification was also carried out (where all the batches are simply stacked one after the other, see Remark 2.1 for further discussion). This lead to even worse results and are not presented for the sake of brevity. Further comparisons with the conventional subspace identification approach are not pursued further.

Remark 2.4. Note that in the present work, online PSD measurements are assumed.

It is, in general, possible to develop models with fewer measurements, as long as the key variables of interest remain observable via the measured variables (see [11] for a demonstration). Another direction of future work will address the problem where PSD measurements are available intermittently, while the other variables are available more frequently.

2.4.2 Predictive Control Of Batch Particulate Processes

This section presents the application of the predictive controller described in Section 2.3.3. In particular, at a sampling instance l , where the current estimate of the states generated by the Luenberger observer is denoted by $\hat{\mathbf{x}}[l - 1]$, and the last control action implemented on the process is denoted by $\mathbf{u}[l]$ the optimal trajectory from the current instance to the end of the batch is computed by solving the following optimization problem:

$$\begin{aligned}
& \min_{\mathbf{U}_f} y_8[l_f - l] \\
& s.t. \quad T_{j,min} \leq u_f[k] \leq T_{j,max}, \quad \forall 0 \leq k \leq l_f - l \\
& \quad y_3[k] + \epsilon_1 \leq y_2[k] \leq y_4[k] - \epsilon_2, \quad \forall k \leq H_c \\
& \quad |u_f[0] - u[l - 1]| \leq \delta, \\
& \quad |u_f[k] - u_f[k - 1]| \leq \delta, \quad \forall 1 \leq k \leq l_f - l \\
& \quad y_9[l_f - l] \geq \gamma + \epsilon_3, \\
& \quad \mathbf{x}[0] = \hat{\mathbf{x}}[l] \\
& \quad \mathbf{x}[k + 1] = \mathbf{A}\mathbf{x}[k] + \mathbf{B}\mathbf{u}_f[k] \\
& \quad \mathbf{y}[k] = \mathbf{C}\mathbf{x}[k] + \mathbf{D}\mathbf{u}_f[k] \quad \forall 0 \leq k \leq l_f - l
\end{aligned} \tag{2.21}$$

where $\mathbf{U}_f = [\mathbf{u}_f[0], \mathbf{u}_f[1], \dots, \mathbf{u}_f[l_f - l]]$ (the remaining input profile) is the decision variable, $l_f = t_f/\Delta_s$ and y_i is the i th element of the output vector y , predicted using the identified model as discussed before. $T_{j,min}$ and $T_{j,max}$ are the constraints on the manipulated variable, u , and set to 30°C and 50°C in the simulation. y_3 and y_4 are the constraints on the solution concentration. The constant δ , chosen to be 2°C/min, is the maximum gradient of the jacket temperature. Note that this rate of change constraint is implemented in a way that ensures both that the first piece of the control action respects this constraint with respect to the last implemented control action, and that the successive control actions respect this constraint as well. γ , chosen as 8.3301×10^9 , denotes the lower bound on the total volume of the crystals growing from the seeds. This constraint on the terminal y_9 represents a desirable quality of the final product and any batch where this constraint is not met

is deemed a ‘failed’ batch. Finally, the last two equations represent the identified discrete time LTI model of the process.

To account for the plant model mismatch, tuning parameters ϵ_1 , ϵ_2 , ϵ_3 and H_c are used to tighten the constraints when implementing the predictive controller. In this work, ϵ_1 , ϵ_2 and ϵ_3 were chosen as 0.0035 g/g , 0.0035 g/g and 0.4×10^9 respectively. The saturation constraints are implemented only 25 steps ahead, and shrunk appropriately as the batch nears completion. Thus, the value of H_c is as follows:

$$H_c = \begin{cases} 25 & l_f - l \geq 25 \\ l_f - l & l_f - l < 25 \end{cases} \quad (2.22)$$

The first piece of the control action is implemented on the process, and the optimization repeated at the next sample time.

Exploiting the fact that the identified model is linear, the MPC optimization problem is formulated as a linear program as discussed below. Consider the estimated subspace state-space model in Equation 2.20. For the input sequence $\mathbf{U}_f^p = [\mathbf{u}_f[0], \mathbf{u}_f[1], \dots, \mathbf{u}_f[p]]$ and initial state as $\mathbf{x}[0]$, the output variable p time steps ahead can be written as

$$\mathbf{Y}[p] = \mathbf{CA}^p \mathbf{x}[l] + \phi_p \mathbf{U}_f^p \quad (2.23)$$

where,

$$\phi_p = \begin{bmatrix} \mathbf{CA}^{p-1}\mathbf{B} & \mathbf{CA}^{p-2}\mathbf{B} & \dots & \mathbf{CB} & \mathbf{D} \end{bmatrix} \quad (2.24)$$

The y_i th measurement, p steps ahead in the future can be written using Equations 2.23 and 2.25 as $Y_i[p] = \mathbf{L}_i \mathbf{Y}[p]$. where

$$\mathbf{L}_i \triangleq \begin{bmatrix} \mathbf{0}_{1 \times (i-1)} & 1 & \mathbf{0}_{1 \times (9-i)} \end{bmatrix} \quad \forall i = 1 \dots 9 \quad (2.25)$$

The terminal constraint on the seeded crystals in the final product can thus be written as:

$$\begin{aligned} \mathbf{L}_9 \mathbf{Y}[l_f - l] &\geq \gamma \\ \implies -\mathbf{L}_9 \phi_{l_f-l} \mathbf{U}_f^{l_f-l} &\leq -\gamma + \mathbf{L}_9 \mathbf{CA}^{l_f-l} x[0] \end{aligned} \quad (2.26)$$

Constraints on the input move is formulated as follows

$$\left| \begin{bmatrix} \mathbf{u}[l] - \mathbf{u}_f[0] \\ \mathbf{u}_f[0] - \mathbf{u}_f[1] \\ \vdots \\ \mathbf{u}_f[l_f - l - 1] - \mathbf{u}_f[l_f - l] \end{bmatrix} \right| \leq \Delta \quad (2.27)$$

$$\Rightarrow \begin{bmatrix} 1 & -1 & 0 & \cdots & 0 \\ 0 & 1 & -1 & \cdots & 0 \\ & \ddots & \ddots & \ddots & \\ 0 & \cdots & 0 & 1 & -1 \\ -1 & 1 & 0 & \cdots & 0 \\ 0 & -1 & 1 & \cdots & 0 \\ & \ddots & \ddots & \ddots & \\ 0 & \cdots & 0 & -1 & 1 \end{bmatrix} \begin{bmatrix} u[l-1] \\ \mathbf{U}_f^{l_f-l} \end{bmatrix} \leq \Delta \quad (2.28)$$

Further, the constraints on the concentration, $y_3 \leq y_2$ can be formulated as

$$\begin{bmatrix} \mathbf{L}_3 - \mathbf{L}_2 \\ \vdots \\ \mathbf{L}_3 - \mathbf{L}_2 \end{bmatrix} \circ \Pi \mathbf{U}_{(H_c-1)} \leq - \begin{bmatrix} \mathbf{L}_3 - \mathbf{L}_2 \\ \vdots \\ \mathbf{L}_3 - \mathbf{L}_2 \end{bmatrix} \circ \begin{bmatrix} \mathbf{C} \\ \mathbf{CA} \\ \vdots \\ \mathbf{CA}^{(H_c-1)} \end{bmatrix} \mathbf{x}[0] \quad (2.29)$$

where, Π is a Toeplitz matrix given by

$$\Pi = \begin{bmatrix} \mathbf{D} & \mathbf{0} & \mathbf{0} & \cdots & \mathbf{0} \\ \mathbf{CB} & \mathbf{D} & \mathbf{0} & \cdots & \mathbf{0} \\ \mathbf{CAB} & \mathbf{CB} & \mathbf{D} & \cdots & \mathbf{0} \\ & \ddots & \ddots & \ddots & \\ \mathbf{CA}^{(H_c-2)}\mathbf{B} & \cdots & \mathbf{CAB} & \mathbf{CB} & \mathbf{D} \end{bmatrix} \quad (2.30)$$

Similarly, $y_2 \leq y_4$ can be written as

$$\begin{bmatrix} \mathbf{L}_2 - \mathbf{L}_4 \\ \vdots \\ \mathbf{L}_2 - \mathbf{L}_4 \end{bmatrix} \circ \Pi \mathbf{U}_{(H_c-1)} \leq - \begin{bmatrix} \mathbf{L}_2 - \mathbf{L}_4 \\ \vdots \\ \mathbf{L}_2 - \mathbf{L}_4 \end{bmatrix} \circ \begin{bmatrix} \mathbf{C} \\ \mathbf{CA} \\ \vdots \\ \mathbf{CA}^{(H_c-1)} \end{bmatrix} \mathbf{x}[0] \quad (2.31)$$

Here, \circ denotes the Hadamard product. The transformation of the control problem into a linear problem allows fast solutions and enables real time implementation of the predictive controller.

Remark 2.5. In the proposed MPC formulation, as stated previously, the measurements fed to the MPC are first filtered with a moving horizon filter to mitigate the effects of measurement noise. The use of a filter represents standard practice, and in the present case enables a ‘fair’ comparison between the PI and the proposed MPC since both controllers are provided the same filtered measurement for feedback control. A comparison with a first principles based approach is not pursued here because, as already stated, if a good first principles model is already available, its use will naturally lead to better control performance. The comparison is thus restricted to implementations that do not require the development of a first principles model. In particular, the focus in the present manuscript is on addressing the fact that the batch processes is a particulate process (defined inherently through evolution of particle size distributions) and to demonstrate the robustness of the approach to variability.

Remark 2.6. In this work, the objective was to minimize the number of fines in the product at end of the batch. Depending on the type of batch crystallizer, the

objective can vary, and can be readily accommodated in the proposed formulation. For instance, the quality of crystals could be dependent more explicitly on the shape of the CSD. An example of a desired shape could be a requirement of narrow distribution of crystals. To handle these, the proposed model would have to be extended to capture more of the state variables and connect it with an appropriately built 'quality' model. This remains a subject of future work for distributed parameter systems.

Closed-loop Simulations Results

The subspace state-space model based linear MPC strategy, proposed in this work, is applied on 50 different batches to examine the effectiveness of the proposed approach. The method is also compared with two other classical control strategies, namely, open loop linear cooling and PI controller based trajectory tracking. It should be noted here that these batches are different from the ones used for identification with the initial conditions generated in a similar fashion.

Table 2.5 summarizes the value of μ_3^n obtained for 50 different batches under three different control strategies, i.e., open-loop with linear cooling, trajectory tracking with PI controller and a data-driven MPC with the formulation specified in Equations 2.21. Figure 2.5 compares the variability of the terminal μ_3^n achieved under different control schemes. It is evident from the results that the proposed MPC scheme lowered the volume of fines on an average by over 27% and 30% compared to PI and linear cooling strategy respectively, while satisfying the process constraints in all the batches. Further, the variability in volume of fines in the final product is least for MPC compared to other control schemes.

Figure 2.6 shows the closed loop profile for the batch for which the MPC yields the best performance. Note that when implementing MPC, the initial 10 minutes of operation is still under the PI control. During this time, the Luenberger observer estimates the current state of the process. Then the controller is switched to MPC till the end of the batch. It can be observed from Figure 2.6 that in the MPC, input trajectory deviates from the PI trajectory after 10 minutes to drive the process to the optimal product specifications.

Table 2.5: Comparison of control strategies for 50 batches

Control method	$\bar{\mu}_3^n$	$\min(\mu_3^n)$	Number of failed batches
Linear cooling	1.5446×10^9	1.2525×10^9	0
PI	1.4709×10^9	1.1863×10^9	0
MPC	1.0802×10^9	9.4983×10^8	0

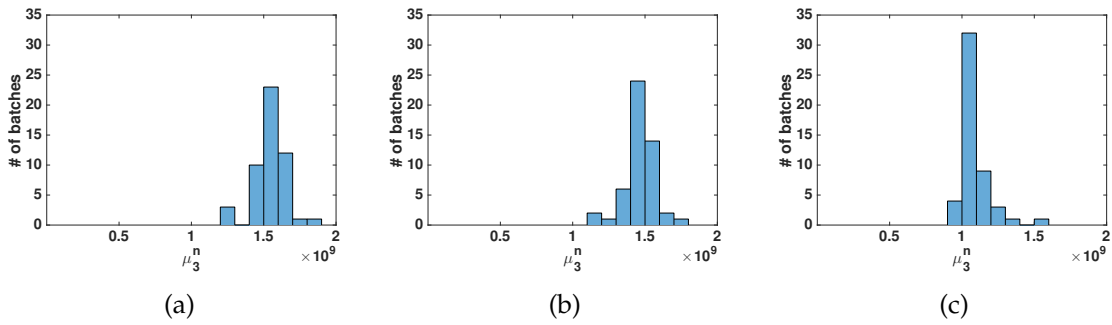


Figure 2.5: Distribution of μ_3^n for process under (a) Linear cooling, (b) PI and (c) MPC.

To further probe the efficiency of the proposed method, the control schemes are compared for the case where the constraint on the terminal μ_3^s (value of γ) is further increased by 1.5×10^9 from the previous case, to reflect the requirement of increase in the product quality. For the set of test batches 24% and 62% batches violate constraints under linear cooling and PI, respectively, and as such do not

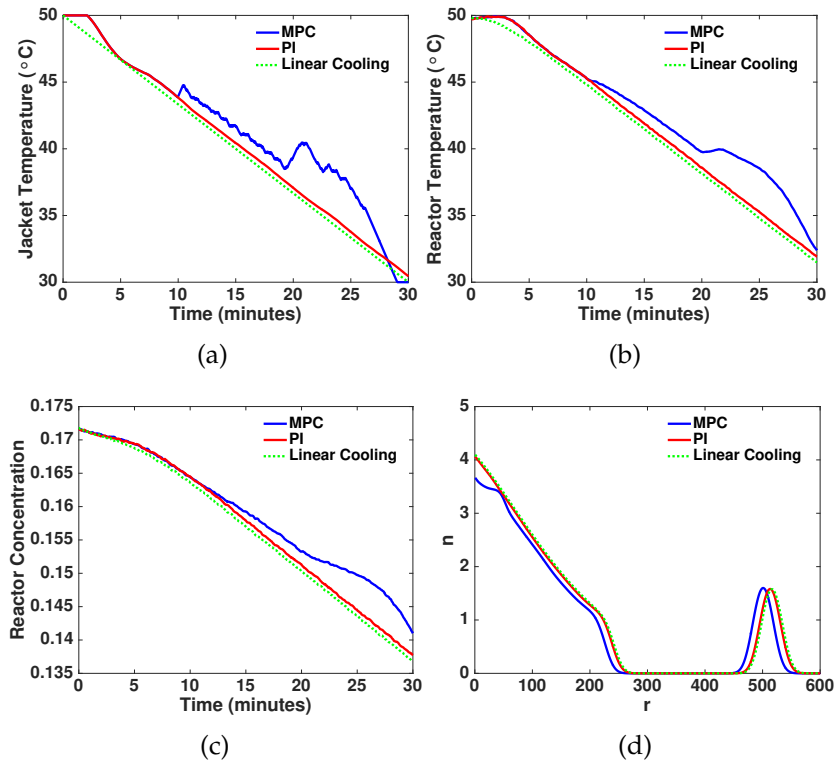


Figure 2.6: Results corresponding to best MPC batch scenario: (a) Input profiles, (b) Reactor temperature, (c) Reactor concentration and (d) Final CSD.

produce the desired product. In contrast, only 4% of the batches result in loss of product under the MPC.

2.5 Robustness Evaluation in Presence of Time Varying Parameters

To reflect process variability, the crystallization process was simulated with b varying randomly with a standard deviation of 0.001 around its nominal value, and U decreasing by 0.5% (as a consequence of fouling) in every successive batch.

2.5.1 Model Identification

The process with varying parameters was simulated for 20 batches, among which 15 batches were used for identification and rest for validation. A state-space model of order 31 was identified using subspace identification for batch as discussed before.

2.5.2 Closed-loop Results

The state-space model identified using the subspace identification was deployed within the previously explained MPC design to control 50 different batches with parameters b and U varying as before. It should be noted that none of these batches were used in the identification batches. The performance of the proposed framework, compared against PI and linear cooling methodologies, are summarized in Table 2.6. As can be noted, the proposed approach resulted in a performance improvement of 21.34% and 7.84% in comparison to PI and Linear cooling respectively. It is important to recognize that the closed-loop performance under the PI controller happens to be poorer than the one under linear cooling. This is not because of poor tuning of the PI controller. The PI controller continues to do a good job of tracking the reference trajectory. It just so happens that with the change in process dynamics due to parameter variation, tracking the same reference trajectory for the temperature ends up resulting in production of more fine particles compared to the nominal linear cooling strategy. The other key point illustrated in these simulations is not so much as to how the MPC continues to do better than the other approaches, but the fact that the MPC continues to generate on-spec product, with improved quality. The temperature and concentration

profiles along with the terminal CSD for the scenario with best MPC performance are illustrated in Figure 2.7. In summary, these results illustrate the robustness of the approach to effectively utilize the available historical batch database to efficiently control a process with varying parameters.

Table 2.6: Comparison of control strategies for 50 batches in presence of time varying parameters

Control method	$\bar{\mu}_3^n$	$\min(\mu_3^n)$	Number of failed batches
Linear cooling	1.3136×10^9	1.1695×10^9	0
PI	1.5391×10^9	1.0450×10^9	0
MPC	1.2106×10^9	8.9552×10^8	0

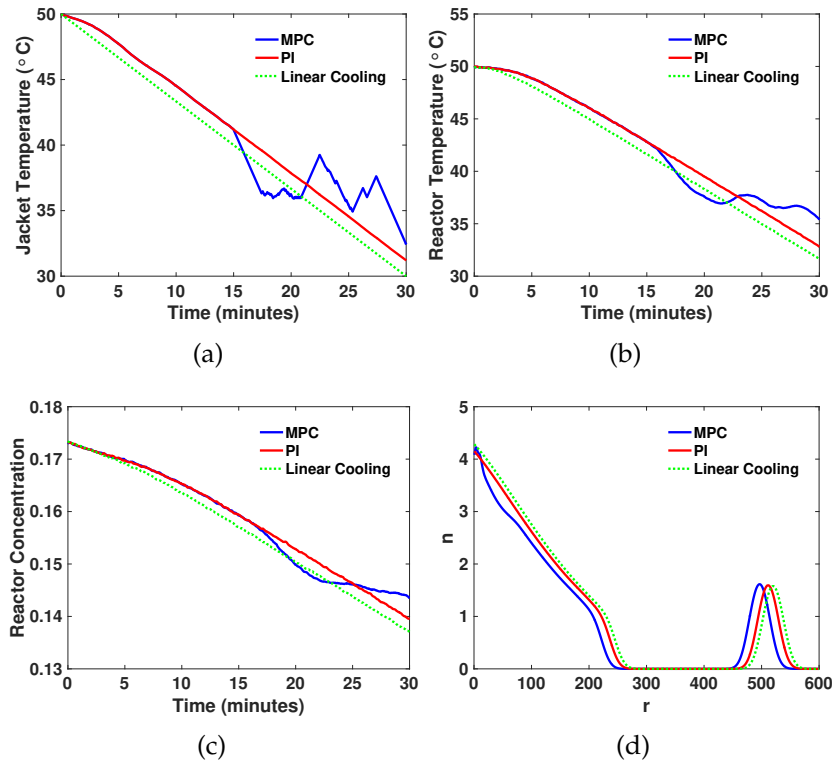


Figure 2.7: Results corresponding to best MPC batch scenario in presence of time varying parameters: (a) Input profiles, (b) Reactor temperature, (c) Reactor concentration and (d) Final CSD.

Remark 2.7. Latent variable based models that are inherently linear time varying models linearized around a mean trajectory, are another excellent tool to model and control batch processes and have found widespread applications [71, 41]. These approaches, because of the necessity to mean center the trajectories, require the identification of some alignment variable (or for the batches to be of the same length). In these approaches, nonlinearity is captured by building as many (as required) models (the time varying matrices or loadings). In the proposed method, nonlinearity is captured instead by utilizing a sufficiently higher order LTI model. A comparison of the proposed approach with the PLS based approaches [11] shows that the proposed method compares favorably to the PLS based approach. The comparison, therefore, is not repeated in the current study.

2.6 Conclusions

In this work, a novel data driven model identification and predictive control approach for particulate processes is proposed. Subspace identification method adapted to accommodate batch data structure is used to identify a linear time-invariant state-space model of the process. The identified model is then deployed within MPC to achieve a particle size distribution with desired characteristics. The simulation results show the merits of the proposed approach in terms of improved quality, the ability to achieve a different product specification and robustness to time varying process parameters.

Chapter 3

Utilizing Big Data for Batch Process Modeling and Control

The results of this chapter have been published as:

JOURNAL PUBLICATIONS:

- A. Garg and P. Mhaskar. Utilizing big data for batch process modeling and control. *Computers & Chemical Engineering*, 2018, Submitted

3.1 Introduction

In this age of digitalization, massive amount of data are generated by various sensing devices and is typically referred to as big data. It is generally characterized by 3 Vs namely, the requirements to handle large volumes, a variety of data, and data with high velocity (see, e.g., [56]). In some instances, additional parameters - establishing veracity and value, are included to characterize the challenges associated with big data. Several of these challenges (such as those related to handling large databases) are best addressed within the fields of computer science and business analytics applications. An aspect of big data that falls within the realm of process control problems is that of handling data variety and veracity.

In the context of process control, data variety would refer to availability of different types of process measurements such as temperatures and pressures data along with infrared spectroscopy, acoustic, or video/image data. The key distinction in these data types is in the structure of data. For instance, in a crystallization process, temperature and concentration measurements are collected with respect to time and is a two-dimensional dataset, however, data collected from spectroscopy (particle size distribution) is a three dimensional dataset with measurements varying both with respect to time and particle size. The challenge then lies in adapting the data-driven approaches to simultaneously handle such variety in modeling and eventually use it for control. In case the modeling approach is not able to simultaneously handle two dimensional and three dimensional measurements, alternative would be to reduce the particulate size distribution measurements (or any higher dimensional data) to two dimensional measurements [24]. Similarly, the data veracity refers to uncertainty in data which

may stem from missing / corrupt measurements in data historian, non-uniform sampled measurements etc. The scope of the present work is restricted to handling data variety with application to batch crystallization process, and we make contributions both in the areas of modeling and control.

Model development generally takes one of two paths- so called first principles modeling, where the structure of the model is given by governing equations (appropriate balances, laws of thermodynamics), or data driven model, where the structure of the model is chosen based on simplicity of model development (albeit cognizant of the ability to predict process dynamics). Both models, however have parameters that need to be identified/determined, and this can only be done via measurements. In this sense, the availability of more data (or variety of data) generally increases the ability to capture the process dynamics better and thus presents an opportunity for advanced control implementation.

The presence of variety of data (henceforth referred to as data variety), however, poses a challenge with first principles model based control. In this approach, the model complexity increases in order to capture data variety. For instance in case of a particulate process, while the temperature and concentration measurements can be described using ordinary differential equations, prediction of particle size distribution requires population balance equations. Although results exist in the literature where first principles based approach have been successfully used for control (for instance see, [63]), use of alternative, data driven approaches (also referred to as data analytics) remains attractive due to the abundance of data and the associated simplicity of model development [17, 52]. For instance, mid-course correction based control strategy for the control

particle size distribution (PSD) in an emulsion semi-batch polymerization was proposed in [16] to drive it to a desired end-point. The approach utilized the available online and offline measurements for prediction of the final PSD using partial least squares (PLS) models, and then compute the required mid-course corrections, with the 'timing' of this mid-course correction based on heuristics. In [52], another PLS modeling approach was used for predicting the final PSD. The number of states of a distributed parameter process obtained after applying the discretization based solution strategies presented earlier for the solution of PBEs are very high, often resulting in ill-conditioned and uncontrollable systems. In order to overcome this, a principle component analysis (PCA) based model order reduction method was proposed in [53]. In this approach, a linear time varying (LTV) model was obtained by transforming the original model into a reduced order model which was subsequently used in the linear MPC framework to obtain the product with a desired PSD.

Over the past several decades, data analytics in process systems engineering has gained prominence. Largely, methods have been developed and applications demonstrated for traditional data (for instance, see [18]) with limited results illustrating robust archiving (volume) aspect of the big data in batch processes [39]. Some applications of neural network or machine learning based modeling and control of batch processes (not necessarily using data variety) have been demonstrated in the literature[36, 13], however, largely machine learning based approaches have emerged for classification kind of problems such as in the area of fault detection [33, 50, 69].

Among other data-driven modeling approaches, latent variable technique is

one method that has been used widely for modeling and control of batch quality. The simplest implementation of these methods uses batch-wise unfolding strategy with each row representing the batch duration. However, unequal batch duration is problematic with this unfolding strategy and inevitably requires batch alignment [38, 39]. Therefore, as the mapping between future variable trajectories and real time domain are unclear, these approaches are more suitable for batch monitoring than control. A multi-model approach was proposed in [3] that did not require batch length alignment and utilized clustering algorithms to build the multiple models. Recently in [11], a batch quality modeling and control approach based on subspace identification was proposed that too doesn't require batches to be aligned for building the model (due to 'state' dependence instead of 'time'). While these recent results are based on building models using traditional data, they presents an opportunity to be adapted to handle the big data modeling problem.

Motivated by these considerations, this paper presents the framework to utilize big data aspects for modeling and control of batch particulate process using a dynamic subspace identification based approach coupled with a static product quality model. The key contributions of the present work are a) a dynamic and quality model to handle both two dimensional and three dimensional measurements i.e. the data variety and b) a novel MPC design with explicit model validity constraints. The rest of the paper is organized as follows: Section 3.2 presents first-principles based model and dynamics of seeded batch crystallizer. Section 3.3 outlines the proposed approach for handling data variety in the batch subspace identification framework for modeling and control of batch crystallizer. The section discusses two formulations: a) minimizing the volume of fines in the

final product by leveraging the variety of measurements and b) control of shape of the particle size distribution in the product. The former case is compared to traditional control practice while the latter's superior ability to achieve desired PSD shape is demonstrated. Finally, concluding remarks are made in Section 3.4.

3.2 Preliminaries

This section reviews a first principles model of a seeded batch crystallizer that will be used for validating the proposed big data based modeling and control approach.

3.2.1 Seeded Batch Crystallizer: Modeling and Dynamics

The manufacturing of crystals, such as potassium sulfate, is often carried out in a batch process (see [60] for a first principles model of the batch process, [63] for first principles based reduced order modeling and control and [24] for traditional data driven modeling and control implementations).

In a first principles model described in Equation (3.32), the evolution of the crystal size distribution (CSD), $n(r, t)$, is described using the population balance equation (PBE) while the evolution of reactor temperature, T and the solute concentration, C are described by two ordinary differential equations.

$$\begin{aligned} \frac{\partial n(r, t)}{\partial t} + G(t) \frac{\partial n(r, t)}{\partial r} &= 0, \quad n(0, t) = \frac{B(t)}{G(t)} \\ \frac{dT}{dt} &= -\frac{UA}{MC_p}(T - T_j) - \frac{\Delta H}{C_p} 3\rho k_v G(t) \mu_2(t) \\ \frac{dC}{dt} &= -3\rho k_v G(t) \mu_2(t) \end{aligned} \quad (3.32)$$

where ρ is the density of crystals, k_v is the volumetric shape factor, U is the overall heat-transfer coefficient, A is the total heat-transfer surface area, M is the mass of solvent in the crystallizer, T_j is the jacket temperature, ΔH is the heat of reaction, C_p is the heat capacity of the solution, and μ_2 is the second moment of the CSD given by

$$\mu_2 = \int_0^{\infty} r^2 n(r, t) dr \quad (3.33)$$

The nucleation rate, $B(t)$, and the growth rate, $G(t)$, are given by

$$\begin{aligned} B(t) &= k_b e^{-E_b/RT} \left(\frac{C - C_s(T)}{C_s(T)} \right)^b \mu_3, \\ G(t) &= k_g e^{-E_g/RT} \left(\frac{C - C_s(T)}{C_s(T)} \right)^g \end{aligned} \quad (3.34)$$

where E_b and E_g are the nucleation and the growth activation energy respectively. Further, b and g relates the nucleation and growth rate to supersaturation, C_s is the saturation concentration of the solute (Equation 3.36), and μ_3 is the third moment of the CSD given by

$$\mu_3 = \int_0^{\infty} r^3 n(r, t) dr \quad (3.35)$$

The saturation and metastable concentrations corresponding to the solution temperature T are calculated using Equation 3.36. The solution concentration is

required to be between these two concentrations during the entire batch run.

$$\begin{aligned} C_s(T) &= 6.29 \times 10^{-2} + 2.46 \times 10^{-3}T - 7.14 \times 10^{-6}T^2 \\ C_m(T) &= 7.76 \times 10^{-2} + 2.46 \times 10^{-3}T - 8.10 \times 10^{-6}T^2 \end{aligned} \quad (3.36)$$

The dynamics of the seeded batch crystallization process were simulated using a second-order accurate finite difference method with 1000 discretization points. Process parameters values used in this study are summarized in Table 3.7.

Table 3.7: Parameter values for the seeded batch cooling crystallizer of Eqs.3.32–3.34. [63, 24]

Parameter	Value	Unit	Parameter	Value	Unit
b	1.45		g	1.5	
k_b	285.0	$1/(s \mu m^3)$	k_g	1.44×10^8	$\mu m/s$
E_b/R	7517.0	K	E_g/R	4859.0	K
ΔH	44.5	kJ/kg	C_p	3.8	$kJ/K \cdot kg$
M	27.0	kg	ρ	2.66×10^{-12}	$g/\mu m^3$
k_v	1.5		t_f	30	min
$T(0)$	50	$^{\circ}C$	$C(0)$.1742	g/g
UA	0.8	$kJ \cdot s \cdot K$			

In a typical CSD for a seeded batch crystallization process, there is a significant gap between the crystals formed by nucleation and those growing from the seeds during the batch duration. The two moments models correspond to the crystals growth from seeds and nucleation [63, 24]. To be precise, the i th moments can be defined as,

$$\begin{aligned} \mu_i^n &= \int_0^{r_g} r^i n(r, t) dr \\ \mu_i^s &= \int_{r_g}^{\infty} r^i n(r, t) dr, \quad i = 0, 1, 2, 3. \end{aligned} \quad (3.37)$$

The superscripts, n and s stands for nucleation and seed respectively, with $r_g =$

$300\mu m$ being the radius defined to demarcate two groups of crystals. In other words, $\mu_3^n[t_f]$ and $\mu_3^s[t_f]$ quantifies the total volume of fines and the total volume of crystals grown from seeds at the end of the batch (denoted by time t_f).

One simple control objective is to achieve final product with minimum volume of fines along with a desired growth of crystals while respecting the constraints on manipulated input, and concentration. In more general terms, however, given the dependence of the product quality on the particle size distribution, the control objective is best formulated as one of achieving a desired particle size distribution.

3.3 Handling data variety in modeling and control of batch processes

Subspace identification methods are an alternative to the classical input-output methods and have gained prominence particularly in the last two decades. The objective is to identify a linear time-invariant (LTI) state-space model, that is estimating the system matrices along with its order (number of states). Different algorithms for subspace identification, such as canonical variate analysis (CVA) [43], numerical algorithms for subspace state space system identification (N4SID) [51] and multivariable output error state space algorithm (MOESP) [66], have been shown to fall under a unifying framework [65] with difference in the weighting matrix used for singular value decomposition (SVD) step.

Subspace identification methods are non-iterative and utilize matrix algebra to compute the unknowns (see, e.g., [64]). Specifically, they involve the use of efficient matrix factorization methods such as SVD and QR factorization for

their implementation. On the contrary, classical system identification techniques are iterative optimization based algorithms that involve minimizing prediction error (PEM) using efficient algorithms such as maximum likelihood estimation (MLE) and expectation maximization (EM). These approaches have been widely studied and possess well established theoretical properties [46, 27, 58, 72, 70]. The existing classical and subspace identification algorithms, however, are designed primarily for continuous systems and are not directly capable of handling batch data structure. Thus, modeling of batch processes using subspace identification techniques requires a recently developed batch version of the subspace identification algorithm as presented in [11, 20, 12].

In this section, first the subspace state space model identification of the batch crystallization process, adapted to accommodate the variety of measurements, is presented. This is followed by the design and application of a model predictive control (MPC) formulation where the quality is characterized through volumes of fines and crystals grown from seeds. Next, a MPC is designed and implemented that enables specification of desired particle size distribution.

3.3.1 Model identification

To identify a data-driven model, a database consisting of 30 different batches was assumed to be available in which a PI controller tracked the temperature trajectory. The input moves are restricted between 50°C and 30°C and the gradient within 2°C/min using a saturater in conjunction with the PI controller. The parameters of the PI controller are listed in Table 3.8. The nominal seed size distribution is given

below;

$$n(r, 0) = \begin{cases} 0 & r < 250\mu m \\ 0.0032(300 - r)(r - 250) & 250 \leq r \leq 300\mu m \\ 0 & r > 300\mu m \end{cases} \quad (3.38)$$

Table 3.8: PI controller parameters

Parameter	Value
Controller gain, K_c	0.1
Reset time, T_i	1

To reflect raw material and initial condition variability across different batches, the initial reactor temperature, reactant concentrations and seed size distribution were chosen from a zero mean Gaussian distribution around their nominal initial values (as given in Table 3.7 and Equation (3.38)). The variance of the Gaussian distribution was chosen as 0.01, $1e^{-6}$ and 0.0025 for temperature, concentration and seed distribution respectively.

For the purpose of model development, data is generated by running 30, half hour batches under feedback control with control implementation every ($\Delta_s =$) 3 seconds. The training data consists of 15 regular batches, and the other where a pseudo random binary signal (PRBS) was superimposed on the reactor temperature tracking trajectory.

The measurements of concentration and reactor temperature, along with the CSD (through techniques such as laser light scattering) are assumed to be available online, albeit subject to measurement noise. Thus, all the measurements include a

measurement noise drawn from a random Gaussian distribution with zero mean and a standard deviation of 0.001 (appropriately scaled for each variable). As often done in practice, the measurements are filtered before being implemented online; in the present simulations a moving average filter with window size 5 was utilized.

As mentioned before, a key step in a subspace identification algorithm is the use of SVD, which requires the input and output data to be arranged in Hankel matrices. In case of subspace identification for continuous processes, Hankel matrices consists of training data collected around a desired steady-state condition by conducting identification experiments. For batch processes, no such steady state exists, and more importantly, given the significant transient dynamics observed during a batch process, data from a single batch would not yield a model with sufficient validity. Therefore, subspace identification algorithms available for continuous processes are not directly applicable for batch processes and requires a specific adaptation of the database as discussed below.

Let $\mathbf{y}^{(b)}[k]$ denotes the output measurements of a seeded batch crystallizer, where b denotes the batch index and k is the sampling instant since the batch initiation.

The output vector for the crystallizer consists of 15 measurements as mentioned later in this section. The Hankel submatrix for the outputs of a batch b is similar to the ‘standard’ Hankel matrix and is given by:

$$\mathbf{Y}_{1|i}^{(b)} = \begin{bmatrix} \mathbf{y}^{(b)}[1] & \mathbf{y}^{(b)}[2] & \cdots & \mathbf{y}^{(b)}[j^{(b)}] \\ \vdots & \vdots & & \vdots \\ \mathbf{y}^{(b)}[i] & \mathbf{y}^{(b)}[i+1] & \cdots & \mathbf{y}^{(b)}[i+j^{(b)}-1] \end{bmatrix} \quad (3.39)$$

For subspace identification of a batch process, the key step then is to construct a pseudo-Hankel matrix such that it enables the use of data from multiple batches. However, a simple concatenation of data from the batches would incorrectly suggest that the end of one batch is the beginning point of another. Therefore, the individual matrices from each batch is horizontally concatenated to obtain a single pseudo-Hankel matrix corresponding to the input and output data. The pseudo-Hankel matrix, thus takes the following form.

$$\mathbf{Y}_{1|i} = \begin{bmatrix} \mathbf{Y}_{1|i}^{(1)} & \mathbf{Y}_{1|i}^{(2)} & \cdots & \mathbf{Y}_{1|i}^{(25)} \end{bmatrix} \quad (3.40)$$

Similarly, Hankel matrices can be constructed for the input data. This approach for handling multiple batches enables implementation of the subspace identification method for batch processes. Further, unlike time-dependent modeling approaches such as latent variable methods, it does not impose any constraint on the length of different batches. The reader is referred to [11, 20] for theoretical discussion of this approach and its application to various applications.

The training batch database consisting of input and output data were used to identify a LTI state-space model of the process using the subspace identification approach discussed above. A parsimonious state space model order of 40 was selected based on the observed trade-off between model fitting and validation. The identified model is thus of the following form.

$$\begin{aligned} \mathbf{x}[k+1] &= \mathbf{A}\mathbf{x}[k] + \mathbf{B}\mathbf{u}[k] \\ \mathbf{y}[k] &= \mathbf{C}\mathbf{x}[k] + \mathbf{D}\mathbf{u}[k] \end{aligned} \quad (3.41)$$

where $\mathbf{y} = [T \ C \ C_s \ C_m \ n_i]'$ and $\mathbf{u} = T_j$. Here $n_i \triangleq n(0.6 * i, t) \forall 0 \leq t \leq 30$ min and $i \in \{1, 100, 200, 300, \dots, 1000\}$. Note that 1000 discretization points were used for solving the first principles crystallization model, and the 1000 measurements are assumed to be available. Even though we have measurements corresponding to 1000 discretization points of the crystal radii range, a much smaller (coarser) sample is used for model identification to avoid identifying a very high order model of the process. However, for final quality prediction, the fine CSD (all 1000 points) is predicted using the terminal subspace states.

From the 30 batches database, first 25 were used for model identification while the last 5 batch were used for model validation. To validate the identified model on a new batch, the primary step is to obtain state estimate of the process from measurements. In the present work, this is accomplished by using a standard Luenberger observer of the form:

$$\hat{\mathbf{x}}[k + 1] = \mathbf{A}\hat{\mathbf{x}}[k] + \mathbf{B}\mathbf{u}[k] + \mathbf{L}(\mathbf{y}[k] - \hat{\mathbf{y}}[k]) \quad (3.42)$$

where \mathbf{L} is the observer gain and is designed based on the desired eigenvalues of $(\mathbf{A} - \mathbf{L}\mathbf{C})$ using *place* command in MATLAB. The observer poles are placed randomly in the unit circle while ascertaining they are not close to unity circle. The initial state estimate is chosen based on the estimated initial state of a training batch. To validate the identified model, first the observer is converged to a state estimate such that the prediction of the outputs match the observed values. Then this state estimate along with the remainder of the input sequence and the identified model is used to predict the outputs for the remainder of the batch. The predicted outputs can be compared to the measured outputs to gauge the quality

of the identified model. Results for validation of one of the batch are shown in Figure 3.8. The validation results demonstrate the viability of using the identified model for feedback control within an MPC formulation.

As mentioned before, the measurements used for model identification used only a fraction of the CSD measurements. This coarse distribution can be used to predict the finer CSD at the batch termination by augmenting the subspace identification model with a linear model which relates the model states to the fine CSD as follows.

$$Q_{t_f} = L_m x[t_f] + e \quad (3.43)$$

Here Q_{t_f} , L_m , $x[t_f]$ and e denote terminal CSD measurements, least squares solution of the model, terminal states of the subspace model and white noise respectively. This model augmented with subspace model completes the description of the batch crystallization process. The approach elegantly handles the data variety.

Recall that the quality measurements are available online (the PSD with a fine discretization). Therefore, to determine L_m from training database, CSD measurements for all times except the first 5 minutes (before which the observer may not have converged), are used. This improves the accuracy of the estimates obtained in comparison to using just the terminal CSD measurements. This model facilitates the prediction of terminal CSD during the batch operation based on predictions of the terminal states obtained from the subspace identification model (as demonstrated in Figure 3.9).

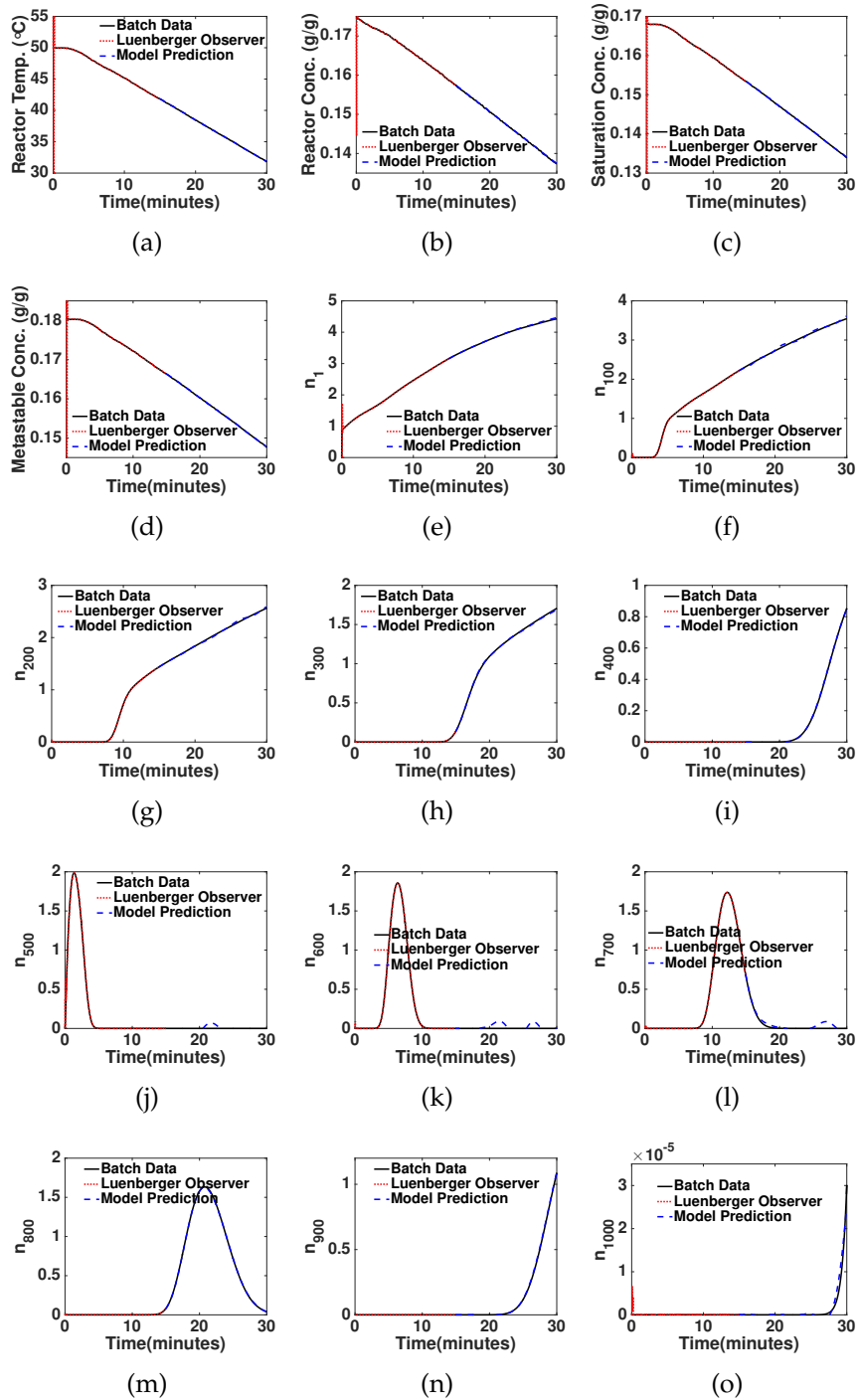


Figure 3.8: Validation results for identification: (a) Reactor temperature, (b) Reactor concentration, (c) Saturation concentration, (d) Metastable concentration, (e) n_1 , (f) n_{100} , (g) n_{200} , (h) n_{300} , (i) n_{400} , (j) n_{500} , (k) n_{600} , (l) n_{700} , (m) n_{800} , (n) n_{900} and (o) n_{1000} .

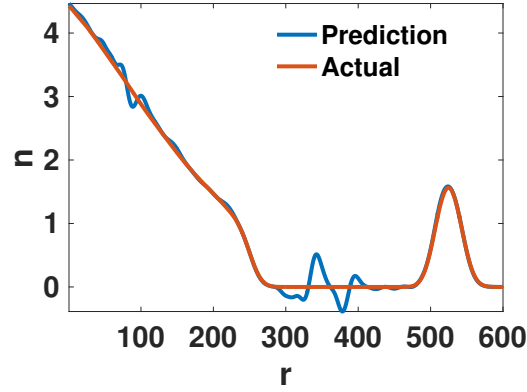


Figure 3.9: Quality model prediction of the CSD at batch termination based on predicted terminal state estimates from 15 minutes onward.

The quality model relating the subspace states to the CSD can be written as follows:

$$\hat{Q}_{t_f} = L_m \hat{x}[t_f] \quad (3.44)$$

Remark 3.1. The use of big data (the variety aspect) in modeling the batch crystallization process through a combination of a dynamic and quality model aids in the capability of the model to predict the particle size distribution throughout the batch. In absence of such an approach, one would need to reduce the PSD measurements to two dimensional measurements, as in [24] through the use of moments, and at best then only predict the moments in the identified model. In contrast, the model developed in the present manuscript is able to predict a (coarser) CSD evolution through the batch, and then utilizes the subspace states at the end of the batch (not the coarse CSD alone) to predict the final product quality (a the finer CSD). The ability to predict the terminal distribution opens up the possibility of controlling the ‘shape’ of the distribution in the final product, as

presented in Section 3.3.3.

3.3.2 Predictive control of volume of fines in batch particulate processes

This section presents the design and application of a subspace state-space model based predictive controller with explicit model validity constraint. The control objective is to minimize volume of fines while ensuring that the total volume of crystals grown from seeds is above a specified threshold. In the closed-loop control structure, the PBM, together with the mass and energy balances of Equation 3.32 are used as a test bed for the process while the identified subspace state space model is deployed within the MPC for the predictions. As with validation tests for the model building, the Luenberger observer is used to estimate the state of the process, and only after a certain duration into the batch, the MPC is initiated. During this initial period (15 minutes), the trajectory tracking PI control is used to track the same trajectory that is tracked under PI control.

Constraints on the concentration, the manipulated input and desired end-point quality are incorporated as input and output constraints in the MPC optimization problem. Consider the current state estimate from the Luenberger observer be denoted by $\hat{\mathbf{x}}[l - 1]$, and the last control action implemented on the process is denoted by $\mathbf{u}[l]$. Then the optimal control trajectory from current sampling instance l to the end of the batch is computed as follows:

$$\begin{aligned}
& \min_{\mathbf{U}_f} \zeta_1 \hat{Q}_{t_f}[l_f - l] \\
& \text{s.t. } T_{j,min} \leq u_f[k] \leq T_{j,max}, \quad \forall 0 \leq k \leq l_f - l \\
& \quad \hat{y}_3[k] + \epsilon_1 \leq \hat{y}_2[k] \leq \hat{y}_4[k] - \epsilon_2, \quad \forall k \leq H_c \\
& \quad |u_f[0] - u[l - 1]| \leq \delta, \\
& \quad |u_f[k] - u[k - 1]| \leq \delta, \quad \forall 1 \leq k \leq l_f - l \\
& \quad \zeta_2 \hat{Q}_{t_f}[l_f - l] \geq \gamma \\
& \quad \hat{\mathbf{x}}[0] = \hat{\mathbf{x}}[l] \\
& \quad (1 - \alpha)\mathbf{x}_d \leq \hat{\mathbf{x}}[l_f] \leq (1 + \alpha)\mathbf{x}_d \quad \forall l_f - 150 \leq k \leq l_f \\
& \quad \hat{\mathbf{x}}[k + 1] = \mathbf{A}\hat{\mathbf{x}}[k] + \mathbf{B}\mathbf{u}_f[k] \\
& \quad \hat{\mathbf{y}}[k] = \mathbf{C}\hat{\mathbf{x}}[k] + \mathbf{D}\mathbf{u}_f[k] \quad \forall 0 \leq k \leq l_f - l
\end{aligned} \tag{3.45}$$

Where,

$$\begin{aligned}
\zeta_1 \hat{Q}_{t_f} &= \sum_{r=0}^{r_g} r^3 n(r, t_f) \\
\zeta_2 \hat{Q}_{t_f} &= \sum_{r=r_g}^{\infty} r^3 n(r, t_f)
\end{aligned} \tag{3.46}$$

Further, $\mathbf{U}_f = [\mathbf{u}_f[0], \mathbf{u}_f[1], \dots, \mathbf{u}_f[l_f - l]]$ denotes the remaining input trajectory and is the decision variable in the stated MPC formulation, $l_f = t_f/\Delta_s$ and the i th element of the output vector y is denoted by y_i and the identified state space model is used for its prediction as discussed before. The constraints on the manipulated variable, u used in the present work are $T_{j,min} = 30^\circ\text{C}$ and $T_{j,max} = 50^\circ\text{C}$. The constraints on the solution concentration are represented

by y_3 (saturation concentration) and y_4 (metastable concentration). Further, the maximum gradient of the jacket temperature is enforced as $\delta = 2^\circ\text{C}/\text{min}$ in the simulations throughout the batch. In addition, the total volume of the crystals growing from the seeds is forced to be above the minimum requirement of $\gamma = 8.3301 \times 10^9$. This desired quality requirement on the final product is represented by the constraint on $\zeta_2 \hat{Q}_{t_f}$. Lastly, the identified discrete time LTI state space model of the process is represented by the final two equations.

As a linear model is estimated to represent the dynamics of a nonlinear process, its important to include model validity constraint to restrict too much deviation of the process from state-space where model predictions will be reasonable. This is achieved by including the bound on the terminal state the process is allowed to reach. In this work, the MPC is forced to reach within 5% bound ($\alpha = 0.05$) of x_d , which is chosen as the average of the terminal states from the training batches. Further, this constraint is invoked only in last 150 control moves for two reasons. First, it reduces the complexity of the MPC optimization problem by reducing the number of constraints when the control horizon is large, thereby improving the solution time. Second, as discussed in [20], the open-loop prediction's accuracy is increased as more data is available (i.e., as the batch operation furthers in time) and thus the constraint becomes more meaningful.

Tuning parameters ϵ_1 , ϵ_2 and H_c are used to tighten the constraints when implementing the predictive controller in order to account for the plant-model mismatch. In this work, ϵ_1 and ϵ_2 were chosen as 0.003 g/g and 0.001 g/g respectively. The saturation constraints are implemented only 30 steps ahead, and shrunk appropriately as the batch nears completion. Thus, the value of H_c is as

follows:

$$H_c = \begin{cases} 30 & l_f - l \geq 30 \\ l_f - l & l_f - l < 30 \end{cases} \quad (3.47)$$

The first move of the control action is implemented on the process, and the optimization is repeated at the next sampling time. Due to the identified state space model being linear, the MPC optimization is formulated and implemented as a linear program.

A hierarchical strategy was used in this work to solve the MPC optimization problem. The default algorithm used for solution was dual-simplex and for cases where an optimal solution was not found, the constraints were relaxed by changing ϵ_1 to 0.002 or removing the constraint on desired terminal quality. In case an optimal solution is not obtained even after relaxations, the next move from previously obtained solution, if available, is implemented. Else, the MPC switched to interior-point-legacy algorithm and the solution obtained is implemented after passing through a saturater to enforce the input constraints.

Closed-loop control simulations

The LTI state space model based linear MPC with explicit model validity constraints is proposed in this work. To validate the effectiveness of this framework, it is used for control of 25 different batches. Further, the approach is compared against an open loop linear cooling and a PI controller based trajectory tracking approach. Note that the batches used for control scheme validation were

different from the ones used for model identification.

The volume of fines (quantified as μ_3^n) obtained in 25 control batches under three different control schemes, i.e., the open-loop control strategy of linear cooling, PI controller based trajectory tracking and the proposed MPC formulation. The variability in the volume of fines (μ_3^n) achieved across different batches under the different control schemes are shown in Figure 3.10. It can be observed from the results that the proposed MPC formulation resulted in lower volume of fines on an average by 15.60% and 19.61% when compared to PI based trajectory tracking and linear cooling strategy respectively, while satisfying the process constraints in all the batches. Further, the variability in the final product quality (volume of fines) is least for MPC compared to other control schemes.

In Figure 3.11, the closed loop profile corresponding to the batch for which the MPC yields the best performance is shown. Note that in MPC controlled batches, PI controller is used for the initial 15 minutes of operation. This is necessary for the Luenberger observer to estimate the current state of the process, following which the controller is switched to the proposed MPC till the end of the batch. It can be observed from Figure 3.11 that during MPC implementation, the input trajectory deviates from the PI trajectory after 15 minutes to drive the process to the optimal product specifications.

Table 3.9: Comparison of control strategies for 25 batches

Control method	μ_3^n	$\min(\mu_3^n)$	Number of failed batches
Linear cooling	1.5676×10^9	1.2991×10^9	0
PI	1.4931×10^9	1.2317×10^9	0
MPC	1.2602×10^9	1.0499×10^9	0

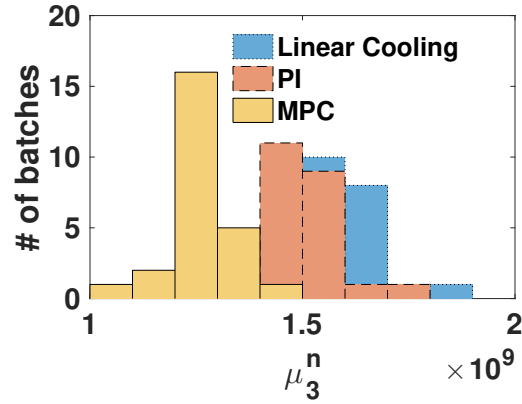


Figure 3.10: Distribution of μ_3^n for process under Linear cooling, PI and MPC.

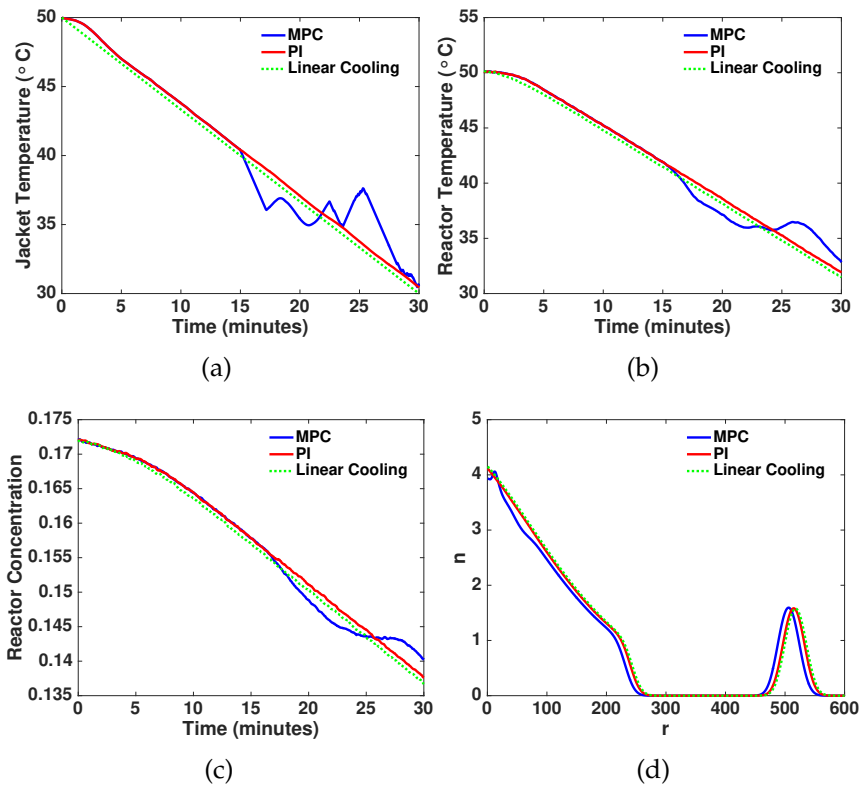


Figure 3.11: Results corresponding to MPC batch with lowest achieved μ_3^n : (a) Input profiles, (b) Reactor temperature, (c) Reactor concentration and (d) Final CSD.

3.3.3 Predictive control of shape of the particle size distribution

This section presents predictive control formulation for achieving a desired shape of the particle size distribution by the termination of batch. The key idea behind directly controlling the shape of the PSD is that the properties of the product are determined by the entire distribution. Hence, shape control may be more appropriate, where tighter product quality is required, than using lumped values of the distribution such as moments. The proposed approach is based on subspace state-space model as discussed before. The approach models the data variety (particle size distribution) and thus makes it suitable for direct control of the distribution shape. The control objective is, therefore, to achieve a specified distribution by the termination of the batch while respecting the constraints on the process dynamics by manipulating the jacket temperature. As in the earlier formulation, the PBM, together with the mass and energy balances are used as a test bed for validation of the proposed approach. During the initial 15 minutes, the PI control is used to track a predefined trajectory. After this the following quadratic MPC formulation is implemented. That is, at any sampling time l (after controller has been switched to MPC), the optimal input trajectory from the current instance to the end of batch is computed as the solution of following optimization.

$$\begin{aligned}
& \min_{\mathbf{U}_f} (\hat{Q}_{t_f}[l_f - l] - q_{des})M(\hat{Q}_{t_f}[l_f - l] - q_{des})^T \\
& s.t. \quad T_{j,min} \leq u_f[k] \leq T_{j,max}, \quad \forall 0 \leq k \leq l_f - l \\
& \quad \hat{y}_3[k] + \epsilon_1 \leq \hat{y}_2[k] \leq \hat{y}_4[k] - \epsilon_2, \quad \forall k \leq H_c \\
& \quad |u_f[0] - u[l - 1]| \leq \delta, \\
& \quad |u_f[k] - u[k - 1]| \leq \delta, \quad \forall 1 \leq k \leq l_f - l \\
& \quad \zeta_2 \hat{Q}_{t_f}[l_f - l] \geq \gamma \\
& \quad \hat{\mathbf{x}}[0] = \hat{\mathbf{x}}[l] \\
& \quad (1 - \alpha)\mathbf{x}_d \leq \hat{\mathbf{x}}[l_f] \leq (1 + \alpha)\mathbf{x}_d \quad \forall l_f - 150 \leq k \leq l_f \\
& \quad \hat{\mathbf{x}}[k + 1] = \mathbf{A}\hat{\mathbf{x}}[k] + \mathbf{B}\mathbf{u}_f[k] \\
& \quad \hat{\mathbf{y}}[k] = \mathbf{C}\hat{\mathbf{x}}[k] + \mathbf{D}\mathbf{u}_f[k] \quad \forall 0 \leq k \leq l_f - l
\end{aligned} \tag{3.48}$$

where, \mathbf{M} is the weighting matrix and q_{des} is the desired distribution profile and rest of the notations are as defined in the earlier formulation. The values of the tuning parameters for this case were $H_c = 25$, $\epsilon_1 = 0.0041 \text{ g/g}$ and $\epsilon_2 = 0.0011 \text{ g/g}$. The MPC optimization problem is formulated and implemented as a constrained quadratic program as the identified model is linear.

Closed-loop control simulations

The proposed quadratic MPC with explicit model validity constraints is applied on 25 different batches to examine the effectiveness of the proposed method. The advantage with the proposed formulation over the previous formulation is that it allows the control practitioner to explicitly provide the desired shape of

the distribution that is required at the end of the batch. This is possible due to explicit modeling of PSD and formulating the optimization as presented. This demonstrate merits of using variety of data for modeling and control of batch particulate processes.

Figure 3.3.3 shows the terminal PSD profiles for the best and worst batches obtained using the proposed control approach. Note the MPC was implemented for the second half of the batch (15 minutes), prior to which PI control was implemented. This initial duration serves as a mechanism for estimating the current state of the process using Luenberger observer.

Table 3.10 summaries the results obtained using the proposed approach for 25 simulation batches. The proposed control design not only enables reaching the target PSD, also reduces the average variability across different batches, compared to the training batches. Note that the lowest SSE for the training batches is expectedly zero as the desired CSD shape was chosen from the training batches. The proposed control design, however, is able to match the desired PSD on average even when starting from other initial conditions.

Table 3.10: Control results for 25 batches

Control formulation	Average SSE	Lowest SSE	Largest SSE	Number of failed batches
Predictive control	12.48	3.78	72.90	0
Training batches	19.70	0	61.83	0

3.4 Conclusions

In this work, a novel batch subspace identification model based predictive controller with explicit model validity constraint, capable of handling data variety,

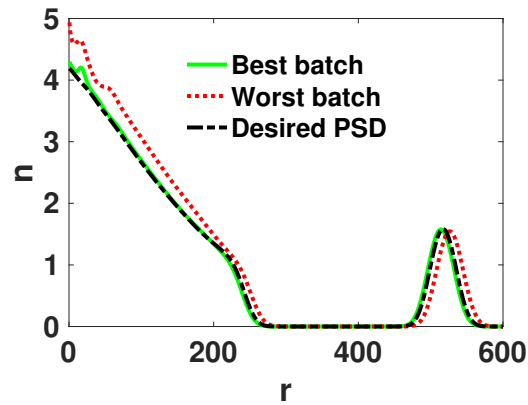


Figure 3.12: Terminal PSD for the best and worst case scenario

for batch particulate processes is proposed. The batch subspace identification method was adapted to handle data variety using a combination of a dynamic and static final CSD model, which is subsequently deployed within MPC. The effectiveness of the proposed approach in terms of improved product quality are demonstrated through two different formulations: a) minimizing the volume of fines in the final product by leveraging the variety of measurements and b) control of crystal size distribution shape in the product.

Chapter 4

Subspace-Based Model Identification of a Hydrogen Plant Startup Dynamics

The results of this chapter have been published as:

JOURNAL PUBLICATIONS:

- A. Garg, B. Corbett, P. Mhaskar, G. Hu, and J. Flores-Cerrillo. Subspace-based model identification of a hydrogen plant startup dynamics. *Computers & Chemical Engineering*, 106:183–190, nov 2017

REFEREED CONFERENCE PROCEEDINGS:

- A. Garg, B. Corbett, P. Mhaskar, G. Hu, and J. Flores-Cerrillo. Development of a high fidelity and subspace identification model of a hydrogen plant startup dynamics. In *2017 American Control Conference (ACC)*, volume 106, pages 2857–2862. IEEE, may 2017

4.1 Introduction

Hydrogen is an indispensable chemical component extensively used in petroleum and chemical industries. An economic way to commercially produce hydrogen is to utilize steam methane reforming (SMR) [42]. SMR process operation (like most other operations) undergoes scheduled startup and shutdown procedures which is sometimes initiated due to the need for regular maintenance and sometimes by unforeseen circumstances. Startups/shutdowns are implemented using standard operating procedures (SOPs). These procedures present various constraints and challenges such as constraints on the reformer exit temperature and firebox pressure [15]. Further, a typical startup involves a series of operations such as ramping various flows, introducing certain flows, along with making discrete decisions such as starting up certain parts of the unit. Thus, the startup time is not fixed and varies based on the decisions taken at various stages. Startups and shutdowns are fairly resource intensive operations, and stand to gain from optimizing the startup procedure via operating procedure synthesis (OPS).

A key requirement for OPS is a good model for the startup process. There exist several modeling approaches that are well suited for small scale processes (see [5] for an excellent review) but difficult to implement to large chemical units. Out of these approaches, dynamic simulation based strategies are most prominent. In these approaches, dynamic simulations are used to select the best startup scenarios. The detailed models allow a good description of the startup dynamics and are valuable from a process analysis standpoint. One of the key contributions of the present work is the development of a detailed first principles model for the hydrogen unit startup, with appropriate adaption of the plant startup SOP. Note

however that such detailed first principles models pose computational challenges when directly embedded in optimization problems, and thus existing SOP synthesis approaches utilize heuristics in an attempt to determine optimal profiles (e.g. see [62, 73, 75, 61]). Performance of a more rigorous optimization necessitates the use of simpler models that can capture the startup/shutdown dynamics, and yet be amenable for online implementation. One of the contributions of the present work is the recognition of the startup/shutdown process as a batch like process that opens up the possibility of adapting data-driven batch modeling techniques to identify models that capture the startup process dynamics reasonably well, and yet are not too computationally complex.

While a variety of a data-driven modeling techniques exist for modeling and control of batch processes, not all of these are suitable for the problem at hand. One approach that has found wide variety of applications is partial least squares (PLS), which models the process in a projected latent space [16]. PLS models are in essence time-varying linear models, linearized around mean past trajectories, and thus require the batches to be of same length, or to find an appropriate alignment variable. As indicated earlier, the inherent variabilities of the startup procedure do not result in startups of equal length.

In one recently proposed approach [3] the models were based on the ‘current measurements’ of the process instead of the ‘time’. These developments were followed by contributions in the area of integration of these data-driven models with model predictive control formulations [4, 3]. More recently a subspace identification based batch control approach was proposed in [11] where an LTI state-space model of the batch process is identified, and does not require the

training batches to be of equal length. The problem of optimizing hydrogen startups thus stands to gain from these recent results. Note that while the approach in [11] has subsequently been adapted to detailed simulations of an electric arc furnace [59] and particle size distribution (PSD) control [25], it has not been applied yet on a process of the present complexity, using real data, and to model startups.

Motivated by these considerations, in this work we address the problem of determining a data driven model for the startup of a hydrogen plant. The paper is organized as follows. First necessary background on hydrogen production process and system identification are presented in Section 4.2. Section 4.3 presents the modifications necessary to adapt a detailed first principles model in UniSim design to enable simulating the startup and shutdown phase. Although the primary focus of the proposed approach is to identify reduced order data-driven model of the process, the development of a detailed first principles model serves two key purposes. Firstly, it enables the generation of startup and shutdown (simulated) data of the process which can be used to test/develop the data-driven modeling approach. Secondly, a detailed simulator capable of mimicking the startup/shutdown can serve as a good analysis tool for control practitioners. Before implementing subspace identification methods to identify a reduced order linear time-invariant model of the process, the suitability of a linear model to explain the dynamics of a finite duration nonlinear process is illustrated through simulations in Section 4.4.1. Then, an LTI data-driven model of the process using subspace identification based method is identified in Section 4.4.2. Simulation results illustrate the prediction capabilities of the identified model validated

against the detailed first principles simulation model. Next, the approach is implemented on data collected from a Praxair hydrogen unit, and validated in Section 4.4.3. Finally, a few concluding remarks are presented in Section 4.5.

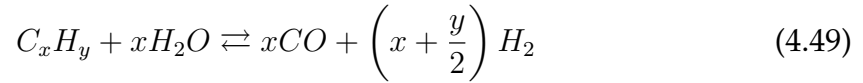
4.2 Preliminaries

This section presents an overview of the hydrogen production process, and subspace identification approaches.

4.2.1 Process Description

Hydrogen is commercially manufactured by steam methane reforming, where natural gas (NG) and superheated steam are fed to a chemical reactor called reformer, which consists of catalyst tubes filled with nickel reforming catalyst as depicted in Figure 4.13. Natural gas is first purified by removing any liquid that may have condensed due to low ambient temperature. It is then split into two streams. Most of the natural gas is compressed as the feed to the reformer. A small amount is used as fuel to provide heat for the reformer. The steam is produced from water by a steam system in the heat recovery block. The NG feed stream is heated using downstream process heat and further processed by removing any unfavorable compounds to the reformer catalyst. Under normal conditions, the pressure of the NG fuel is controlled by an upstream valve, and the flow rate of the NG fuel is controlled by a downstream valve. The majority of the hydrogen is

produced in the reformer through the following chemical reactions:



Reaction 4.49 is known as reforming and reaction 4.50 is also called shift conversion. Both the reactions are reversible. The overall reaction is endothermic. Reformer exit temperature (RET) is an important process variable for this process and is expected to be kept at a specific value by heating the reformer. This heat is provided by burning the off-gas from the pressure swing adsorber (PSA) and NG fuel stream. The NG fuel stream is used to regulate the reformer exit temperature under nominal operating scenarios. Moreover, the temperature is affected by the flow rates of the combustion air and the superheated steam.

The reformer effluent process gas passes through a reactor, where additional hydrogen is produced by shifting most of the carbon monoxide in the process gas to carbon dioxide and hydrogen through reaction 4.50. The reactor effluent stream then passes through the heat recovery and is sent to the PSA, where the hydrogen is produced. The PSA process is based on the physical adsorption phenomena. High volatile compounds with low polarity such as hydrogen are practically non-adsorbable compared to water, nitrogen, carbon monoxide, ammonia, methane, sulfur compounds and hydrocarbons. Most of the impurities in the gas can be selectively adsorbed, resulting in high purity hydrogen. During normal operation, the off-gas out of the PSA is used as the primary fuel that provides heat for the reformer.

The combustion heat resulting from the ignition of air and fuel in burners heat the reformer tubes. A fan is used to supply air to the burners and another one draws the combustion products, which are termed flue gas, out of the reformer firebox. The firebox pressure should not reach its lower and upper limits for safety. If the pressure is too low, the fire can be extinguished. If it is too high, it may impose safety hazards to facility and personnel. The pressure is controlled by adjusting the position of the suction louvers of Fan 2. As the louvers open, the fan draws more flow, resulting in a lower pressure. Conversely, as the louvers close, the fan draws less flow to increase the pressure.

The focus of the present work is modeling of the startup process. A typical startup involves ramping the natural gas fuel to reach a sufficient reformer exit temperature, introduction of natural gas feed and steam, regulation of nitrogen flow in the reactor tubes. It also requires making discrete decisions such as starting up the PSA, recirculating the tail gas from the PSA and ramping up to full capacity in several stages. Specific details of the startup procedure are omitted due to confidentiality reasons.

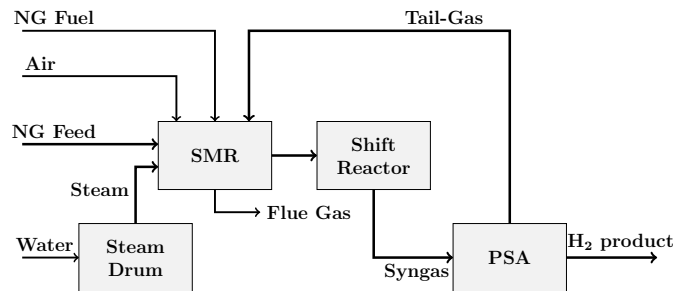


Figure 4.13: A schematic of the hydrogen production process

4.2.2 Subspace Identification

Subspace identification methods are a class of model identification methods that are non-iterative in nature and identify a state-space linear time invariant model, identifying the system matrices along with the order of the system. These methods utilize efficient matrix factorization methods such as singular value decomposition (SVD) and QR factorization (a matrix factored into Q and R matrices where, Q is an orthogonal matrix and R is an upper triangular matrix) for their implementation. This is in contrast to classical system identification techniques, which are iterative optimization based algorithms that minimize the prediction error (PEM) using efficient methods such as maximum likelihood estimation (MLE) and expectation maximization (EM) algorithm. These methods offer well established theoretical properties and have been widely studied [46, 27, 58, 31, 72, 70]. However, most of the existing classical and subspace identification approaches focus on data obtained from continuous operation.

Among subspace identification algorithms, some of the widely used techniques include canonical variate analysis (CVA) [43], numerical algorithms for subspace state space system identification (N4SID) [51] and multivariable output error state space algorithm (MOESP) [66]. It has been shown that these algorithms can be interpreted as a singular value decomposition of a matrix weighted differently in each method [65]. Apart from these, several other application specific algorithms equivalent to the standard subspace identification have been proposed [68, 45, 67]. Broadly, subspace identification methods can be categorized into deterministic, stochastic, and combined deterministic stochastic methods (see, e.g., [64] for an excellent overview). The key distinction among these is the way in which process

noise and disturbances are handled. In the present work, the focus will be on adaptation of deterministic identification for batch-like (startup) processes.

The deterministic identification problem can be described as follows: If p measurements of the input $u_k \in \mathbb{R}^m$ and the output $y_k \in \mathbb{R}^q$ are given which are generated by the following unknown deterministic system of order n :

$$\mathbf{x}_{k+1}^d = \mathbf{A}\mathbf{x}_k^d + \mathbf{B}\mathbf{u}_k, \quad (4.51)$$

$$\mathbf{y}_k = \mathbf{C}\mathbf{x}_k^d + \mathbf{D}\mathbf{u}_k, \quad (4.52)$$

where $x_k \in \mathbb{R}^n$ denotes the system state at a sampling instant k , the task is to determine the order n and the system matrices $\mathbf{A} \in \mathbb{R}^{n \times n}$, $\mathbf{B} \in \mathbb{R}^{n \times m}$, $\mathbf{C} \in \mathbb{R}^{q \times n}$, $\mathbf{D} \in \mathbb{R}^{q \times m}$, up to within a similarity transformation. Note that if subspace identification is utilized to identify the system dynamics for a linear system, an exact identification will yield subspace states that are typically a transformation of the original system states. For the case of approximation of nonlinear dynamics, the identified states (including the number) may not be the same as that of the original nonlinear system's state space representation. The traditional subspace identification methods are designed to handle continuous data. Thus, the traditional subspace identification method is not directly applicable to situations where data is available from multiple startups. This manuscript presents one such approach for startup processes.

4.3 Detailed First Principles Model Development

To serve as a test bed, a UniSim Design model of the hydrogen production unit capable of simulating the plant startup and shutdown dynamics was first developed. To this end, a UniSim design model capturing nominal production phase provided by Praxair Inc. was suitably modified to incorporate the startup and shutdown simulation capabilities. A brief description of the necessary steps are provided here to serve as guidelines to adapt other dynamic simulation models built for simulating nominal continuous operation (around some steady-state equilibrium point) of the plant.

To enable startup simulation, the flowsheet requires several modifications. For instance, the control configurations from the P&ID are required to be incorporated in the model. Apart from these, several dummy controllers are required to mimic the manual operations by the operator during the course of startup/shutdown. In shutdown phase simulation, it is not possible to drive the model to a complete shutdown state due to the limitations of simulator. Therefore, the flows were reduced to a nominal low value which can simulate the process without running into numerical issues. This minimal state is treated as shutdown state in the simulation. The startup procedure is then implemented on this attained shutdown state. Note that the goal of the first principles model development in this work was only to capture the key startup and shutdown trends (validated against real startup data). This model can be then used as a test bed for the application of the proposed identification approach.

Note that the SOP available from plant operations was not amenable for direct implementation in a simulated environment. Therefore, a 'minimalistic' SOP

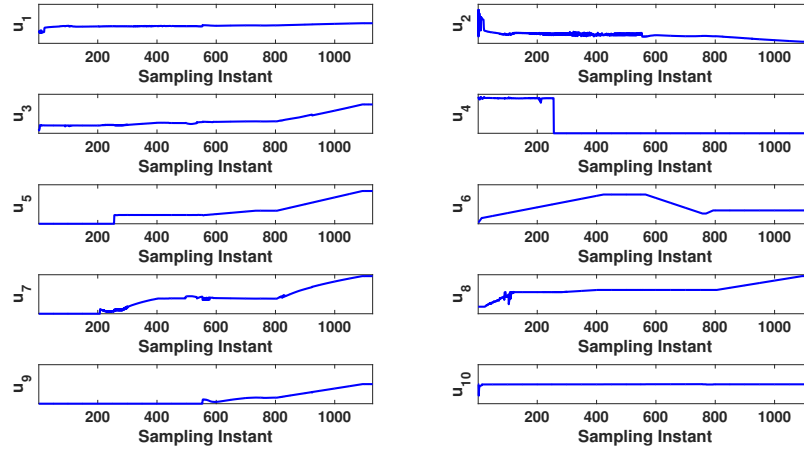


Figure 4.14: Simulated startup: Manipulated variables profile

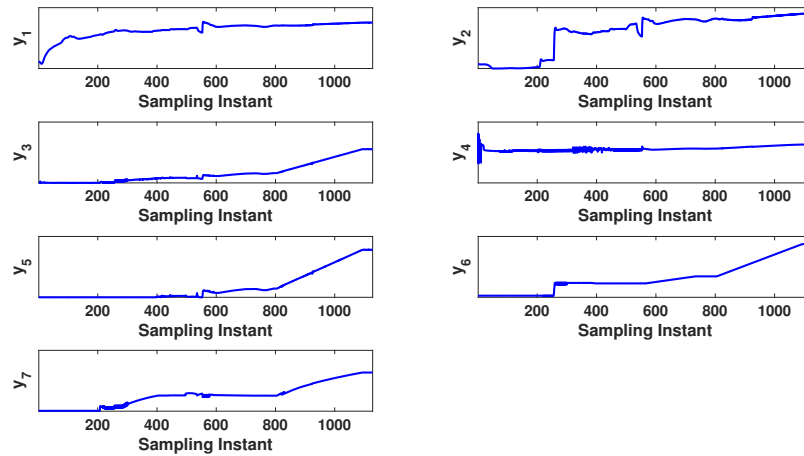


Figure 4.15: Simulated startup: Output variables profile

implementable in the UniSim design model was developed along the lines of real plant SOP. Data from several startups is generated by implementing this adapted SOP. For implementing the modified SOP in UniSim design, any of the following two approaches can be used. Either, the startup strategy be defined

within UniSim design itself using Event Schedulers (as done in the present work) or using a Matlab-UniSim interface to drive the process using Matlab. However, for implementing a closed loop control strategy the latter approach might be more suited and will be the subject of future work. One such simulated startup manipulated and output profiles are illustrated in Figures 4.14 and 4.15 (showing the scaled manipulated inputs and measured outputs, respectively). While specific details of the inputs and outputs remain confidential, the inputs include various gas flow rates and the outputs include temperatures and pressures.

4.4 Identification of State-Space Model

We recognize that the startup phase can be treated as a batch process. Thus, consider the output measurements of a startup batch denoted as $\mathbf{y}^{(b)}[k]$, where k is the sampling instant since the startup initiation and b denotes the startup index. The output Hankel matrix for a batch b is the same as a ‘standard’ Hankel matrix, given by:

$$\mathbf{Y}_{1|i}^{(b)} = \begin{bmatrix} \mathbf{y}^{(b)}[1] & \mathbf{y}^{(b)}[2] & \cdots & \mathbf{y}^{(b)}[j^{(b)}] \\ \vdots & \vdots & & \vdots \\ \mathbf{y}^{(b)}[i] & \mathbf{y}^{(b)}[i+1] & \cdots & \mathbf{y}^{(b)}[i+j^{(b)}-1] \end{bmatrix} \quad (4.53)$$

where, index i is a user-chosen number of Hankel rows and $i+j^{(b)}-1 = N^b$, where N^b is the total number of data points in the b th batch.

The above Hankel matrix cannot be directly utilized for the identification of the subspace model using existing identification techniques, because as is, it allows

inclusion of data from a single batch. The remainder of the startups also cannot be simply concatenated to this matrix because that would implicitly assume that the end of one startup is the beginning of another startup. The key then is to build a Hankel-like matrix for each startup in a way that enables use of data across startups. This is achieved by horizontally concatenating the individual matrices, from each startup, to form a single pseudo-Hankel matrix for both input and output data. This is done without (incorrectly) assuming that the end point of one startup is the beginning of another. Thus, we define pseudo-Hankel matrix of the following form:

$$\mathbf{Y}_{1|i} = \begin{bmatrix} \mathbf{Y}_{1|i}^{(1)} & \mathbf{Y}_{1|i}^{(2)} & \cdots & \mathbf{Y}_{1|i}^{(nb)} \end{bmatrix} \quad (4.54)$$

Where nb is the number of batches in the training data. Similarly, pseudo-Hankel matrices for input data are formed. This approach for handling multiple batches nicely satisfies the requirements for subspace identification. A distinctive feature of this approach is that, it does not impose any constraint on the length of different batches. The reader is referred to [11] for detailed discussion on this approach.

Construction of appropriate Hankel-like matrices for input and output enable determination of state trajectories using any of the wide variety of subspace identification algorithms available in the literature. In the present work, a deterministic subspace identification algorithm presented in [48] is used. A result of the concatenation of the Hankel matrices is that the identified state trajectories will be comprised of concatenated state estimates for each training batch, determined on the same basis. Mathematically the identified state trajectories are

represented as:

$$\hat{\mathbf{X}}_{i+1}^{(b)} = \begin{bmatrix} \hat{\mathbf{x}}^{(b)}[i+1] & \cdots & \hat{\mathbf{x}}^{(b)}[i+j^{(b)}] \end{bmatrix} \quad (4.55)$$

$$\hat{\mathbf{X}}_{i+1} = \begin{bmatrix} \hat{\mathbf{X}}_{i+1}^{(1)} & \hat{\mathbf{X}}_{i+1}^{(2)} & \cdots & \hat{\mathbf{X}}_{i+1}^{(nb)} \end{bmatrix} \quad (4.56)$$

Once this state trajectory matrix is obtained, the system matrices can be estimated easily using methods like ordinary least squares. Note the regression problem must be set up carefully so state trajectories from each batch are only related to the outputs and inputs from that batch. This is achieved as shown below:

$$\mathbf{Y}_{reg}^{(b)} = \begin{bmatrix} \hat{\mathbf{x}}^{(b)}[i+2] & \cdots & \hat{\mathbf{x}}^{(b)}[i+j^{(b)}] \\ \mathbf{y}^{(b)}[i+1] & \cdots & \mathbf{y}^{(b)}[i+j^{(b)}-1] \end{bmatrix} \quad (4.57)$$

$$\mathbf{X}_{reg}^{(b)} = \begin{bmatrix} \hat{\mathbf{x}}^{(b)}[i+1] & \cdots & \hat{\mathbf{x}}^{(b)}[i+j^{(b)}-1] \\ \mathbf{u}^{(b)}[i+1] & \cdots & \mathbf{u}^{(b)}[i+j^{(b)}-1] \end{bmatrix} \quad (4.58)$$

$$\begin{bmatrix} \mathbf{Y}_{reg}^{(1)} & \cdots & \mathbf{Y}_{reg}^{(nb)} \end{bmatrix} = \begin{bmatrix} \mathbf{A} & \mathbf{B} \\ \mathbf{C} & \mathbf{D} \end{bmatrix} \begin{bmatrix} \mathbf{X}_{reg}^{(1)} & \cdots & \mathbf{X}_{reg}^{(nb)} \end{bmatrix} \quad (4.59)$$

The above procedure allows determining the system dynamics from a set of training startups. One of the key 'tuning parameter' in identifying the model is the number of subspace states. In general, higher number of subspace states result in better fit in the training set, but could likely lead to over-fitting, and poor prediction for a fresh startup. This is avoided by choosing the tuning parameter on the basis of cross validation, that is, utilizing a startup that was not part of the training set. The validation of the model (and eventual use as a model within a

feedback control tool) however also requires the use of a state estimator. This is because for a new batch, only the initial outputs are available as measurements, and not the value of the subspace states for that particular batch. If the subspace model is integrated from an arbitrary initial (subspace states) condition, it is unlikely that the model will be able to predict the dynamics of the new batch. An integral feature of the subspace identification approach for batch processes, therefore, it to use a state estimator for the initial duration of the batch to first estimate the subspace state trajectory for the initial duration of the batch. It is important to note that the potential use of the model in a closed-loop setting relies on its ability to predict future outputs for candidate input moves. The state estimator, however, can only be utilized to determine the current state estimates. After the initial duration, therefore, prediction of the outputs for the rest of the batch (without using the state estimator) is used for validation of the identified model.

In the present work, a Luenberger observer is used to illustrate the approach. However, the method is not restricted to this choice of estimator/observer. Any other estimator, such as Kalman filter, or moving horizon estimator (MHE) can be readily used. Thus, to validate the model, for the initial part of the batch, a standard Luenberger observer of the following form is used to first determine good estimates of the states (based on convergence of the measured output):

$$\hat{\mathbf{x}}[k + 1] = \mathbf{A}\hat{\mathbf{x}}[k] + \mathbf{B}\mathbf{u}[k] + \mathbf{L}(\mathbf{y}[k] - \hat{\mathbf{y}}[k]) \quad (4.60)$$

where \mathbf{L} is the observer gain, picked to ensure that $(\mathbf{A} - \mathbf{L}\mathbf{C})$ is stable, k is the current sampling instant, $\hat{\mathbf{x}}$ is the state estimate, \mathbf{y} denotes the measurement and

\hat{y} is the output prediction obtained using the estimated model. The poles of the observer are placed appropriately in the unit circle.

Another decision that must be made when dealing with a fresh startup is determining the initial condition for the subspace model. One reasonable way of picking the initial state estimates is, for instance, the average of states in the training data set. The observer is initialized at $k = 0$ and is updated with measurements until $k = l$, such that outputs converge. Then for $k = l + 1$ onwards, the identified LTI model is used to predict forward for validation purposes.

Once the model predictions are obtained, the prediction errors in the process outputs are quantified using mean absolute scaled error (MASE)[34]. The specific expression for computing MASE is given as follows

$$\text{MASE} = \frac{\sum_{t=1}^T |e_t|}{\frac{T}{T-1} \sum_{t=2}^T |Y_t - Y_{t-1}|} \quad (4.61)$$

where, e_t is the prediction error and Y_t is the measured value of a variable at any sampling instant t .

Remark 4.1. One could argue that it should be possible to carry out subspace identification individually on each training batch using existing identification approaches to determine state trajectories for each batch, and then identify a single dynamic model from the resulting state trajectories. However, doing so would necessitate reconciling the different state projections realized for each training batch, which is simply not possible. One of the principal advantages of the proposed approach is that by combining multiple batches in the pseudo-Hankel matrix a common subspace basis is selected for all training batches. As a result, the state trajectories identified for each training batch are consistent (as demonstrated

by equation 4.59).

Remark 4.2. As mentioned earlier, the proposed approach readily permits use of batches of varying durations. However, it should be noted that, in this approach, each observation has equal weight. Therefore, a batch of greater duration will have a correspondingly greater influence in the identified model. Practically however, this result is appropriate since longer batches contain more information about the dynamics of the system. This additional information is a direct result of the greater number of measurements and inputs perturbations available in longer duration batches. This has the implication that longer duration batches may play a greater role in guaranteeing persistent excitation as later discussed in Conjecture 1.

4.4.1 Illustrative Simulations for Batch Subspace Identification Methodology

In this section, the capabilities of the proposed data-driven modeling methodology is illustrated and discussed with the aid of simulations. In particular, the objective is to illustrate improved prediction ability by using higher number of states in the identified model. To this end, consider a switched system described as follows

$$x[k+1] = \begin{cases} 0.7x[k] + 0.5u[k] & \text{if } x[k] \leq 0 \\ 0.9x[k] + 0.5u[k] & \text{if } 0 < x[k] < 0.4 \\ 0.4x[k] + 0.5u[k] & \text{if } x[k] > 0.4 \end{cases} \quad (4.62)$$

$$y[k] = x[k] \quad (4.63)$$

The state of this single state process is assumed to be measured and treated as process output. A set of 5 batches were generated for this process. The first 4 batches were used for training while the last batch is used for validation. A PRBS input signal was designed such that for two of the batches, the process starts in mode 2 and goes to mode 3 and stays there, while for the other three batches, the process goes from mode 2 to mode 3 and switches back to mode 2 for a short duration. Two models are identified, one with a single state, and another with two states. The validation results and the corresponding error evolution is shown in Figures 4.16 and 4.17 respectively.

These simulations are presented to illustrate two key points. The first is that using a higher number of states allows the model identification procedure to better capture the dynamics of the process in different regions, by the higher flexibility in choosing the corresponding state trajectories. Thus, it is expected that the model using say two subspace states should perform better than a subspace model with a single state. The second key point is the use of the observer, which as the process evolves and transits from one operation region to another, allows the model to 'learn' the current dynamics of the process better. Thus, in Figure 4.17, compared to the error evolution of the prediction using the state estimates at the 20th time instance, the error is significantly lower for the prediction using the state estimate at the 60 time instant.

Remark 4.3. For identification of a process model, a key requirement is to have a rich data set. In continuous processes, operating around a nominal steady state, sufficient excitation of the input signal is in general difficult, especially for closed-loop data. However, in a process like startup/shutdown, this excitation

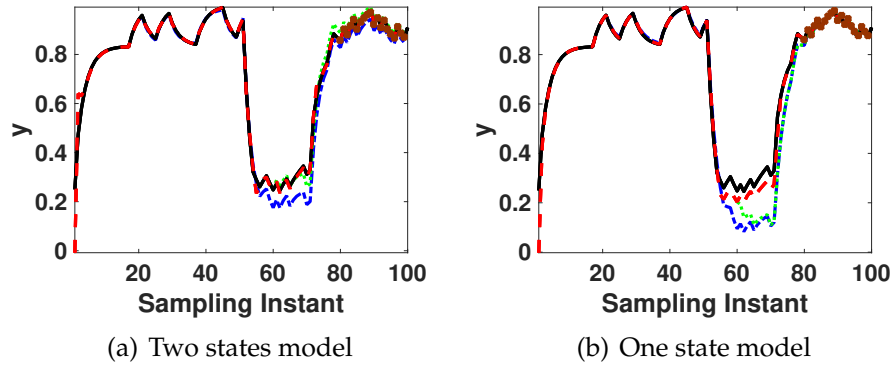


Figure 4.16: A Luenberger observer (red) is used to estimate the initial condition of the identified state space model till 20th, 60th and 80th sampling instant and then the identified model predictions are shown by blue dashed lines, green dotted lines and brown circles respectively. Black lines denote the plant output. The simulation illustrates the the prediction error goes down as the updated state estimate is used.

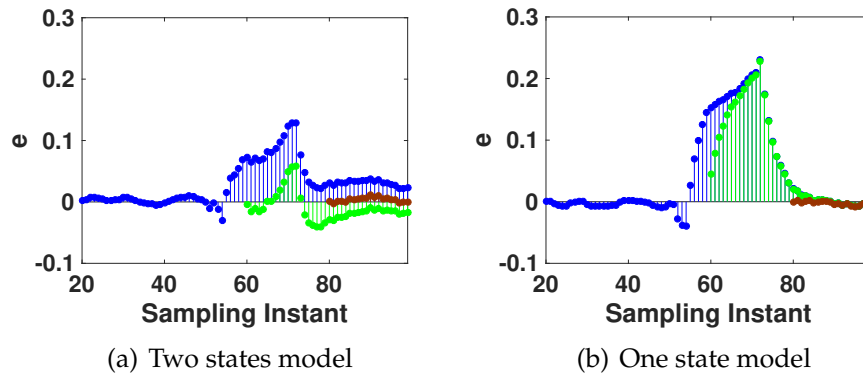


Figure 4.17: Residual plot from 20th, 60th and 80th sampling instants onward

occurs naturally since the process is never really at steady state, and the variation in feedstocks (and even operating procedure) provides variations across batches. The proposed approach, by recognizing startup/shutdown process as a batch-like process and using the datasets across different startup/shutdown scenarios, exploits the richness in the data to identify a reasonable model of the process, as demonstrated in this work.

To understand the benefits of using multiple batches for identification, we recognize that we are identifying a linear model of an appropriate order from the data. The order of the model that can be uniquely identified from the data depends on the ‘excitation’ of the input signal. To conjecture that data from multiple batches makes the identification data set richer, we first invoke a definition of persistence of excitation from classical system identification literature[46, 76]:

Definition 1. A quasi-stationary signal $u(t)$, with the spectrum $\Phi_u(\omega)$, is said to be persistently exciting of order n if, for all filters of the form

$$M_n(q) = m_1q^{-1} + \dots + m_nq^{-n} \quad (4.64)$$

the relation

$$|M_n(e^{i\omega})|^2\Phi_u(\omega) \equiv 0 \quad (4.65)$$

implies that $M_n(e^{i\omega}) \equiv 0$

A frequency domain interpretation of this definition is that, $u(t)$ is persistently exciting of order n , if $\Phi_u(\omega)$ is different from zero at at least n points in the interval $-\pi < \omega \leq \pi$ [46].

Building on this frequency domain interpretation, consider p different batch datasets with inputs and outputs denoted as $\mathbf{u}_1, \dots, \mathbf{u}_p$ and $\mathbf{y}_1, \dots, \mathbf{y}_p$ respectively. Also, the input spectrum is denoted as Φ_1, \dots, Φ_p . Then, we conjecture that the use of multiple batches improves the identifiability of a model by essentially improving its order of excitation in the inputs. Formally, this is stated as follows:

Conjecture 1. For batches B_1, \dots, B_p , let the set of frequencies different from zero

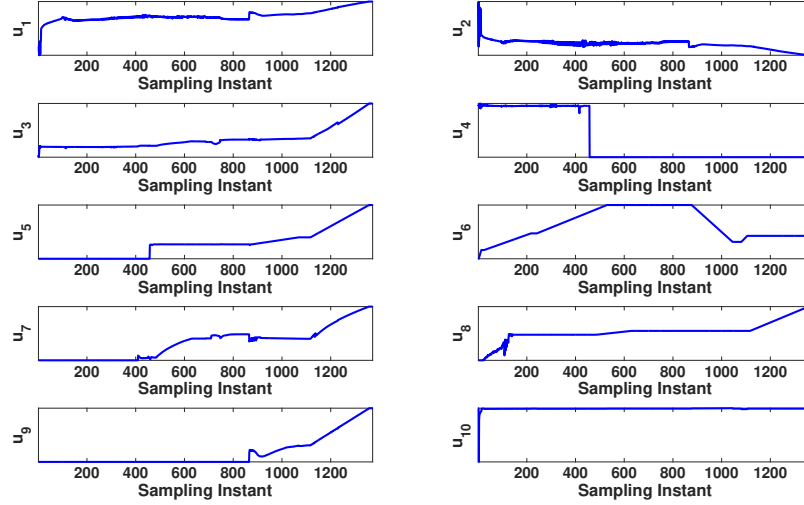


Figure 4.18: Manipulated variables for the validation batch

in the input spectrum for each batches be denoted as Ψ_1, \dots, Ψ_p , then the overall persistence of excitation in the input for the multiple batches can be given by the number of frequencies in the set Ψ^b , where

$$\Psi^b = \Psi_1 \cup \dots \cup \Psi_p \quad (4.66)$$

that is, number of unique frequencies in all the batches that are different from zero.

Thus, including multiple batches implies that the order of the model that can be identified will be at least as much as that identified using a single batch. We next present a modified definition of persistent excitation for batch data sets.

Definition 2. The inputs from multiple batches are said to be *persistently exciting* if Ψ^b contains all the frequencies in the interval $-\pi < \omega \leq \pi$.

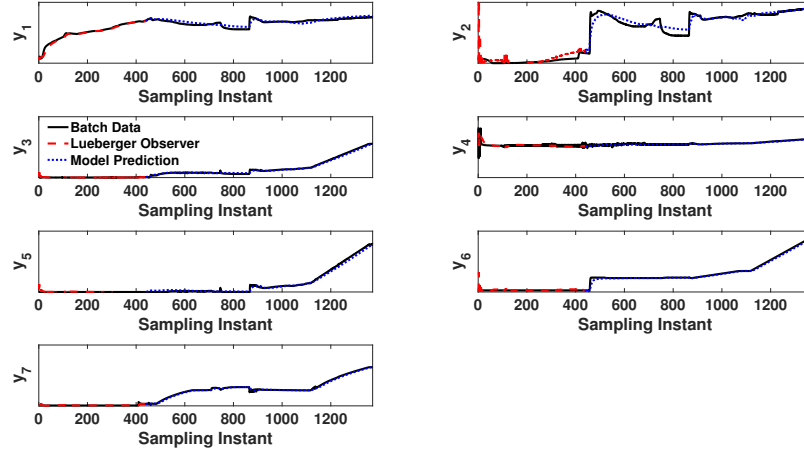


Figure 4.19: Validation results

Table 4.11: MASE for validation results in Figure 4.19

Outputs	y_1	y_2	y_3	y_4	y_5	y_6	y_7
MASE	12.88	10.19	5.82	0.97	7.43	9.64	4.85

4.4.2 Model Identification & Validation for Simulated Data

A database of 5 historical startup batches and 1 identification batch corresponding to step test around the nominal operating phase for different inputs were used as training datasets for the subspace identification algorithm. The database included batches ranging from 1560 to 6840 sampling instant duration. They consists of 10 manipulated variables and 7 outputs as illustrated in Figures 4.14 and 4.15. The variability among different startups is captured by suitably altering the various event triggers in the startup recipe. All the startups thus are of different lengths i.e., have a different startup time. A subspace state space model of order 52 was estimated (see Remark 4.4 for a discussion on this). Note that it was verified that the input signal for the simulated batches was persistently exciting, resulting in

the ability of the data to identify the appropriate underlying model.

The identified model was validated on another startup batch and the results are presented in Figure 4.19. For validation, Luenberger observer was utilized until outputs converge (this happens at 440th sampling instant). Then, the estimated LTI model is used to make the output predictions for the remainder of batch using the remainder of the input profile and the current state estimate as shown in Figure 4.18. As can be seen from Figure 4.19, the model predictions matches the simulated data (the prediction errors in the validation batch are quantified in Table 4.11). In essence, the identified LTI model is able to capture the complex nonlinear dynamics sufficiently well.

Remark 4.4. Note that the high order of the model is a direct consequence of the requirement to capture process nonlinearity of a complex system. It is important to recognize the distinction (and similarity) between models obtained using latent variable methods. While not directly applicable to the present application, a latent variable model [16] for batch processes typically includes far fewer latent variables or states. However, the model parameters are not necessarily any less. The latent variable models include ‘loadings’ corresponding to each sampling instance. Thus the reduced number of latent variables is offset by the number of loadings (matrices of the linear time varying model) that need to be determined. One of the key benefits of the proposed approach is that it enables capturing process nonlinearity, without any higher model complexity than the latent variable approaches. Further, the use of higher number of states did not result in any numerical issues in the present work.

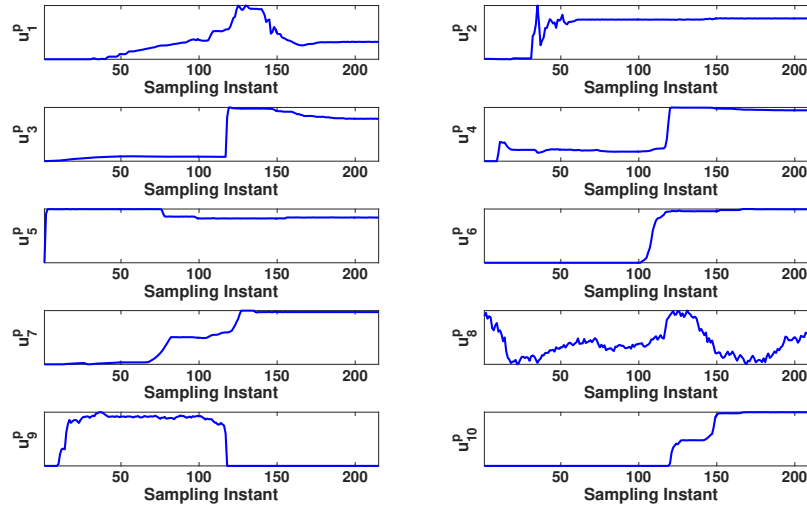


Figure 4.20: Input profiles for the validation startup batch from plant

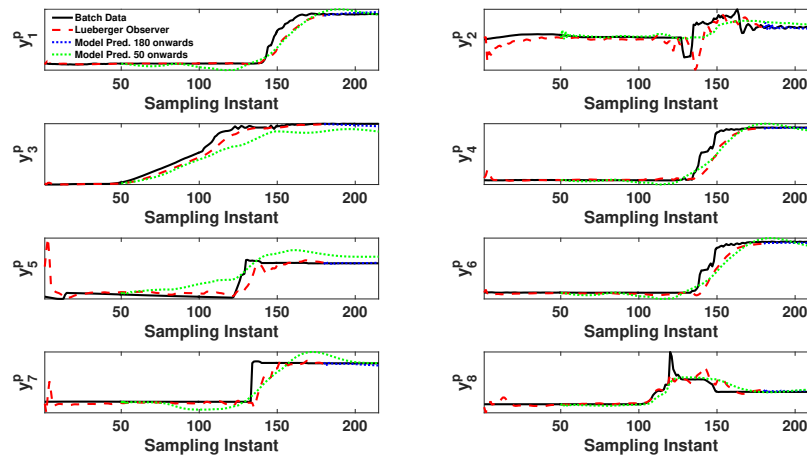


Figure 4.21: Output profiles prediction for plant data, with open loop prediction starting from 50 (dotted lines) and 180 (solid blue line) sampling instance. The red dashed line shows outputs from the Luenberger observer.

4.4.3 Model Identification & Validation for Plant Data

The proposed approach was next utilized to model data from a hydrogen unit startup. In this work, 4 datasets corresponding to cold startup of a hydrogen unit

Table 4.12: MASE for validation results in Figure 4.21 for predictions starting from 50th sampling instant onwards

Outputs	y_1^p	y_2^p	y_3^p	y_4^p	y_5^p	y_6^p	y_7^p	y_8^p
MASE	11.35	4.59	15.46	8.21	30.25	9.89	23.76	4.59

of Praxair Inc. were used to model the startup dynamics while the model was validated using another startup from the same plant. The dataset consisted of 10 manipulated and 8 output variables. A model of order 46 was estimated. It should be noted that all the startups were of different duration. For the validation batch, input profiles and the outputs along with predictions are shown in Figures 4.20 and 4.21 respectively. Some of the manipulated and output variables in the plant historian are different from the ones used for simulated study. This is because not all measurements are stored in the historian and thus can't be used for model estimation.

For the validation data set, the Luenberger observer was utilized until outputs converge. Then, the estimated LTI model is used to make the output predictions for the remainder of batch using the inputs as shown in Figure 4.21. The dashed lines show the outputs from the Luenberger observer. Note that the estimated output predictions staying reasonably close to the observed measurements simply shows that the observer is well tuned. The Luenberger observer outputs alone are not sufficient from a closed-loop implementation perspective. The key for closed-loop implementation is the ability of the model to predict future output behavior for a candidate input profile from a certain point into the batch. These are shown by the dashed green and solid blue lines in Figure 4.21, where the predictions are made starting from sampling instant 50 and 180, respectively. It can be seen that

the open loop predictions are reasonably good even starting from 50th sample (see Table 4.12 for a quantitative error measure) and improve considerably for the case where the predictions are made from 180th sampling instant onward. The identified model is thus an excellent candidate for closed-loop control and optimization.

Remark 4.5. Note that during the startup, various streams were turned on at different points for the training and validation data. This however does not necessitate building different models. The very fact that all these stream flowrates are inputs that are part of the modeling and validation datasets enables capturing the effect of these inputs on the process dynamics. In essence, the ability of the model to capture the dynamics follows from the fact that varying the inputs to an LTI system does not make the system time-varying.

Remark 4.6. The initial duration, over which the outputs converge serves as an important adaptive mechanism in the proposed approach, and is consistent with latent variable approaches where the scores for a particular batch can only be reasonably well estimated after some data from the new batch has been collected. In particular, the initial period where the observer ‘estimates’ the state for the new batch provides the proposed approach with the ability to ‘learn’ of the variations in the new batch, including variation in feedstock, and to account for the differences in the dynamics that result from that.

4.5 Conclusion

This work presents a data-driven model of the hydrogen production unit. To this end, a detailed first principles model of the entire plant was developed in UniSim Design, capable of simulating the startup and shutdown phase. Several simulated startups were used as training database for identification of reduced order data-driven model. An LTI data-driven model of the process using subspace identification based methods was estimated along with a simulation based study to demonstrate the suitability of linear models to approximate nonlinear dynamics. Simulation results demonstrate the prediction capabilities of the identified model and its suitability for deployment in an optimization framework.

Chapter 5

Model Predictive Control of Uni-Axial Rotational Molding Process

The results of this chapter have been published as:

JOURNAL PUBLICATIONS:

- A. Garg, F. P. C. Gomes, P. Mhaskar, and M. R. Thompson. Model predictive control of uni-axial rotational molding process. *Computers & Chemical Engineering*, 2018, Submitted

REFEREED CONFERENCE PROCEEDINGS:

- A. Garg, F. P. C. Gomes, P. Mhaskar, and M. R. Thompson. Data-driven control of rotational molding process. In *2019 Indian Control Conference (ICC)*, 2019, Submitted

5.1 Introduction

Rotational Molding, also known as rotomolding or rotational casting, is a batch process used for the processing of plastics through distinct heating and cooling phases [30]. In this process, a mold filled with a powdered charge is slowly rotated in a heated oven, resulting in the softened material being dispersed and sticking to the walls of the mold. In order to produce an even wall thickness, the mold is continuously rotated at all times both during the heating and cooling phase. The key process objectives are to obtain consistent high-quality products from one batch to another while avoiding unfinished parts with incomplete curing or degradation due to prolonged overheating. The challenges are to reject significant variability in the initial charge, and to determine 'recipes' to enable production of user-specified product quality. Given the significant nonlinearity and complexity of the process dynamics, first principles/mechanistic model based control strategies to address these challenges remain non-viable.

The current rotational molding processes therefore utilize an open loop, recipe-based policy. Significant experimental effort is invested in determining an input trajectory that yields the desirable product. The approach is predicated on the assumption that the desired product quality can be obtained by simply repeating previous successful input profiles. These approaches thus do not require a model and are easy to implement; however, the open-loop nature of the approach makes it susceptible to disturbances, and requires an entirely new set of experiments to determine the process operation for a different desired product quality. One approach to partially reject disturbances in the rotomolding process is trajectory tracking [1]. In this approach, a predefined set-point trajectory for a measured

process variable, such as internal mold air temperature, is tracked. The challenge with the trajectory tracking approach is that even with perfect tracking, it may not result in the desired quality, as the relationship between the measured/tracked variable and final quality may change significantly with changes in the process conditions across batches. The remedy is the use of a model based control strategy where the model is able to capture the relationship between the manipulated inputs and the final quality variables. A popular model-based control approach, MPC, has widely been studied for the control of batch processes [6, 4, 3], owing to the ability to utilize model predictions in the computation of the control actions in a way that respects process and input constraints. The approaches in [6, 4, 3] are, however, predicated on the use of a good first principles model, which is not readily available for the rotomolding process.

The lack of first principles models, and the abundance of historical data have motivated the development of models requiring minimal first principles knowledge, determined from past batch data, and their use for batch control. A variety of approaches for the development of data-driven models have been proposed. One popular approach is partial least squares (PLS), captures the essence of the process dynamics in a projected latent space [16, 18]. The model structure is similar to time-varying linear models, with the model predicting deviations from mean past trajectories. The specific model structure requires the batches to be the same length, or to recognize an appropriate alignment variable.

Rotomolding batches are not necessarily of the same duration, and more importantly, often need to be run for different times, where the run time itself is a decision variable. The PLS based modeling and control approaches do not remain

readily implementable in such scenarios.

To account for these limitations, a multi-model approach was proposed in [3]. More recently, adapting results for model designs for continuous processes ([46, 37, 54]), a subspace identification based batch modeling and control approach was proposed [11] where a linear time invariant (LTI) state-space model of the batch process is determined. The approach draws on the utilizing higher number of 'states' as needed to capture the process (nonlinear) dynamics. One of the major advantages to this approach is that it facilitates accommodating variable duration batches without the need for aligning different batch lengths, as demonstrated through different applications [11, 20, 24]. The approach thus appears well suited for adaption to rotomolding quality control.

Motivated by these considerations, this work presents a subspace identification based state-space modeling and control approach for a rotational molding process to achieve desired quality specifications. The objectives in this work are to reduce the variability in product quality across different batches and demonstrate the ability of the proposed approach to achieve specified product quality requirements. The novel contributions of the present work are a) subspace identification based state space model of the heating cycle coupled with a static product quality model and b) a linear programming based model predictive control design that enables optimizing for quality while also choosing the best batch duration for a uni-axial rotational molding process; a uni-axial process was chosen to start developing this novel control system since it is easier to include sensors, even though bi-axial processes are the norm in the industry. The rest of the paper is organized as follows: Section 5.2 describes the rotational molding

process, followed by a review of subspace identification approaches for batch processes. In Section 5.3, the proposed approach for modeling and control of a uni-axial rotational molding process is presented along with results from its application to an experimental setup. Finally, concluding remarks are made in Section 5.4.

5.2 Preliminaries

A brief overview of the uni-axial rotational molding process is presented in this section, followed by the subspace identification based modeling approach for batch processes.

5.2.1 Rotational Molding Process

Rotational molding (RM) is a widely used processing technique to produce seamless hollow plastic components mainly due to its simplicity and low operating cost. Each batch can be characterized by two distinct phases: heating and cooling. During the heating phase, powder resin is deposited and melted on the mold wall, trapping some air bubbles in between the coalescing molten particles. Thus, additional heating is required to drive the system to temperatures well above the melting temperature to allow the diffusion of entrained gases out of the polymer melt, a process also known as sintering [32]. However, excessive exposure to high temperature and oxygen inside the mold can cause thermo-oxidative degradation of the product. After completion of the heating phase, the mold is removed from the oven and cooled down using a directed stream of cold

air (or aerosolized water) to solidify the molded plastic. Due to the absence of shear in the process, a good distribution of the particles during sintering is only possible for a limited range of thermoplastic powders, polyethylene (PE) being the most commonly used [49]. The RM market potential is known to be limited by the lack of process control strategies to ensure good product quality while expanding the processing window.



Figure 5.22: Experimental setup for rotational molding

The experimental setup used in this study is shown in Figure 5.22. It consists of three manipulated inputs namely, actuator signals to left and right side oven heaters and a compressed air supply. Traditionally, in a laboratory-scale uni-axial rotational molding unit, heating is applied mostly through radiant panels inside the oven with still air. However, in this work, a supply of compressed air is introduced to provide additional control over the internal mold temperature. It

results in reduced heat losses due to increased convective heat transfer because of recirculation of the air inside the oven. This also constitutes a novel contribution in the present work. Note that the value of the manipulated input is converted into a ON-OFF signal by LabView such that ON time (out of 10s sampling time) is proportional to the value of the control action (between 0 and 100). In the modeling and control calculation, therefore, a continuous value of the heating control action is used. The variable that is available for online measurements is the internal mold temperature. The product specifications are quantified through measurements described in the next Section (see Table 5.13 for the list of input, online measured and quality variables).

The material used is a high density polyethylene (PE), Exxon Mobil™ HD 8660.29, donated by Imperial Oil Ltd., milled and sieved (35 mesh) in powder form for rotational molding applications. Each batch is initiated with a loading of 100g of the polyethylene powder into a cubic metallic mold with coated surfaces and a glass window for visual inspection. The mold is then closed and covered by an oven with two heated plates at temperatures varying from 300 to 340°C, and rotated at a speed of 4 RPM. Temperatures are monitored and recorded using a thermocouple installed to measure the internal air of the mold. In order to improve air circulation and promote cooling when required, a stream of compressed air (100 psi) is installed from the back of the oven and controlled (ON/OFF) by a solenoid. A LabView (National Instruments) interface is developed to control the heated plates and change the heating profile. At the designated curing point the oven is removed and forced cooling is promoted with a forced air of approximately 2.5 m/s. After reaching an internal air temperature below 80°C, the mold is opened

and the sample removed. The finished product is a cube of dimensions $85\text{mm} \times 85\text{mm} \times 3\text{mm}$ without top and bottom faces as shown in Figure 5.23. The process control challenge is to determine the control moves (heater actions and compressed air flow rate) online to achieve good product quality. To address this challenge, a model quantifying the relationship between the input moves and the product quality is needed, so it can be used within a model predictive control approach to determine the control action. Before presenting the modeling approach, the experimental quality measurement procedures are described.

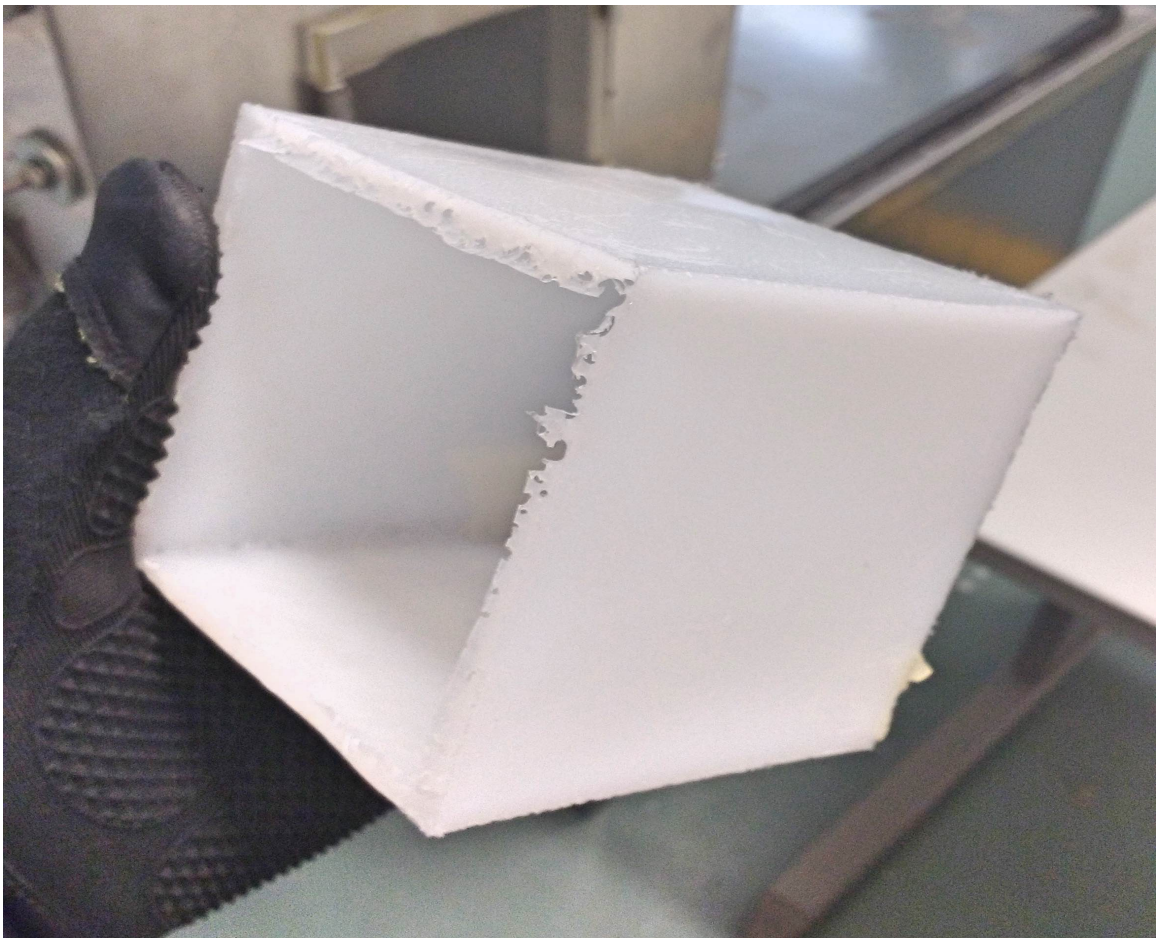


Figure 5.23: Finished product

Quality Measurements

Two nondestructive methods are used to measure and quantify product quality: ultrasonic and surface imaging. For the ultrasonic tests, two transducers (F30a and R15, Physical Acoustics Corp.) are affixed using high vacuum grease to the top of one of the cubic surfaces and separated by a 55mm center-to-center distance. A sequence of signals are generated from 135 to 165 kHz, propagated through the sample and recorded at a 4 MHz acquisition rate (National Instruments DAQ) as shown in Figure 5.24. The resultant signals are converted from time-domain to frequency domain using a fast-Fourier transformation. Each sample is analyzed by an averaged spectrum of 32 collected spectra with 0.4 kHz resolution from 1 to 1000 kHz. The quoted 'ultrasonic amplitude value' is calculated from the average of the maximum amplitude peak from the 32 spectra measured.

Surface image analysis is done on one of the cube faces. A thin layer of copper and graphite lubricant is applied to fill in surface voids reminiscent of trapped bubbles so that they stand out in images, with any excess removed using a paper tissue. A digital image captures a $40\text{mm} \times 40\text{mm}$ area and is post-processed to enhance contrast of surface voids. After the nondestructive analyses, samples are cut and prepared for the destructive (impact) tests. For the dart drop impact test, parts are stored for one day at a freezing temperature of -40°C . A standard dart weight of 6.804 kg is dropped from predetermined heights following a step-wise procedure (if the previous sample failed, decrease dart height by 0.1524 m; or if sample did not fail, increase height by 0.1524 m). Final impact energy is calculated from the minimum impact height that promotes failure of at least 50% of the samples. A minimum of nine samples are required for each processing condition.

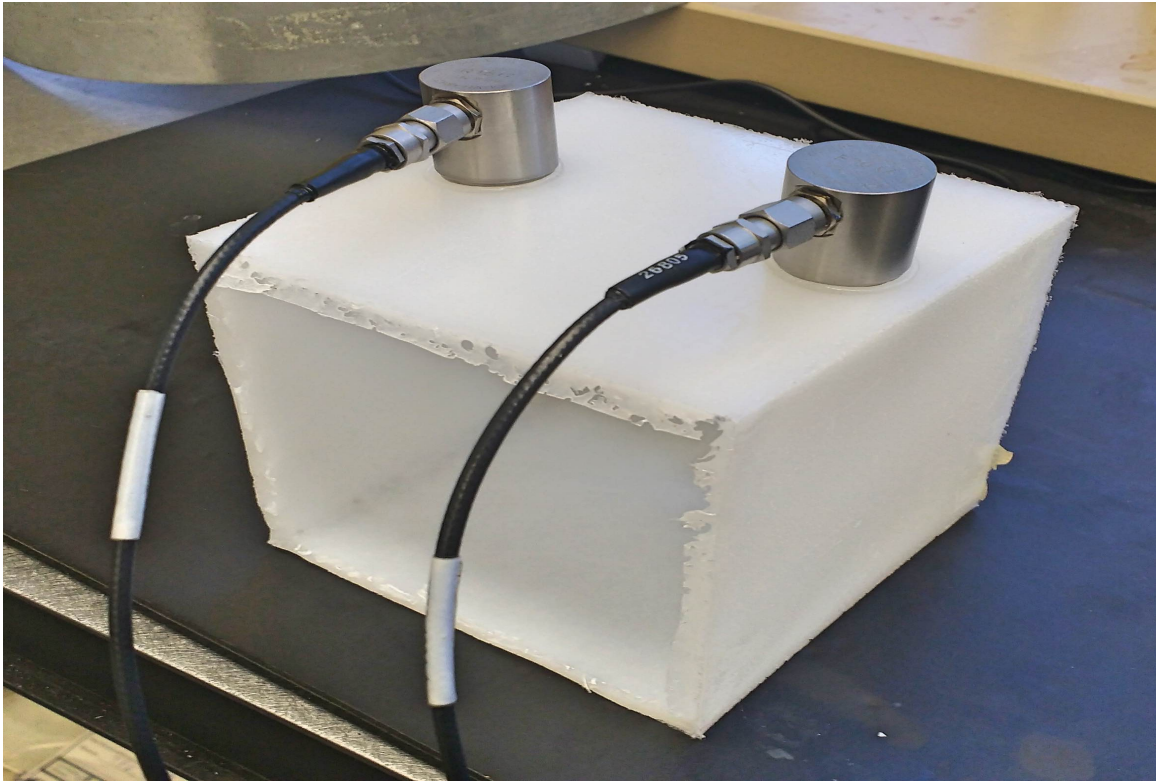


Figure 5.24: Molded product with two ultrasonic transducers affixed to the top of one of the cubic surfaces using high vacuum grease for non-destructive (ultrasonic) testing

A 30 mm square is cut for rheology test. A frequency sweep test is performed on a 25mm parallel plate rheometer (DHR TA Instruments), from 0.1 to 200 s^{-1} , with a 0.15 strain at a temperature of 190°C. The oscillatory data is converted to a viscosity-shear rate curve using a Cox-Merz transformation and a Cross model (see Equation (5.67)) was fit to obtain the zero-shear viscosity parameter (η_0). The test is repeated three times for each sample tested and statistical variation is calculated using a 95% confidence interval. Specifically, the viscosity is calculated

using the following equation:

$$\eta = \eta_{\infty} + \frac{\eta_0 - \eta_{\infty}}{1 + (C\dot{\gamma})^m} \quad (5.67)$$

where η is viscosity, η_0 is the zero-shear viscosity parameter, η_{∞} is the infinity-shear viscosity parameter, m is the Cross rate constant, $\dot{\gamma}$ is the shear rate constant and C is the Cross time constant. For this, the oscillatory data was converted to a viscosity (η) against shear rate ($\dot{\gamma}$) curve using a Cox-Merz transformation and a Cross model (Equation (5.67)) was fit using TRIOS software (TA Instruments) to obtain the zero-shear viscosity parameter (η_0). Other parameters were not evaluated for these experiments. Only the zero-shear viscosity was considered as a representative parameter for the thermo-oxidative degradation.

Table 5.13: Variables for the rotational molding process

Manipulated input	Measured output	quality variables
Left heater control action	Internal mold temperature	sinkhole area coverage (%)
Right heater control action		average ultrasonic spectra amplitude (dB)
Compressed air supply control action		Impact energy (Kg.m)
		Zero-shear viscosity (Pa - s)

5.2.2 Subspace Identification for Batch Processes

To achieve good quality control, a model is needed that can predict the quality variables for a given sequence of input moves, to use within an optimization framework to determine the optimal input moves (that will yield the desired quality). In the present manuscript, this is achieved by first building a dynamic model that can predict the internal mold temperature, and then building another model that can predict the final quality using the end point prediction of the

dynamic model. The dynamic model is built using the subspace identification method.

Subspace identification methods can be broadly categorized into deterministic, stochastic, and combined deterministic stochastic methods to identify linear dynamic models from process data. The key difference between these methods is the way in which process noise and disturbances are handled. In the present work, deterministic identification algorithms have been used. The deterministic identification problem can be explained as follows: If s measurements of the input $u_k \in \mathbb{R}^m$ and the output $y_k \in \mathbb{R}^l$ are given, the task is to determine the order n of a linear time invariant system of the following form (and the associated system matrices $\mathbf{A} \in \mathbb{R}^{n \times n}$, $\mathbf{B} \in \mathbb{R}^{n \times m}$, $\mathbf{C} \in \mathbb{R}^{l \times n}$, $\mathbf{D} \in \mathbb{R}^{l \times m}$ up to within a similarity transformation):

$$\mathbf{x}_{k+1}^d = \mathbf{A}\mathbf{x}_k^d + \mathbf{B}\mathbf{u}_k, \quad (5.68)$$

$$\mathbf{y}_k = \mathbf{C}\mathbf{x}_k^d + \mathbf{D}\mathbf{u}_k, \quad (5.69)$$

Unlike classical system identification (see, e.g., [58]), subspace methods are non-iterative and compute the unknowns using matrix algebra (see, e.g., [64, 55]). Different algorithms within subspace identification such as canonical variate analysis (CVA) [43], numerical algorithms for subspace state space system identification (N4SID) [51] and multivariable output error state space algorithm (MOESP) [66] have been shown to differ only in the weighting of the matrix used at the singular value decomposition step [65]. The existing results however are designed primarily for continuous processes (see, e.g., [68, 57, 54]). In these cases,

the training datasets are collected from identification experiments done around a desired steady-state condition and can readily be incorporated in the Hankel matrices formation step of the subspace identification algorithm. However, in case of batch processes, a meaningful steady-state is not available around which a model can be identified. Instead, a model for the transient dynamics of the process is required. Therefore, the nature of data collection for batch processes requires specific adaptation of the database, and subspace identification algorithm.

To this end, consider the output measurements of a batch process denoted as $\mathbf{y}^{(b)}[k]$, where k is the sampling instant since the batch initiation and b denotes the batch index. The output Hankel matrix for a batch b is given by:

$$\mathbf{Y}_{1|i}^{(b)} = \begin{bmatrix} \mathbf{y}^{(b)}[1] & \mathbf{y}^{(b)}[2] & \cdots & \mathbf{y}^{(b)}[j^{(b)}] \\ \vdots & \vdots & & \vdots \\ \mathbf{y}^{(b)}[i] & \mathbf{y}^{(b)}[i+1] & \cdots & \mathbf{y}^{(b)}[i+j^{(b)}-1] \end{bmatrix} \quad (5.70)$$

Unlike continuous processes, where the measurements comprises of one set of data, in batch operation, data is often available from multiple past batches. A simple concatenation of the data from the past batches into one ‘continuous’ dataset would result in the incorrect assumption of the starting point of one batch being similar to the end-point of the previous batch (which is not the case in practice). The key then is to form a single pseudo-Hankel matrix for both input and output data, recognizing the batch nature of the data, and is done by forming pseudo-Hankel matrices of the following form [11]:

$$\mathbf{Y}_{1|i} = \begin{bmatrix} \mathbf{Y}_{1|i}^{(1)} & \mathbf{Y}_{1|i}^{(2)} & \cdots & \mathbf{Y}_{1|i}^{(nb)} \end{bmatrix} \quad (5.71)$$

where, nb is the number of batches used for training. Similarly, pseudo-Hankel matrices for input data are formed. A distinctive feature of this approach is that, unlike time-dependent modeling approaches such as PLS, it does not impose any constraint on the length of different batches.

The deterministic algorithm presented in [48], and adapted in [11] is used for modeling in this work; however, the approach can be used with any of the standard subspace identification algorithms with appropriate adaptations. The key step of obtaining state trajectories involves computing SVD of the pseudo-Hankel matrix as follows. Let SVD of $\mathbf{H} = \begin{bmatrix} H_1 \\ H_2 \end{bmatrix}$ be given by

$$\mathbf{H} = \begin{bmatrix} U_{11} & U_{12} \\ U_{21} & U_{22} \end{bmatrix} \begin{bmatrix} S_{11} & 0 \\ 0 & 0 \end{bmatrix} V^t \quad (5.72)$$

then, the state vector can be computed as $U_q^t U_{12}^t H_1$. Here,

$$\mathbf{H}_1 = \begin{bmatrix} \mathbf{Y}_{1|i} \\ \mathbf{U}_{1|i} \end{bmatrix} \quad (5.73)$$

$$\mathbf{H}_2 = \begin{bmatrix} \mathbf{Y}_{1+i|2i} \\ \mathbf{U}_{1+i|2i} \end{bmatrix} \quad (5.74)$$

and U_q is defined through SVD of $U_{12}^t U_{11} S_{11}$ as

$$U_{12}^t U_{11} S_{11} = \begin{bmatrix} U_q & U_q^\perp \end{bmatrix} \begin{bmatrix} S_q & 0 \\ 0 & 0 \end{bmatrix} \begin{bmatrix} V_q^t \\ V_q^{\perp t} \end{bmatrix} \quad (5.75)$$

Once the state trajectories are obtained, the system matrices are computed using ordinary least squares as discussed in Chapter 4.

5.3 Data Driven Modeling and Control of a Rotational Molding Process

In this section, first a dynamic model is developed that is able to predict the internal mold temperature, and product quality, for a candidate input trajectory. This model is then utilized within an MPC formulation to achieve desired product quality.

5.3.1 Model Identification

In this process there are three inputs (control action for two heaters and a compressed air supply) and one output (mold internal temperature). For the purpose of model identification, historical data from 21 different batches (Figure 5.25) are used. Out of these, 15 were used for modeling and 6 for validation. The training batches are designed to provide a sufficiently rich data set, with the heating being turned off at significantly different mold temperatures. This variation provides richness to the data for better identification of a model which covers a large operating space of the process. Having obtained the data, first, a direct implementation of the data driven modeling approach [11] to describe the entire process dynamics (heating as well as cooling with additional input variable as the constant fan speed active during the cooling phase) were attempted. The resulting model did not achieve acceptable prediction (results showing the poor

prediction capability of the model are omitted for the sake of brevity).

Therefore, a model only for the heating phase is identified in this work. Further, the internal mold temperature ‘takes off’ after the powder melts, with each batch melting around the same temperature. While the subspace identification approach is able to describe nonlinearities over the operating range, this (state induced) change in the dynamics is too drastic to be able to be captured adequately by a single linear time invariant model. One possible recourse is to develop ‘time dependent’ or ‘phase dependent’ models (as is traditionally done in PLS based approaches). Such a modeling strategy would necessarily require indexing with respect to time, and therefore invalidate the time invariant nature of the model (and the ensuing utilization within an optimization framework to determine the processing time). Instead, in the present manuscript a single model is developed; however, the data from the initial part of the process is first used to estimate the current state of the process which helps the model recognize the dynamics of the present batch, and the model based controller only turns on after the powder melts.

Subsequently, a state-space model of order 3 is identified using the subspace identification approach for batch as described in Section 5.2. The model order is chosen to ensure good prediction for the batch set aside for cross validation. Note also that the dynamic model (and its validation) in the present work focuses on predicting the internal mold temperature alone and the quality predictions were not considered at this stage. A possible alternative is to validate the model order based on the prediction of both the internal mold temperature and the quality.

Remark 5.1. In this work, the model order is selected based on validation batch predictions. Future work would involve residual analysis development of Akaike

Table 5.14: Quality measurements for training batches, arranged in the increasing order of the MPC objective function values for case 1. Further the row corresponding to the minimum value of the MPC objective function for case 2 is highlighted.

Batches	Q_1	Q_2	Q_3	Q_4	Case 1: MPC objective function value	Case 2: MPC objective function value
Batch 7	1.56	21.23	5.01	6966	4.81	-1.91
Batch 16	3.22	15.70	4.25	6541	4.96	-1.31
Batch 17	1.66	18.47	4.87	6936	5.06	-1.62
Batch 20	5.58	14.38	3.63	6532	5.11	-1.09
Batch 15	2.65	13.97	4.87	6704	5.28	-1.19
Batch 19	6.62	9.15	3.01	6312	5.43	-0.52
Batch 9	7.81	6.30	3.01	6252.5	5.67	-0.23
Batch 18	4.91	8.65	4.25	6542	5.68	-0.59
Batch 21	4.11	7.58	3.63	6510	5.76	-0.43
Batch 12	3.91	6.55	3.63	6447	5.79	-0.33
Batch 5	2.67	16.83	4.25	7522	5.82	-1.33
Batch 4	5.57	7.54	3.01	6645	5.92	-0.33
Batch 3	2.52	10.89	4.15	7024	5.92	-0.78
Batch 2	5.98	6.36	4.15	6561	5.94	-0.33
Batch 1	1.04	16.67	4.87	8088.5	6.38	-1.33
Batch 10	0.99	23.78	5.01	11356.5	8.94	-1.73
Batch 11	0.88	20.17	6.74	11131	9.06	-1.57
Batch 14	0.59	25.06	6.39	11990	9.43	-1.94
Batch 8	0.38	23.42	6.22	12362.5	9.96	-1.72
Batch 13	0.5	22.09	6.39	12659	10.39	-1.58
Batch 6	0.22	23.51	6.39	13418	11.01	-1.65

Information Criterion (AIC) like measures for quantifying parsimonious order selection.

The identified state-space model is then augmented with a linear quality model identified using a least squares approach. For this, the quality measurement of the finished sample across training batches (refer to the first four columns in Table 5.14) is related to the terminal states of the above state-space model through a

linear model of following form.

$$Q_{t_f} = \hat{L}_m x[t_{f_{heat}}] + e \quad (5.76)$$

were Q_{t_f} , \hat{L}_m , $x[t_{f_{heat}}]$ and e denote quality measurements, least squares solution of the model, terminal states of the subspace model and white noise respectively. This model in conjunction with subspace model describes the rotational molding process dynamics completely. Further, $t_{f_{heat}}$ and t_f denotes the time for heating cycle completion and batch termination respectively.

This model facilitates the prediction of product quality during the batch operation based on predictions of the terminal states obtained from the subspace identification model. Mathematically, this can be written as follow.

$$\hat{Q}_{t_f} = \hat{L}_m \hat{x}[t_{f_{heat}}] \quad (5.77)$$

Remark 5.2. A static model is identified for modeling quality in this work. However, a dynamic model for quality can also be estimated where the final quality depends not only on the terminal states but the entire state trajectory.

Remark 5.3. Another modeling approach could include identifying multiple models which captures the dynamics of the process during initial duration of the heating cycle and after the powder has melted completely. Further, instead of predicting the quality based on the states at the end of the heating cycle, the cooling cycle can be modeled (essentially a stochastic model) and the quality then be modeled and predicted based on the terminal states of this model. These avenues are beyond the scope of the present work and will be explored in future

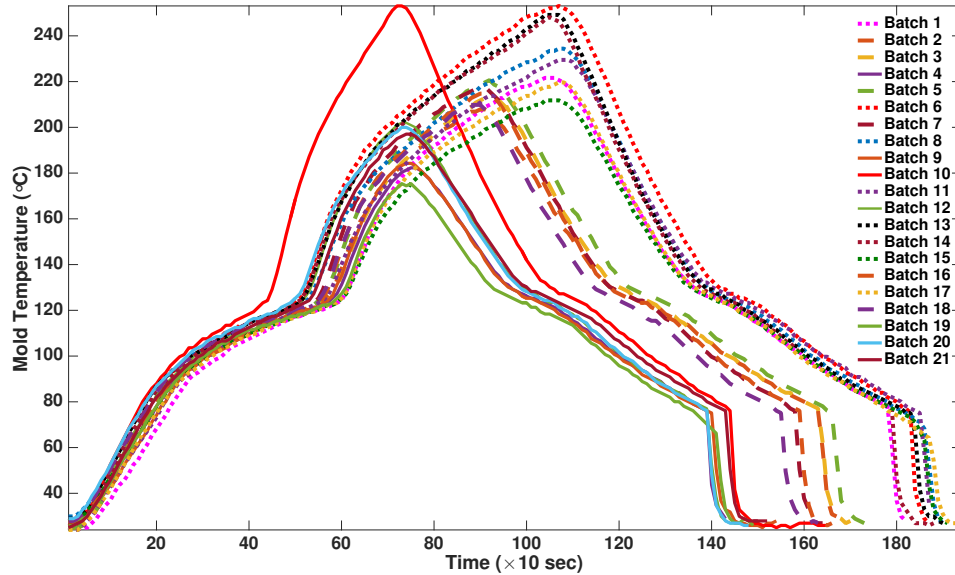


Figure 5.25: Mold internal temperatures for training batches

work.

5.3.2 Predictive Control Of Rotational Molding Process

Once a model which captures the process dynamics reasonably well has been developed, it can be incorporated in a predictive control framework to achieve desired product specifications. This constitutes the second step of the approach. Good model predictions (using state-space model augmented with a quality model) are dictated primarily by two components: initial state estimate and the state-space model matrices. State-space matrices are known once the model is estimated, which also involves determining the initial state of the system for each training batch (based on the entire batch behavior). However, when implementing such an approach in a control framework (i.e., for a new batch), the entire batch

data is unavailable, and thus the application of this approach naturally involves state estimation for the initial batch duration. In this work, this is achieved as follow: first a PI controller is used to track a predefined set-point (300°C) for the two oven temperatures (left and right side heater) to calculate the input moves for the two heaters and a compressed air supply. This is done till the mold internal temperature reaches a predefined threshold temperature (130°C in this work) following which, after an appropriate state estimator has been run to determine state estimates, the controller is turned on. In essence, during the initial time when a PI controller is used, the MPC gathers temperature information corresponding to the phenomena of heating, powder adhesion and melting of the powder in that particular batch, and then uses that information to control the sintering (heating) phase. The Luenberger observer utilized in the present work takes the following form:

$$\hat{\mathbf{x}}[k + 1] = \mathbf{A}\hat{\mathbf{x}}[k] + \mathbf{B}\mathbf{u}[k] + \mathbf{L}(\mathbf{y}[k] - \hat{\mathbf{y}}[k]) \quad (5.78)$$

where \mathbf{L} is the observer gain and is designed based on the desired eigenvalues of $(\mathbf{A} - \mathbf{L}\mathbf{C})$ chosen to be within the unit circle (achieved using the *place* command in MATLAB). After the state estimates have converged, the controller is activated and is used to control the process till the completion of batch heating cycle.

Remark 5.4. Although a Luenberger observer is used in this work, any observer/state estimator can be used to obtain the state estimates. The other key choice is that of the initial guess for the state estimates; they can either be chosen as zero (in the absence of any prior information), or as the average of

the initial identified states in the training data set. More importantly, this initial state estimation period can be understood as the online ‘learning’ aspect of the modeling approach, where the model is ‘tuned’ to the specific dynamics of the present batch.

In continuous operation the objective is that of stabilization, and the process is run continuously, leading to a receding horizon implementation of MPC. Both the control objective, and the control horizon are different for batch operation, and this must be appropriately accounted for in the control design. Note also that in the present application, the heating cycle length (and thus the batch length) is also a decision variable obtained as a solution of MPC.

For the control implementation, the control action is computed every 10s. At a sampling instance l , where the current estimate of the states generated by the Luenberger observer is denoted by $\hat{\mathbf{x}}[l-1]$, and the last control action implemented on the process is denoted by $\mathbf{u}[1]$, the optimal trajectory from the current instance to

the end of the batch is computed by solving the following optimization problem:

$$\min_{\mathbf{U}_f, l_f} \beta \hat{Q}_{t_f}[l_f - l] \quad (5.79a)$$

$$s.t. \quad U_{j,min} \leq u_f[k] \leq U_{j,max}, \quad \forall \quad 0 \leq k \leq l_f - l \quad (5.79b)$$

$$|u_f[0] - u[l - 1]| \leq \delta, \quad (5.79c)$$

$$|u_f[k] - u[k - 1]| \leq \delta, \quad \forall \quad 1 \leq k \leq l_f - l \quad (5.79d)$$

$$\hat{\mathbf{x}}[0] = \hat{\mathbf{x}}[l] \quad (5.79e)$$

$$l_f \in \{t_{switch} + 300, t_{switch} + 350, t_{switch} + 400\} \quad (5.79f)$$

$$\hat{\mathbf{x}}[k + 1] = \mathbf{A}\hat{\mathbf{x}}[k] + \mathbf{B}\mathbf{u}_f[k] \quad (5.79g)$$

$$\hat{\mathbf{y}}[k] = \mathbf{C}\hat{\mathbf{x}}[k] + \mathbf{D}\mathbf{u}_f[k] \quad \forall \quad 0 \leq k \leq l_f - l \quad (5.79h)$$

$$\hat{Q}_{t_f} = L_m \hat{x}[l_f] \quad (5.79i)$$

where,

$$\hat{Q} = \begin{bmatrix} \hat{Q}_1 & \hat{Q}_2 & \hat{Q}_3 & \hat{Q}_4 \end{bmatrix}^T \quad (5.80a)$$

$$\beta = \begin{bmatrix} 10^{-2} & -10^{-1} & -10^{-2} & 10^{-3} \end{bmatrix} \quad (5.80b)$$

Further, $\mathbf{U}_f = [\mathbf{u}_f[0], \mathbf{u}_f[1], \dots, \mathbf{u}_f[l_f - l]]$ (the remaining input profile) is the decision variable (consisting of two heater and air supply control action), l_f is the heating cycle completion time and the set for choosing the l_f is specified based on the experience with the experimental setup regarding the duration of batch lengths, $\delta = \begin{bmatrix} 30 & 30 & 30 \end{bmatrix}^T$ is the allowed rate of change of the input, $U_{j,min}$ and $U_{j,max}$ are the constraints on the manipulated variable. In addition, t_{switch} denotes the time (in sec) at which controller switches to MPC from PI controller.

Equation (5.79b) represents the constraint on the inputs with $U_{j,min}$ and $U_{j,max}$ being $\begin{bmatrix} 0 & 0 & 0 \end{bmatrix}^T$ and $\begin{bmatrix} 100 & 100 & 100 \end{bmatrix}^T$ respectively. Equations (5.79c) and (5.79d) specify the rate constraint on the inputs. Equation (5.79e) specifies the current state estimate obtained from the Luenberger observer at that instant while Equation (5.79f) denotes three allowable values of the duration of the heating cycle. Finally, Equation (5.79i) specifies the quality model to predict the terminal quality of the product using the terminal states predicted by the state space model as specified in the Equations (5.79g)-(5.79h).

One of the key strengths of the proposed formulation is the ability to specify the control objective to reflect the product quality. In particular, to recognize the fact that the desired product quality reflects, in some sense, trading off some of the quality variables against others. This is quantified through the choice of the vector β . In this particular implementation, β is chosen in the following fashion: First, 'reasonable' values of the parameters are chosen based on the relative importance (and magnitudes) of the quality variables. The objective function is then evaluated for the 21 batches in the training data and the batches ranked according to the objective function. The value of the parameters are then tweaked to ensure that the batches which are deemed, qualitatively, to be better are consistent with the objective function value (i.e., the best batches have the lowest objective function value). This is in line with industrial practice where an operator/quality controller could be asked to rank the product in terms of quality, which would then enable picking the parameters of β in a similar fashion.

The above optimization problem is essentially a mixed integer linear program (MILP) but instead solved in a brute force fashion as three linear programs using

linprog in MATLAB. To implement the control algorithm on the experimental setup, MATLAB is interfaced with LabView which in-turn works as a data acquisition system.

5.3.3 Closed-Loop Experimental Results

The proposed modeling and control approach is next implemented on the experimental set ups. Two sets of closed-loop implementations are carried out. The first step was to evaluate the ability of the controller to reject variability and meet product specifications (considering balanced importance given to all quality measurements) and the second step was to evaluate the ability of the controller to achieve new product specifications.

In the first implementation, the controller was tested on five new batches. l_f in all of these batches was selected as $t_{switch} + 350$ by the MPC. The feedback control algorithm achieves excellent quality results with the values obtained meeting the desired product specifications, and more importantly, the average value of the objective function obtained in these MPC batches is 5.06 (see Table 5.15) in comparison to the 4.81–11.01 range (in Table 5.14) with an average of 6.78 obtained in the training batches (also, see Figure 5.26). The corresponding temperature profiles for the internal mold temperatures are as shown in Figure 5.27. From these results, it can be noticed that the thermo-oxidative degradation was minimized with no significant change in viscosity (Q_4) from the base material. However, values of Q_1 - Q_3 achieved an average quality. This formulation would be suitable for applications where effects from degradation should be minimized, such as formation of volatile components that can contaminate rotomolded water tanks.

Table 5.15: Case 1: Quality measurements for MPC batches

Batches	Q_1	Q_2	Q_3	Q_4	MPC objective function value
MPC Batch 1	7.79	9.54	4.67	5891	4.97
MPC Batch 2	7.38	13.98	4.67	5934	4.56
MPC Batch 3	7.06	10.80	3.63	6459	5.41
MPC Batch 4	7.85	10.3	3.63	6401	5.41
MPC Batch 5	7.09	15.37	3.63	6445	4.94

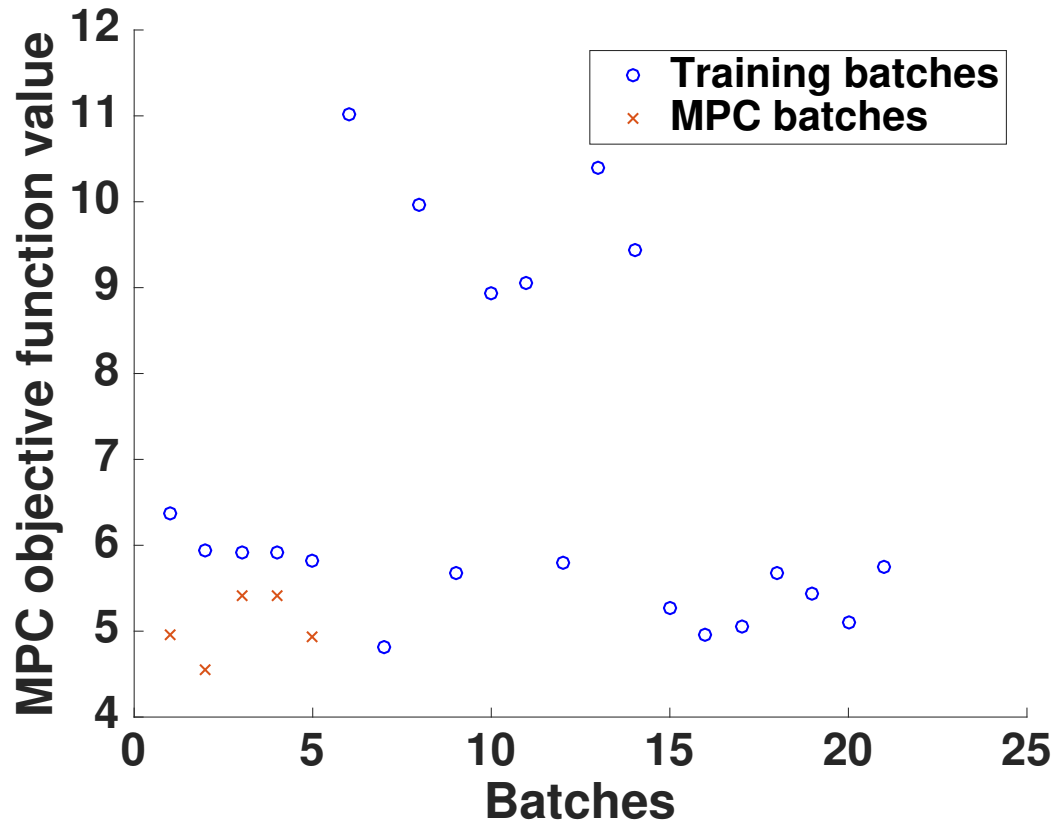


Figure 5.26: Case 1: Comparison of MPC objective function values between training and MPC batches

Remark 5.5. In another work[30], the authors have proposed an alternative to destructive methods for quality assessment using the ultrasonic spectral data.

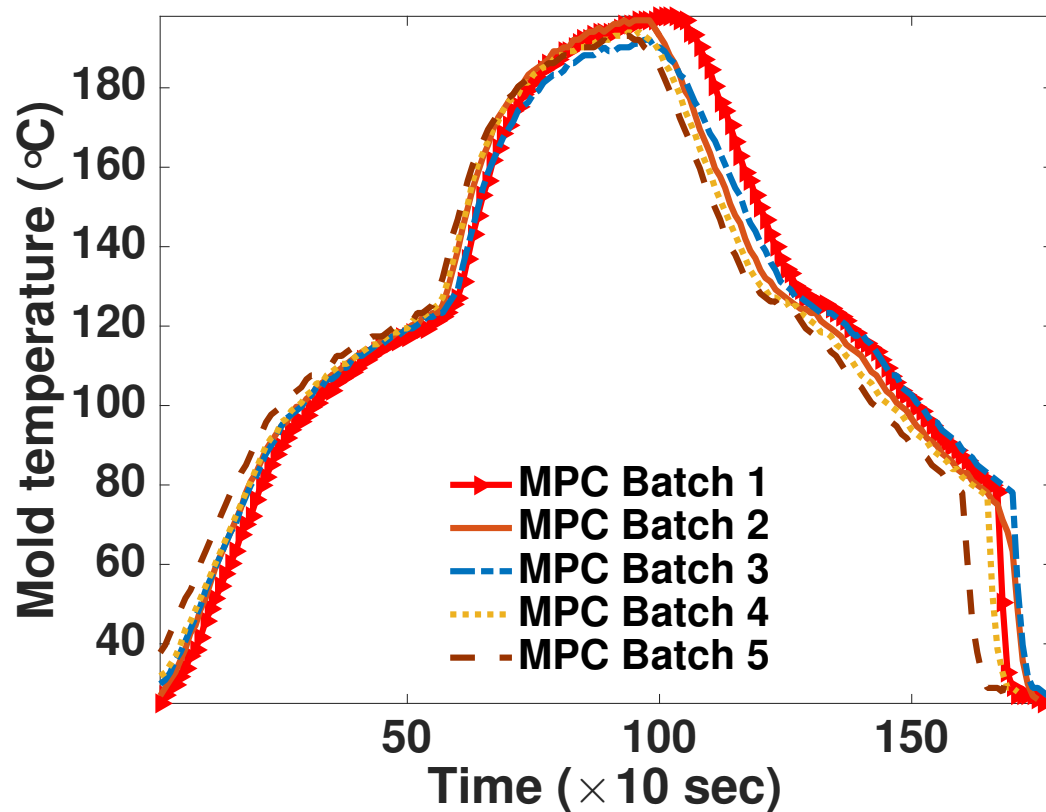


Figure 5.27: Mold internal temperatures for MPC batches

Future work will also focus on predicting the ultrasonic spectral data in order to predict the product quality. Further, machine learning based approaches will be utilized to build a classifier for product quality based on the image of the product. This classifier will be suitably integrated with the state-space model to obtain optimal control using MPC.

Remark 5.6. The framework developed in this work for the control of uni-axial rotational molding process will also be extended to the case of bi-axial rotational molding process. One of the major challenge in the control of bi-axial rotomolding process is the non-availability of the internal mold temperature measurements.

Therefore, alternative source of measuring the internal temperature will be sought and appropriately modeled.

In the second implementation, the efficacy of the proposed approach to obtain a different product quality (for instance, due to a client requirement) is evaluated. For some applications, a small degree of thermo-oxidative degradation can be acceptable with no deterioration of mechanical strength. Thus, the objective function in the earlier formulation was modified such that the training batches with higher impact properties are the ones that result in the lowest values of the objective function. It should be noted that all the quality variables were still considered in this formulations as excessive heating and degradation should still be minimized. Therefore β was changed to the following

$$\beta = \begin{bmatrix} 10^{-6} & -10^{-5} & -10^{-5} & 10^{-4} \end{bmatrix} \quad (5.81)$$

Table 5.16: Case 2: Quality measurements for MPC batches

Batches	Q_1	Q_2	Q_3	Q_4	Case 2: MPC objective function value
MPC Batch 1	1.41	23.18	5.7	8842	-1.9897
MPC Batch 2	1.69	22.98	5.7	9748	-1.8763
MPC Batch 3	1.75	19.99	5.7	8302	-1.7213
MPC Batch 4	1.20	22.53	5.7	9843	-1.8267
MPC Batch 5	1.99	17.30	5.7	7675	-1.5126

Rest of the MPC problem was as stated for the previous case. The results obtained for this scenario are summarized in Table 5.16 (also see Figure 5.28). The internal mold temperature for the MPC batches is as shown in Figure 5.29.

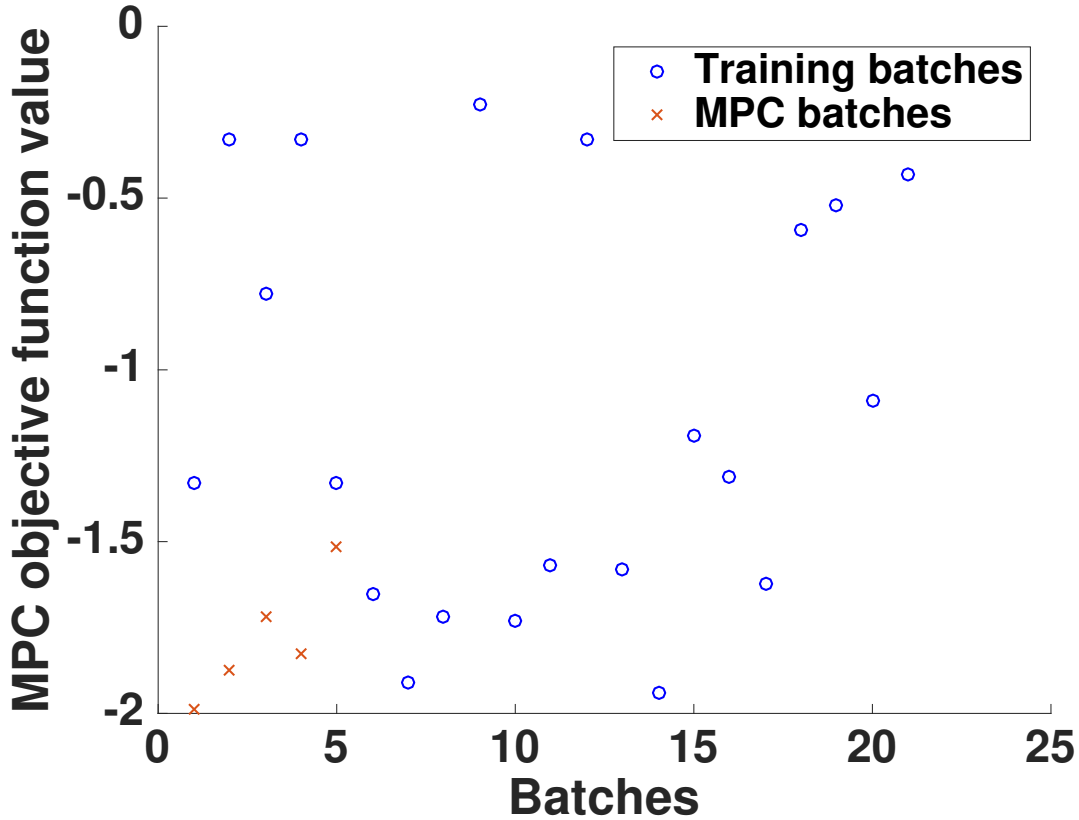


Figure 5.28: Case 2: Comparison of MPC objective function values between training and MPC batches

The product obtained at the end of the batches had lower sintering. It should be noted that the MPC resulted in a sharp increase in the internal mold temperature with reduced batch time ($l_f = t_{switch} + 300$) compared to the previous case where MPC selected a safe heating profile with minimized degradation over a longer batch duration (refer to Figure 5.30 for MPC control moves). This is to facilitate improved sintering in the product, with better mechanical properties, at the expense of some degradation. It demonstrates the capability of the proposed model in predicting the terminal quality effectively and thereby optimizing the

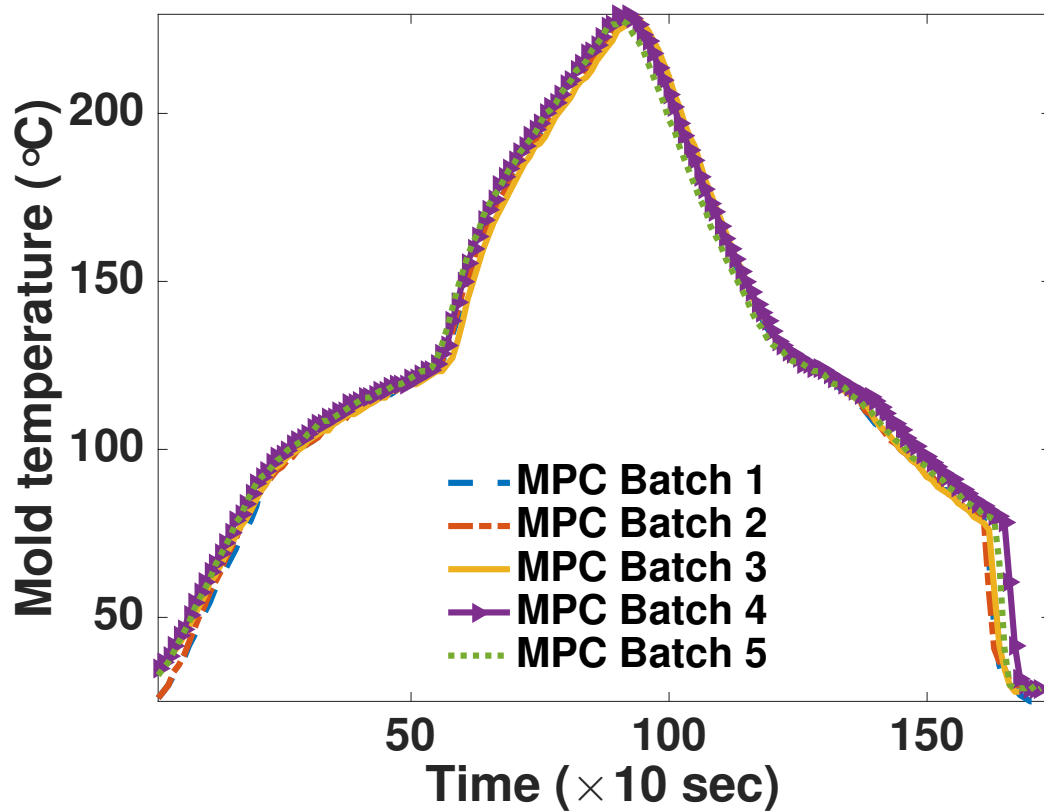


Figure 5.29: Case 2: Mold internal temperatures for MPC batches

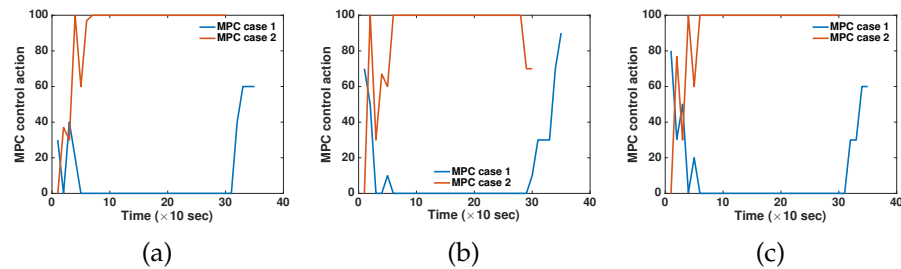


Figure 5.30: MPC control signals (after switching from PI controller) for one candidate batch from the two cases for (a) heater 1, (b) heater 2 and (b) compressed air supply.

process according to the desired quality requirements. Although not pursued in this work, the MPC formulation can readily be adapted to specify constraints on

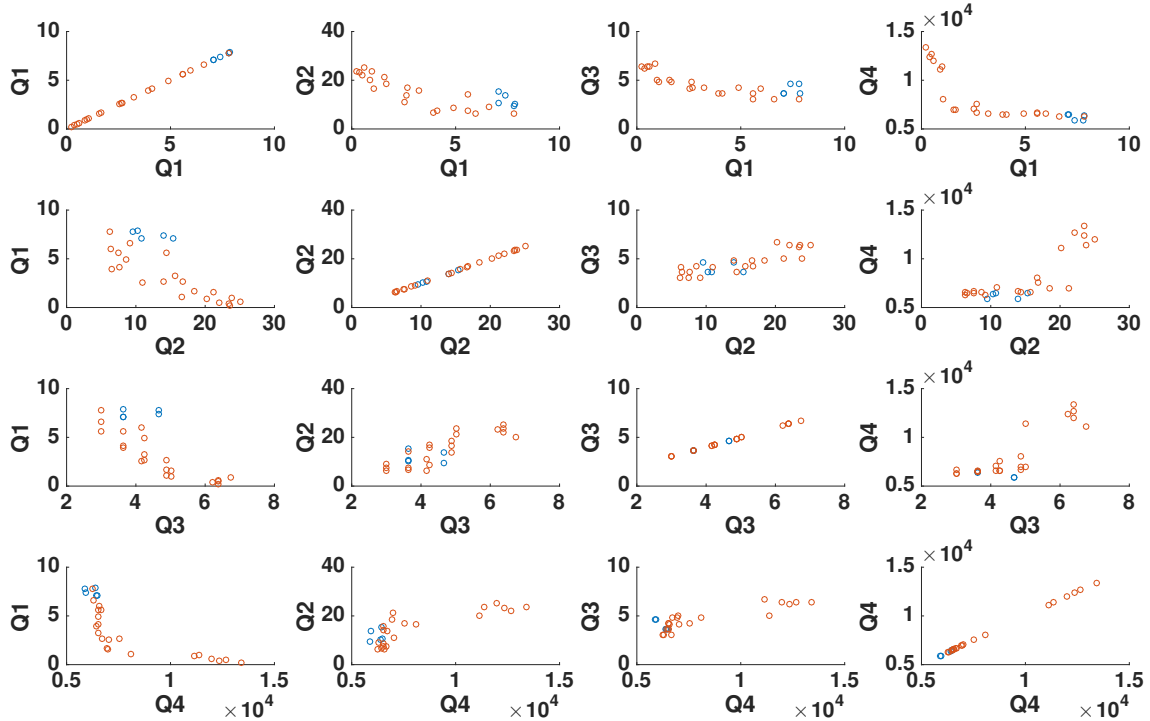


Figure 5.31: Case 1: Scatter plot for the quality values obtained in the training (red circles) and MPC batches (blue circles).

the value of individual quality variables.

Further, in Figure 5.31 it can be noticed that all MPC batches have quality inside the range of training batches. Although an overall balance between quality properties is achieved by the MPC formulation, the MPC batches are located at the extremes of some variables. The scatter plot corresponding to $Q1$ versus $Q4$ demonstrate that control action from MPC was focused on avoiding degradation. Whereas in the second formulation (see Figure 5.32), the scatter plot $Q1$ versus $Q4$ showed that the MPC batches were located slightly above the point of degradation to improve the impact properties. In addition, these scatter plots

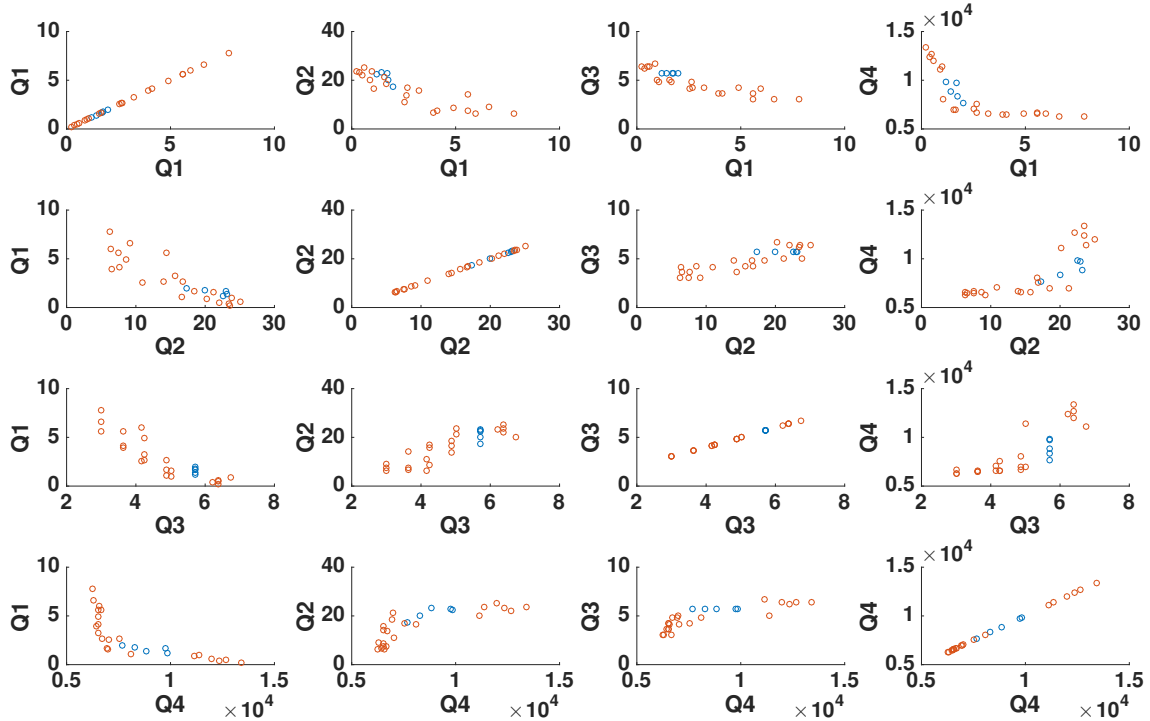


Figure 5.32: Case 2: Scatter plot for the quality values obtained in the training (red circles) and MPC batches (blue circles).

also demonstrate the ability of the proposed modeling and control approach in rejecting the initial product variability and other process disturbances.

Remark 5.7. To implement the proposed approach in an industrial setting, the model can be developed by utilizing the data from plant historian with a few identification experiments, if required. Once the proposed system is in place, the operator would not need any details on the identification or MPC algorithm and the desired product properties can be specified using a simplified interface. Further, for initial training the approach can be developed and provided to a operator in the form of a decision support tool which can aid them in decision

making process with the flexibility to implement the control action they are comfortable with.

5.4 Conclusions

In this work, a novel data-driven model predictive controller for uni-axial rotational molding process is proposed. Batch subspace identification algorithm is used to identify a linear time-invariant state-space model of the process. The identified model is then deployed within MPC to achieve a desired quality of the mold. The results show the merits of the proposed approach in terms of improved quality, variability rejection across difference batches and the ability to achieve the specified grade of product. Future work would be to include the initial raw material information (such as molecular structure information based on rheology flow curves and powder particle size distribution) in the identified model of the process. Such a model would enable prediction of achievable product quality range given information about the resin to be used for rotomolding.

Chapter 6

Conclusions and Future Work

This chapter discusses the main contributions of this work and the directions for future research avenues.

6.1 Conclusions

The research focus in this work is on data-driven modeling and control of batch processes using subspace identification algorithms specifically adapted for batch processes. First, in Chapter 2, we explored the capability of subspace identification in modeling a highly nonlinear and infinite dimensional seeded batch crystallization process described mathematically using population balance equations. A linear model predictive controller (MPC) design with subspace identification model at its heart is shown to achieve a particle size distribution with desired characteristics subject to both manipulated input and product quality constraints in comparison to traditional control practices. In addition, suitability of the proposed approach when subjected to uncertainty and time-

varying parameters is demonstrated. The chapter also emphasized the merits of the proposed modeling approach against using the conventional subspace identification algorithm for continuous processes. The predictions obtained in the latter case were worse than the proposed approach. This underlines the need for including multiple batch datasets for identification of the process dynamics.

In Chapter 2, the PSD measurements were reduced to two dimensional measurements through the use of moments. The consequence of this is that the identified model can only predict the moments and not the entire particle size distribution. To overcome this limitation, in Chapter 3, the use of big data (data variety aspect) in modeling the batch crystallization process through a combination of a dynamic and quality model is presented. It aids in the capability of the model to predict the PSD throughout the batch. Therefore, the proposed approach is able to predict a coarser PSD evolution throughout the batch and utilizes the subspace states at the end of the batch to predict the final product quality i.e., a finer PSD. This resulted in the possibility of directly controlling the 'shape' of the distribution in the final product. Therefore, a novel subspace identification based predictive controller with explicit model validity constraint, capable of incorporating data variety, for a seeded batch crystallization process is proposed. The effectiveness of the proposed approach in terms of improved product quality are demonstrated through two different formulations.

Next, in Chapter 4, the data-driven modeling ideas presented in the previous chapters are extended to an industrial hydrogen plant startup process. Although operation of a hydrogen plant falls under the realm of continuous process, however, due to the nature of startup and shutdown process, it can be categorized

as a batch-like process. The objective in this work was to develop a data-driven model of the hydrogen plant that can be used to predict the evolution of startup. For this, a detailed first principles model of the entire plant was developed in UniSim Design, with the capability to simulate startup and shutdown phase. These simulations were used for identification of a reduced order data-driven model using subspace identification based approach. In addition, simulation based study is presented to demonstrate the suitability of the linear models to approximate nonlinear dynamics. Simulation results as well as application on real plant data demonstrate the prediction capabilities of the identified model.

Finally, in Chapter 5, we utilized these ideas for modeling and online control of an experimental setup. For this, a novel modeling and control approach for uniaxial rotational molding process is proposed. Subspace identification is used to identify a linear time-invariant model of the process, which is then subsequently deployed within MPC to achieve a user-specified product quality. The results demonstrate the efficacy of the proposed framework in terms of improved quality, variability rejection across batches and the ability to achieve specified grade of product.

6.2 Future Work

In this section, directions for future work are outlined.

- With big data gaining popularity in both academia and industry alike, it provides an opportunity for process control practitioners to develop techniques suitable for process industries. Although most of the challenges

that constitutes big data are best handled within the fields of computer science, two of its aspects, data variety and veracity, falls within the realm of process control. While in Chapter 3, handling data variety aspect in the context of a batch crystallization process, the framework can be adapted to handle data varacity. Data varacity refers to uncertainty in the data and in the context of process control, it would mean handling missing and non-uniform measurements. While missing measurements may be a result of corrupt values in the data historian, limitations of the instrumentation system can result in different measurements being collected at non-uniform sampling rate. Therefore, it will be interesting to adapt the subspace identification approach to handle data varacity for modeling and control of batch processes. One possible approach would be to iteratively converge to the values of the missing values such that the estimates are consistent with the subspace identification model.

- In Chapter 4, the predictive capability of the proposed approach on both simulated and industrial startup data was demonstrated. The model has been used to develop a decision support tool for the operator which will aid in predicting the timeline for startup completion. This is important for estimating the availability of the product (hydrogen). These results have been omitted from this thesis as we would like to extend this work to design optimal closed-loop startup strategies using a MPC with the identified model at its core. Further, the developed framework can be used to optimize the plant shutdown as well.
- In Chapter 5, a framework for data-driven model predictive control of

uni-axial rotational molding process is demonstrated. There are a number of research avenues available in this project to further enhance the rotomolding control. Firstly, a static model between initial raw material information (such as molecular structure information based on rheology flow curves and powder particle size distribution) and initial states of the state-space model can be estimated. Such a model would aid in predicting the achievable product quality range given information about the resin being used for rotational molding. Secondly, in another work [30] (not being included in this thesis), we have proposed alternative quality assessment approach using ultrasonic spectral data instead of destructive tests. Extension of this work will focus on predicting the ultrasonic spectral data to gauge the product quality. Further, machine learning based approaches can be used to build a classifier for product quality based on the image of the product. This can then be suitably integrated with the state-space model to optimally control the rotomolding process using MPC. Lastly, the framework will be extended to the case of bi-axial rotomolding. One of the major challenge in this case would be the non-availability of the internal mold temperature measurements. Therefore, alternative source of measuring the internal temperature will be sought and integrated with our approach.

Bibliography

- [1] D. I. Abu-Al-Nadi, D. I. Abu-Fara, I. Rawabdeh, and R. J. Crawford. Control of rotational molding using adaptive fuzzy systems. *Advances in Polymer Technology*, 24(4):266–277, 2005.
- [2] B. Alhamad, J. a. Romagnoli, and V. G. Gomes. On-line multi-variable predictive control of molar mass and particle size distributions in free-radical emulsion copolymerization. *Chemical Engineering Science*, 60(23):6596–6606, 2005.
- [3] S. Aumi, B. Corbett, P. Mhaskar, and T. Clarke-Pringle. Data-based modeling and control of Nylon-6, 6 batch polymerization. *IEEE Transactions on Control Systems Technology*, 21(1):94–106, 2013.
- [4] S. Aumi and P. Mhaskar. Integrating Data-Based Modeling and Nonlinear Control Tools For Batch Process Control. *Aiche Journal*, 58:2105–2119, 2012.
- [5] R. Batres, J. Soutter, S. P. Asprey, and P. Chung. Operating procedure synthesis: science or art. *The Knowledge Engineering Review*, 17(3):S0269888902000498, sep 2002.

- [6] D. Bonvin. Optimal operation of batch reactors—a personal view. *Journal of Process Control*, 8(5-6):355–368, oct 1998.
- [7] D. Bonvin, B. Srinivasan, and D. Hunkeler. Control and optimization of batch processes. *IEEE Control Systems Magazine*, 26(6):34–45, dec 2006.
- [8] P. D. Christofides, N. El-Farra, M. Li, and P. Mhaskar. Model-based control of particulate processes. *Chemical Engineering Science*, 63(5):1156–1172, 2008.
- [9] P. D. Christofides, M. Li, and L. Mädler. Control of particulate processes: Recent results and future challenges. *Powder Technology*, 175(1):1–7, 2007.
- [10] B. Corbett, B. Macdonald, and P. Mhaskar. Model Predictive Quality Control of Polymethyl Methacrylate. *IEEE Transactions on Control Systems Technology*, 23(2):687–692, mar 2015.
- [11] B. Corbett and P. Mhaskar. Subspace identification for data-driven modeling and quality control of batch processes. *AIChE Journal*, 62(5):1581–1601, may 2016.
- [12] B. Corbett and P. Mhaskar. Data-Driven Modeling and Quality Control of Variable Duration Batch Processes with Discrete Inputs. *Industrial & Engineering Chemistry Research*, 56(24):6962–6980, jun 2017.
- [13] Dong, T. J. McAvoy, and E. Zafiriou. Batch-to-Batch Optimization Using Neural Network Models. *Industrial & Engineering Chemistry Research*, 35(7):2269–2276, jan 1996.
- [14] F. J. Doyle, C. a. Harrison, and T. J. Crowley. Hybrid model-based approach to batch-to-batch control of particle size distribution in emulsion

- polymerization. *Computers & Chemical Engineering*, 27(8-9):1153–1163, sep 2003.
- [15] M. Du, P. Mhaskar, Y. Zhu, and J. Flores-Cerrillo. Safe-Parking of a Hydrogen Production Unit. *Industrial & Engineering Chemistry Research*, 53(19):8147–8154, may 2014.
- [16] J. Flores-Cerrillo and J. F. MacGregor. Control of particle size distributions in emulsion semibatch polymerization using mid-course correction policies. *Industrial and Engineering Chemistry Research*, 41(7):1805–1814, 2002.
- [17] J. Flores-Cerrillo and J. F. MacGregor. Control of batch product quality by trajectory manipulation using latent variable models. *Journal of Process Control*, 14(5):539–553, 2004.
- [18] J. Flores-Cerrillo and J. F. MacGregor. Latent variable MPC for trajectory tracking in batch processes. *Journal of Process Control*, 15(6):651–663, 2005.
- [19] A. Garg, B. Corbett, P. Mhaskar, G. Hu, and J. Flores-Cerrillo. Development of a high fidelity and subspace identification model of a hydrogen plant startup dynamics. In *2017 American Control Conference (ACC)*, volume 106, pages 2857–2862. IEEE, may 2017.
- [20] A. Garg, B. Corbett, P. Mhaskar, G. Hu, and J. Flores-Cerrillo. Subspace-based model identification of a hydrogen plant startup dynamics. *Computers & Chemical Engineering*, 106:183–190, nov 2017.
- [21] A. Garg, F. P. C. Gomes, P. Mhaskar, and M. R. Thompson. Model predictive

- control of uni-axial rotational molding process. *Computers & Chemical Engineering*, 2018, Submitted.
- [22] A. Garg, F. P. C. Gomes, P. Mhaskar, and M. R. Thompson. Data-driven control of rotational molding process. In *2019 Indian Control Conference (ICC)*, 2019, Submitted.
- [23] A. Garg and P. Mhaskar. Subspace identification and predictive control of batch particulate processes. In *2017 American Control Conference (ACC)*, pages 505–510. IEEE, may 2017.
- [24] A. Garg and P. Mhaskar. Subspace Identification-Based Modeling and Control of Batch Particulate Processes. *Industrial & Engineering Chemistry Research*, 56(26):7491–7502, jul 2017.
- [25] A. Garg and P. Mhaskar. Subspace Identification-Based Modeling and Control of Batch Particulate Processes. *Industrial & Engineering Chemistry Research*, 56(26):7491–7502, jul 2017.
- [26] A. Garg and P. Mhaskar. Utilizing big data for batch process modeling and control. *Computers & Chemical Engineering*, 2018, Submitted.
- [27] S. Gibson and B. Ninness. Robust maximum-likelihood estimation of multivariable dynamic systems. *Automatica*, 41(10):1667–1682, oct 2005.
- [28] M. Golshan, J. F. MacGregor, M.-J. Bruwer, and P. Mhaskar. Latent Variable Model Predictive Control (LV-MPC) for trajectory tracking in batch processes. *Journal of Process Control*, 20(4):538–550, 2010.

- [29] M. Golshan, J. F. MacGregor, and P. Mhaskar. Latent variable model predictive control for trajectory tracking in batch processes: Alternative modeling approaches. *Journal of Process Control*, 21(9):1345–1358, 2011.
- [30] F. P. C. Gomes, A. Garg, P. Mhaskar, and M. R. Thompson. Quality monitoring of rotational molded parts using a non-destructive technique. ANTEC, 2018.
- [31] R. B. Gopaluni. Nonlinear system identification under missing observations: The case of unknown model structure. *Journal of Process Control*, 20(3):314–324, mar 2010.
- [32] A. Hamidi, S. Farzaneh, F. Nony, Z. Ortega, S. Khelladi, M. Monzon, F. Bakir, and A. Tcharkhtchi. Modelling of sintering during rotational moulding of the thermoplastic polymers. *International Journal of Material Forming*, 9(4):519–530, sep 2016.
- [33] J. Hoskins and D. Himmelblau. Artificial neural network models of knowledge representation in chemical engineering. *Computers & Chemical Engineering*, 12(9-10):881–890, sep 1988.
- [34] R. J. Hyndman and A. B. Koehler. Another look at measures of forecast accuracy. *International Journal of Forecasting*, 22(4):679–688, 2006.
- [35] C. D. Immanuel, Y. Wang, and N. Bianco. Feedback controllability assessment and control of particle size distribution in emulsion polymerisation. *Chemical Engineering Science*, 63(5):1205–1216, 2008.
- [36] B. Joseph and F. W. Hanratty. Predictive control of quality in a batch

- manufacturing process using artificial neural network models. *Industrial & Engineering Chemistry Research*, 32(9):1951–1961, sep 1993.
- [37] R. Kadali, B. Huang, and A. Rossiter. A data driven subspace approach to predictive controller design. *Control Engineering Practice*, 11(3):261–278, mar 2003.
- [38] A. Kassidas, J. F. MacGregor, and P. A. Taylor. Synchronization of batch trajectories using dynamic time warping. *AIChE Journal*, 44(4):864–875, apr 1998.
- [39] T. Kourti. Abnormal situation detection, three-way data and projection methods; robust data archiving and modeling for industrial applications. *Annual Reviews in Control*, 27 II:131–139, 2003.
- [40] T. Kourti. Multivariate dynamic data modeling for analysis and statistical process control of batch processes, start-ups and grade transitions. *Journal of Chemometrics*, 17(1):93–109, 2003.
- [41] T. Kourti, J. Lee, and J. F. Macgregor. Experiences with industrial applications of projection methods for multivariate statistical process control. *Computers & Chemical Engineering*, 20(96):S745–S750, jan 1996.
- [42] J. Kroschwitz and A. Seidel. *Kirk-Othmer Encyclopedia of Chemical Technology*. Number v. 20 in *Encyclopedia of Chemical Technology*. Wiley, 2006.
- [43] W. Larimore. Canonical variate analysis in identification, filtering, and adaptive control. In *29th IEEE Conference on Decision and Control*, pages 596–604 vol.2. IEEE, 1990.

- [44] J. H. Lee and K. S. Lee. Iterative learning control applied to batch processes: An overview. *Control Engineering Practice*, 15(10):1306 – 1318, 2007. Special Issue - International Symposium on Advanced Control of Chemical Processes (ADCHEM).
- [45] Z. Liu, A. Hansson, and L. Vandenberghe. Nuclear norm system identification with missing inputs and outputs. *Systems & Control Letters*, 62(8):605–612, aug 2013.
- [46] L. Ljung. *System Identification: Theory for the User*. Pearson Education, 1998.
- [47] S. M. Miller and J. B. Rawlings. Model identification and control strategies for batch cooling crystallizers. *AIChE Journal*, 40(8):1312–1327, aug 1994.
- [48] M. Moonen, B. De Moor, L. Vandenberghe, and J. Vandewalle. On- And Off-Line Identification Of Linear State Space Models. *International Journal of Control*, 49(1):219–232, 1989.
- [49] K. O. Ogila, M. Shao, W. Yang, and J. Tan. Rotational molding: A review of the models and materials. *Express Polymer Letters*, 11(10):778–798, 2017.
- [50] M. Onel, C. A. Kieslich, Y. A. Guzman, C. A. Floudas, and E. N. Pistikopoulos. Big data approach to batch process monitoring: Simultaneous fault detection and diagnosis using nonlinear support vector machine-based feature selection. *Computers & Chemical Engineering*, 115:46–63, jul 2018.
- [51] P. V. Overschee and B. D. Moor. Two subspace algorithms for the identification of combined\ndeterministic-stochastic systems. [1992] *Proceedings of the 31st IEEE Conference on Decision and Control*, 311(I):75–93, 1992.

- [52] M. Park and M. Dokucu. Regulation of the emulsion particle size distribution to an optimal trajectory using partial least squares model-based predictive control. *Industrial & engineering*, pages 7227–7237, 2004.
- [53] M.-J. Park and F. J. Doyle. Nonlinear model order reduction and control of particle size distribution in a semibatch vinyl acetate/butyl acrylate emulsion copolymerization reactor. *Korean Journal of Chemical Engineering*, 21(1):168–176, 2004.
- [54] N. D. Pour, B. Huang, and S. L. Shah. Subspace Approach to Identification of Step-Response Model from Closed-Loop Data. *Industrial & Engineering Chemistry Research*, 49(18):8558–8567, sep 2010.
- [55] S. J. Qin. An overview of subspace identification. *Computers and Chemical Engineering*, 30(10-12):1502–1513, 2006.
- [56] S. J. Qin. Process data analytics in the era of big data. *AIChE Journal*, 60(9):3092–3100, sep 2014.
- [57] S. J. Qin, W. Lin, and L. Ljung. A novel subspace identification approach with enforced causal models. *Automatica*, 41(12):2043–2053, 2005.
- [58] H. Raghavan, A. K. Tangirala, R. Bhushan Gopaluni, and S. L. Shah. Identification of chemical processes with irregular output sampling. *Control Engineering Practice*, 14(5):467–480, may 2006.
- [59] M. M. Rashid, P. Mhaskar, and C. L. Swartz. Multi-rate modeling and economic model predictive control of the electric arc furnace. *Journal of Process Control*, 40:50–61, apr 2016.

- [60] J. B. Rawlings, S. M. Miller, and W. R. Witkowski. Model identification and control of solution crystallization processes: a review. *Industrial & Engineering Chemistry Research*, 32(7):1275–1296, jul 1993.
- [61] F. Reepmeyer, J.-U. Repke, and G. Wozny. Time optimal start-up strategies for reactive distillation columns. *Chemical Engineering Science*, 59(20):4339–4347, oct 2004.
- [62] N. Scenna, C. Ruiz, and S. Benz. Dynamic simulation of start-up procedures of reactive distillation columns. *Computers & Chemical Engineering*, 22:S719–S722, mar 1998.
- [63] D. Shi, N. H. El-Farra, M. Li, P. Mhaskar, and P. D. Christofides. Predictive control of particle size distribution in particulate processes. *Chemical Engineering Science*, 61(1):268–281, 2006.
- [64] A. K. Tangirala. *Principles of System Identification: Theory and Practice*. Taylor & Francis, 2014.
- [65] P. Van Overschee and B. De Moor. A unifying theorem for three subspace system identification algorithms. *Automatica*, 31(12):1853–1864, 1995.
- [66] M. Verhaegen and P. Dewilde. Subspace model identification Part 1. The output-error state-space model identification class of algorithms. *International Journal of Control*, 56(5):1187–1210, nov 1992.
- [67] M. Verhaegen and A. Hansson. Nuclear Norm Subspace Identification (N2SID) for short data batches. *IFAC Proceedings Volumes (IFAC-PapersOnline)*, 19(2010):9528–9533, jan 2014.

- [68] J. Wang and S. J. Qin. A new subspace identification approach based on principal component analysis. *Journal of Process Control*, 12:841–855, 2002.
- [69] H. Wu and J. Zhao. Deep convolutional neural network model based chemical process fault diagnosis. *Computers & Chemical Engineering*, 115:185–197, jul 2018.
- [70] O. Wu, K. Hariprasad, B. Huang, and J. F. Forbes. Identification of linear dynamic errors-in-variables systems with a dynamic uncertain input using the EM algorithm. In *2016 IEEE 55th Conference on Decision and Control (CDC)*, number Cdc, pages 1229–1234. IEEE, dec 2016.
- [71] Y. Yabuki and J. F. MacGregor. Product quality control in semibatch reactors using midcourse correction policies. *Industrial & Engineering Chemistry Research*, 36(4):1268–1275, 1997.
- [72] X. Yang, W. Xiong, B. Huang, and H. Gao. Identification of Linear Parameter Varying Systems with Missing Output Data Using Generalized Expectation-Maximization Algorithm. *IFAC Proceedings Volumes*, 47(3):9364–9369, 2014.
- [73] X. Yang, Q. Xu, K. Li, and C. D. Sagar. Dynamic Simulation and Optimization for the Start-up Operation of An Ethylene Oxide Plant. *Industrial & Engineering Chemistry Research*, 49(9):4360–4371, may 2010.
- [74] H. Yu and J. Flores-Cerrillo. Latent Variable Model Predictive Control for Trajectory Tracking in Batch Processes: Internal Model Control Interpretation and Design Methodology. *Industrial & Engineering Chemistry Research*, 52(35):12437–12450, sep 2013.

- [75] Y. Zhao, J. Zhang, T. Qiu, J. Zhao, and Q. Xu. Flare Minimization during Start-Ups of an Integrated Cryogenic Separation System via Dynamic Simulation. *Industrial & Engineering Chemistry Research*, 53(4):1553–1562, jan 2014.
- [76] Y. Zhu. *Multivariable System Identification For Process Control*. Elsevier Science, 2001.